Republic of Iraq
Ministry of Higher Education
and Scientific Research
University of Babylon
College of Engineering

Design, Implementation and Performance Analysis of Smart Electrocardiograph (ECG) System

A Thesis

Submitted to the College of Engineering
of the University of Babylon in Partial Fulfillment
of the Requirements for the Degree of Doctor of Philosophy
in Electronics and Communications Engineering

by

Akram Jaddoa Khalaf Ahmed

(B.Sc. 2001)
(H.D. 2002)
(M.Sc. 2013)

Supervised by

Prof. Dr. Samir Jasim Mohammed

November 2021 ***Rabi II 1443***

بِسْمِ اللَّهِ الرَّحْمَنِ الرَّحِيمِ

﴿ نَرْفَعُ دَرَجَاتٍ مَنْ نَشَاءُ وَفَوْقَ كُلِّ ذِي عِلْمٍ عَلِيمٌ ﴾

صَدَقَ اللَّهُ الْعَلِيّ الْعَظِيم

يوسف (٧٦)

Abstract

The electrocardiograph (ECG) is a substantial biomedical body signal showing heart activity and diagnosing cardiovascular diseases. Many researchers investigate heartbeat detection and classification based on ECG to achieve a high-performance method because they concern human life and the advance of wearable technology.

The QRS detection algorithm is essential for ECG signal processing in healthcare applications. In numerous methods, the ECG signal is analyzed to classify different classes of heartbeats. These classes are started from normal or abnormal beats and reach many types based on the classification methods and the variability for database beat types.

A low error QRS-detection and classification algorithm with a low computational is a significant challenge for researchers. The main problem with improving performance is increasing the computation, such as in many existing methods for detection and classification. Moreover, the high computation methods are unsuitable for implementation in wearable devices and low data rate internet applications. On the other hand, for the MIT-BIH arrhythmia database (MBADB), different heartbeat numbers are calculated for researchers depending on the difference in understanding the annotation file.

This thesis developed a high accuracy and low computational wearable healthcare system based on Artificial Intelligence (AI) and the Internet of Things (IoT) using proposed heartbeat detection and classification methods. In order to achieve that: First, a QRS-detection algorithm based on low error detection is designed. The proposed algorithm with a low computation and high-performance is implemented based on novel techniques (Slope-level) for features extraction and hybrid classification by Artificial Neural Networks (ANN) and decision trees. Second, the heartbeats number of the MBADB is standardized after developing a new function for MATLAB Waveform Database Toolbox

(WFDB). Third, a low computation and high accuracy classification method for normal and abnormal heartbeats is developed based on new mixed and reused features using ANN. Fourth, a high accuracy classification method for five classes of heartbeats is designed based on a novel method named Selective-Mask Artificial Neural Network (SMANN) for low computational applications. The SMANN gives ANN a new dimension instead of the serial dimension for deep learning methods. SMANN is a multiple mask ANN, each mask for the selective data will be separated by their properties. Furthermore, A new mixture of features from the reused QRS-detection stage and the other features from the RR-interval and between-RR are used for decreasing the computation for features extraction. Finally, a smart wearable system for heartbeat detection and classification using Node-MCU with IoT is designed and implemented based on the proposed QRS-detection algorithm and the proposed five classes classification method.

The performance of the proposed detection algorithm and the performance of the proposed classification methods are evaluated using the MATLAB program based on MBADB. The evaluation performance results for the proposed QRS detection algorithm are a high sensitivity (99.88%), low error rate detection (0.224%), and a high predictivity of 99.89%. The normality classification method results have an accuracy of 98.97%, sensitivity of 99.42%, and positive predictivity of 99.13%. Then, the results for the five classes classification are high accuracy of 99.92 %; the total classification errors for the SMANN are 80 errors from total heartbeats of 103,192 compared with the 583 errors for the traditional ANN. Thus, SMANN is a new approach for improving performance with low resources. Finally, the accomplished wearable system results were promising for real-time heartbeat detection and classification as online and offline patient monitoring with a low cost about 52$.

To my beloved family

To the memory of my father

To my beloved wife … Noor

Supervisor Certification

I certify that this thesis entitled "**Design, Implementation and Performance Analysis of Smart Electrocardiograph (ECG) System**" was prepared by **Akram Jaddoa Khalaf** under my supervision at the Department of Electrical Engineering, College of Engineering, University of Babylon, as a partial fulfillment of the requirements for the degree of Doctor of Philosophy in Electronics and Communications Engineering.

Signature:

Name: ***Prof. Dr. Samir Jasim Mohammed***

(Supervisor)

Date: / / 2021

In view of the above recommendation, I am forward this thesis for discussion by the Examination Committee.

Signature:

Name: ***Asst. Prof. Dr. Shamam Fadhil Alwash***

(Head of Electrical Engineering Dept.)

Date: / / 2021

Examining Committee Certificate

We certify that we have read this thesis entitled "**Design, Implementation and Performance Analysis of Smart Electrocardiograph (ECG) System**" and as an examining committee, examined the student, "**Akram Jaddoa Khalaf**", in its contents and that in our opinion it meets the standard of a thesis for the degree of Doctor of Philosophy in Electronics and Communications Engineering.

Signature:
Name: ***Prof. Dr. Ahmad T. AbdulSadda*** *(Member)*
Date: / / 2021

Signature:
Name: ***Prof. Dr. Osama Qasim Jumah Al-Thahab*** *(Member)*
Date: / / 2021

Signature:
Name: ***Prof. Dr. Ibrahim Abdullah Merdas*** *(Member)*
Date: / / 2021

Signature:
Name: ***Prof. Dr. Bayan Mahdi Sabbar*** *(Member)*
Date: / / 2021

Signature:
Name: ***Prof. Dr. Laith Ali Abdul-Rahaim***
(Chairman)
Date: / / 2021

Signature:
Name: ***Prof. Dr. Samir Jasim Mohammed***
(Supervisor)
Date: / / 2021

Signature:
Name: ***Asst. Prof. Dr. Shamam Fadhil Alwash***
(Head of Electrical Engineering Dept.)
Date: / / 2021

Signature:
Name: ***Prof. Dr. Hatem Hadi Obeid***
(Dean of College of Engineering)
Date: / / 2021

Acknowledgements

In the name of Allah, Most Gracious, Most Merciful

First and above all, I praise *ALLAH*, the almighty for providing me with this opportunity and granting me the capability to proceed with this thesis.

I present my highest appreciation to my thesis supervisor *Dr. Samir Jasim Mohammed*, for his constant help, encouragement, guidance, patience and support through this research.

I would like to thank my friends and colleagues for their assistance and collaboration. I also thank the staff of the Department of Electrical Engineering for their kind support. Especially, my friend, *Dr. Shamam Alwash*, for constant help, guidance and support through this research.

Finally, I would like to express my deepest gratitude and gratefulness to my family. Especially my mother, my wife *"Noor"*, my sisters, my aunts, and my uncle. The sacrifices; they made during my years of work is simply ineffable, and whose endless love and encouragement enabled me to complete this work.

Table of Contents

List of Symbols

$-QRS^*$	Negative predicted QRS
$+QRS^*$	Positive predicted QRS
ΔHb	Hidden bias correction term
ΔHw	Hidden weight correction term
ΔOb	Output bias correction term
ΔOw	Output weight correction term
b	Bias
bn	The beat number
bn^*	The predicted beat number
d	Desired (target) output
E	energy (Wh).
f	Function
f'	Activation function derivative
$F(n)$	All features
$f(n)$	Features for ANN
F_{max}	The maximum value for each feature
F_{min}	The minimum value for each feature
f_s	Sampling frequency
H	Hidden output
h	hour.
Hb	Hidden layers bias
H_{net}	Hidden layers nets
Hw	Hidden weight (inputs)
$H\delta$	Hidden error information term
i	Index of inputs (features)
j	Index of hidden neurons
k	Index of Selective Masks

l	Index of Outputs Classes
m	Number of inputs (features)
$m(n)$	Filtered ECG signal
m_QRSdec	The mean for 15 values of the QRSdec
n	Number of hidden neurons
N	Number of samples per window
Ob	Output layers bias
$Onet$	Output layers nets
O_{out}	Output output
Ow	Output weight
$O\delta$	Output error information term
P	power (W).
QR_level	The y- value from R point to Q point
QR_slope	The slope from Q point to R
QR_time	The x_values from Q point to R point
*QRS**	Predicted QRS
QRS_level	QR_level + RS_level
QRS_slope	QR_slope + RS_slope
QRSdec	QRS_level × QRS_slope
QS_time	The x_values from Q point to S point
r	Number of Selective Masks
$r(n)$	The Q, R and S level and time values
R+10_slope	The slope from peak R(t) to R(t+10)
R-10_slope	The slope from peak R(t) to R(t-10)
RS_level	The y- value from R point to S point
RS_slope	The slope from R point to S point
RS_time	The x_values from R point to S point
s	Number of Outputs Classes

$s(n)$	ECG original signal
T	time (h)
t	Time sample
t_Q	The time of Q wave for the (bn) beat
t_R	The time of R wave for the (bn) beat
t_S	The time of S wave for the (bn) beat
W	watt.
w	Weight
x	Input
y	Hidden output
y_{net}	Hidden layers nets
α	Learning rate

List of Abbreviations

AAMI	Association for the Advancement of Medical Instrumentation
Acc	Accuracy
AHA	American Heart Association database
AI	Artificial Intelligence
ANN	Artificial Neural Networks
B	Beats
BF	Beat Function
CDS	Clinical Decision Support
CPU	Central Processing Unit
CVDs	Cardiovascular Diseases
DER	Detection_Error_Rate
DSPs	Digital Signal Processors
DSSS	Direct-Sequence Spread Spectrum
ECG	Electrocardiograph
F	Fusion beat
FN	False Negative
FP	False Positive
FPGAs	Field Programmable Gate arrays
GPS	Global Positioning System
HR	Heart Rate
IEEE	Institute of Electrical and Electronics Engineers
IoT	Internet of Things
MBADB	MIT-BIH arrhythmia database
Mbps	Megabits per second
MCU	Microcontroller
MIMO	Multiple-Input and Multiple-Output

MIT-BIH	Massachusetts Institute of Technology- Boston's Beth Israel Hospital
ML	Machine Learning
N	Normal
OFDM	Orthogonal Frequency Division Multiplexing
PP	Positive_Predictivity
Q	Unknown
ReLU	Rectified Linear Unit
S	Supraventricular ectopic
Se	Sensitivity
SMANN	Selective-Mask Artificial Neural Network
Tanh	Hyperbolic Tangent
TCP/IP	Transmission Control Protocol and Internet Protocol
TP	True Positive
V	Ventricular ectopic
WFDB	Waveform Database Toolbox
WHO	World Health Organization
Wi-Fi	Wireless Fidelity

List of Figures

List of Tables

Publications

A research paper has been published, consisting of the developed and evaluated algorithm for QRS-detection based on low error detection, high accuracy, and low computation.

Title: "***A QRS-Detection Algorithm for Real-Time Applications***,"

By: Akram Jaddoa Khalaf, Samir Jasim Mohammed,

Publisher: International Journal of Intelligent Engineering and Systems.

A research paper has been published, consist of verifying the MIT-BIH arrhythmia database according to the number of heartbeats using a simple function for WFDB.

Title: "***Verification and Comparison of MIT-BIH Arrhythmia Database Based on Number of Beats***,"

By: Akram Jaddoa Khalaf, Samir Jasim Mohammed,

Publisher: International Journal of Electrical and Computer Engineering (IJECE).

A research paper has been accepted which consists of developing and evaluating a normal and abnormal heartbeat classification method based on the artificial neural network.

Title: "***Low Computation Heartbeat Classification Based on ECG Using Artificial Neural Networks***,"

By: Akram Jaddoa Khalaf, Samir Jasim Mohammed,

Publisher: 3rd International Scientific Conference of Alkafeel University (ISCKU 2021) / Journal "AIP Conference Proceedings".

A research paper has been published, consisting of the developed and evaluated method for five-classes heartbeats classification based on SMANN to improve the performance with low computational processes. Moreover, a smart wearable system for heartbeats detection and classification using Node-MCU with IoT is implemented based on the QRS-detection proposed algorithm and the five-classes classification proposed method.

Title: "***A Wearable Heartbeats Classification System Based on A New Method (Selective-Mask Artificial Neural Network)***,"

By: Akram Jaddoa Khalaf, Samir Jasim Mohammed,

Publisher: International Journal of Online and Biomedical Engineering (iJOE).

Chapter 1: Introduction

Contents

Chapter One:
Introduction

1.1 Overview

This chapter presents the research background, literature review and discusses the importance of designing and implementing the smart wearable healthcare system. It presents the background and literature review that formulates the foundation of this thesis. The literature review also shows related and relevant methods and algorithms for the QRS-detection, classification, and wearable system. Then the scope of research is presented. Next, the research aims with objectives are described after the research problem identifying. Finally, the chapter has concluded the outline of the thesis chapters.

1.2 Research Background

Globally, the major diseases that cause death are cardiovascular diseases (CVDs), with 31 % of all worldwide deaths, almost eighteen million deaths caused by CVDs. This number may reach to 24 million in 2030 because of the growing global population. Figure 1.1 shows the global cause of death according to 2016 WHO reports [1].

People are dying each year due to CVDs; an electrocardiograph (ECG) is an essential and usable way of diagnosing CVDs since it is simple to use and offers valuable knowledge about heart health. The ECG is the process of reading the heart's electrical signal over time. For different biomedical applications like heart rate measuring, unnormal diagnosing, biometric identification, and movement recognition, the ECG is an efficient non-invasive tool [2]. Also, this signal shows the heart functionality for the cardiologist to diagnose arrhythmias that is one of the CVDs. The field for ECG signal processing developed significantly because of the seriousness of CVDs according to the high percentage of death.

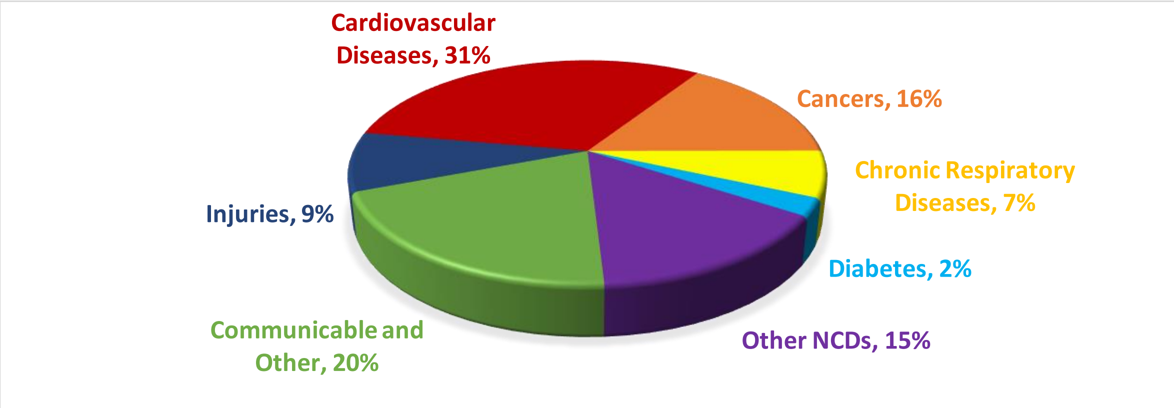

Figure 1.1 Global diagram of death percentages [1]

According to the Science Direct and IEEE research database, there is significant attention in the ECG signal processing and classification field. A survey has been done for existing research using specific keywords until 18/6/2021, as shown in Figure 1.2. From the overall signal processing research in ScienceDirect, the ECG signal processing is 40%, and the ECG signal classification is 15%. Moreover, the ECG signal processing is 51%, and the ECG signal classification is 8% from the overall IEEE signal processing research.

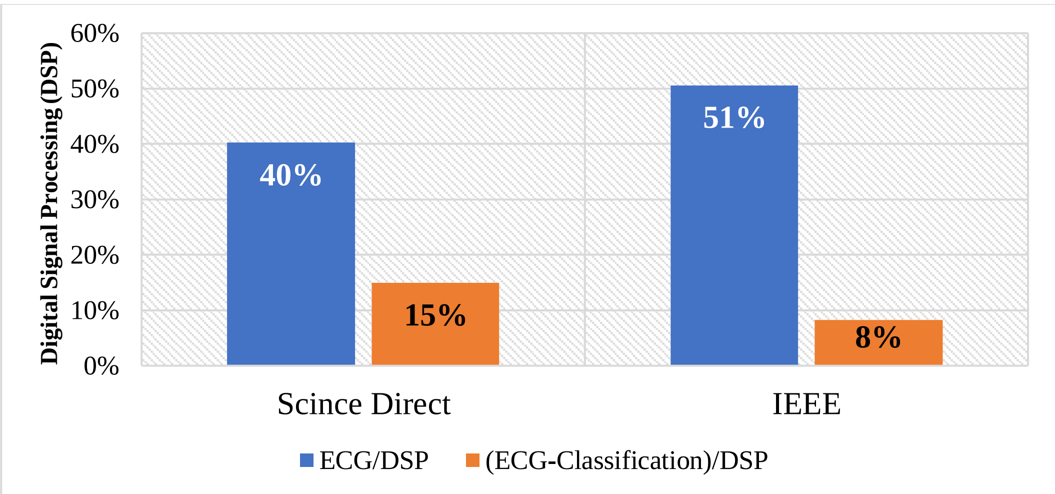

Figure 1.2 Types of research in the corresponding field

Arrhythmias are a heartbeat abnormality with a too fast, too slow, or irregular rhythm and are detected and classified by ECG signals. Arrhythmias are the most common causes of death among CVDs. So, accurate arrhythmias detection and classification have been of great concern in biomedical signal processing studies. Moreover, the advancement of communication like IoT and electronics like the reliable microcontrollers [2-4].

The heartbeat with normal rhythm consists of the waves P-QRS- T, as shown in Figure 1.3 [2, 4, 5]. In ECG signal processing, QRS-complex detection is essential for most applications because it is the highest energy part for the ECG signal. However, the detection analysis is not easy because the noise affected the ECG signal and physiological variability for patients; moreover, the similarity between some cases of T wave with QRS-complex characteristics. In addition to, muscular noise, electrode motion effects, power-line interference, and baseline wandering are the noise sources that affect the ECG signals [6, 7].

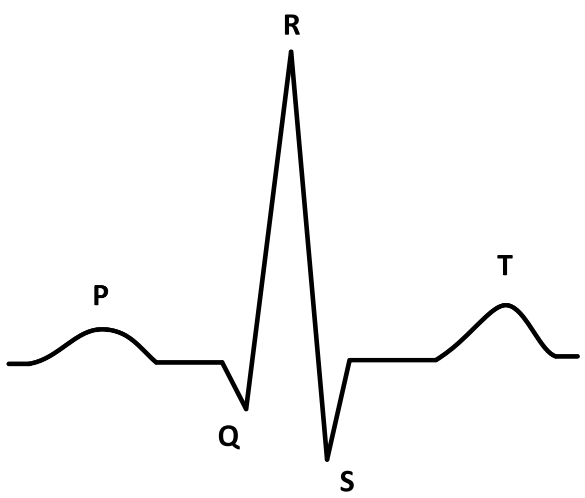

Figure 1.3 The normal (ideal) ECG signal

Numerous studies for classification have been developed in recent decades. Detecting and classifying arrhythmias is an important topic in biomedical fields because it provides details regarding CVD [8]. The ECG beats should be processed to find any cardiac anomalies. However, the long-time ECG signal processing from the hospital monitoring system or wearable healthcare for online monitoring is a big challenge for an individual, and it takes a very long time [9].

Automated arrhythmia classification provides excellent suitability for doctors and helps the patients for monitoring their conditions. Typically, it is not achievable in many regions because of financial and medical services issues. Reducing the demand for physicians and care providers encourages the need for a low-cost, safe, and automatic framework for wearable healthcare monitoring devices [9]. On the other hand, real-time or long-time monitoring systems are concerned with a single-lead ECG signal to allow the patients to have a natural life [10]. There are many challenges for arrhythmia classification: the selected section may not show the arrhythmia, the ECG signal variability depending on age or gender, large data may cause classification errors, and the noise for ECG signal [9].

The applications for real-time biomedical signal processing development are rapidly increasing because they relate to human life and the development of wearable devices. The cloud computing and internet of things (IoT) play significant role to improve many applications; healthcare applications are at the top of these applications [11]. On the other hand, the QRS detection field seems to be saturated because many algorithms are proposed. Despite that, the development of wearable devices and the healthcare system make a new challenge to increase the algorithm efficiency, performance, and portability [6, 12]. Moreover, to reduces the memory storage and transmit low data rate for wearable devices. Many advanced techniques and tools are still not used for future improvement [7, 13].

Artificial Neural Networks (ANN) are essential Machine Learning (ML) techniques for classification and recognition problems such as heartbeat classification [14, 15]. ML is a part of Artificial Intelligence (AI) that makes computers for programming themselves according to the input data to solve a problem. It attempts to provide computers with cognitive abilities in order to train them to learn and solve issues like human brain intelligence. Artificial intelligence cannot duplicate human intellect, but computers can only be taught to do certain human brain functions [16].

Wearable devices are small-sized devices that sense, collect, and upload different physiological data to provide a better quality of life. Reducing power usage and improving communication are required for meeting these objectives. Thus, there is an increased need for mobile devices that offers a tangible method to improve daily living that smartphones cannot provide. These devices, such as phones, smartwatches, electronic clothing, wireless body area networks, and others, are referred to as wearables [17].

The technology of wearable devices has attracted the attention of academics and healthcare providers in the recent years. The reasons for wearable device development are due to the enormous advantages such as real-time or long-time home monitoring [18]. Moreover, the wearable devices technological progress made in communication like IoT and electronics like the reliable microcontrollers. Since IoT features, consider as a promising technology for many applications; one of these applications is healthcare to improve the quality of life and save human life. The IoT is a new context of modern wireless telecommunications based on interaction and cooperation using a unique address between various objects like sensors, actuators, devices, etc., for common goals. [19].

Different databases are widely used to evaluate different applications that were proposed in many studies for ECG signals analysis [2]. The ECG databases are available now, such as Massachusetts Institute of Technology (MIT) - Boston's Beth Israel Hospital (BIH) databases, QT database, and the database of American Heart Association (AHA). The first ECG standard material available for testing and performance evaluation is the MIT-BIH arrhythmia database

(MBADB). Arrhythmia analyzers manufacturers found that working with the MBADB and AHA databases spurred them to use market competition as a means of proving objectively quantifiable performance. This is credited to the MBADB database, which serves both fundamental research and medical device development and evaluation. It has comprised variable ECG signals with a variable: noise, artifacts, beat types, and wave shapes [7, 20].

Different ECG databases like the MIT-BIH database are widely used for training, testing, and evaluating the performance of existing methods. The MIT-DIH arrhythmia database contains variable ECG signals, and variable arrhythmia types make this database used by many researchers [20]. It consists of 15 heartbeats types. Based on AAMI, the MBADB beats are categorized into five types, as shown in Table 1.1.

Table 1.1 MBADB and AAMI standards [21]

<table>
<tr><th colspan="2">MIT-BIH annotations</th><th colspan="2">AAMI</th></tr>
<tr><td>N</td><td>Normal beat</td><td rowspan="5">N</td><td rowspan="5">Normal</td></tr>
<tr><td>L</td><td>Left bundle branch block beat</td></tr>
<tr><td>R</td><td>Right bundle branch block beat</td></tr>
<tr><td>e</td><td>Atrial escape beat</td></tr>
<tr><td>j</td><td>Nodal (junctional) escape beat</td></tr>
<tr><td>A</td><td>Atrial premature beat</td><td rowspan="4">S</td><td rowspan="4">Supraventricular ectopic</td></tr>
<tr><td>a</td><td>Aberrated atrial premature beat</td></tr>
<tr><td>J</td><td>Nodal (junctional) premature beat</td></tr>
<tr><td>S</td><td>Supraventricular premature</td></tr>
<tr><td>V</td><td>Premature ventricular contraction</td><td rowspan="2">V</td><td rowspan="2">Ventricular ectopic</td></tr>
<tr><td>E</td><td>Ventricular escape beat</td></tr>
<tr><td>F</td><td>Fusion of ventricular and normal</td><td>F</td><td>Fusion beat</td></tr>
<tr><td>/</td><td>Paced beat</td><td rowspan="3">Q</td><td rowspan="3">Unknown</td></tr>
<tr><td>f</td><td>Fusion of paced and normal beat</td></tr>
<tr><td>Q</td><td>Unclassifiable beat</td></tr>
</table>

1.3 Literature Review

In this section, the QRS-detection existing algorithm and the heartbeats classification existing methods are reviewed. The QRS-detection algorithms are considered because it detects the highest energy waves in the ECG signal, which is the QRS-complex or heartbeats. Furthermore, the arrhythmia classification algorithm based on QRS-detection is more popular than the ECG processing without heartbeat detection [22]. Finally, the existing wearable devices are reviewed with the proposed system advantages over the previous systems.

1.3.1 QRS Detection

Many researchers have been developed various QRS-detection algorithms, methods, and techniques based on different concepts. Each approach depends on the application is designed, so some methods are used for real-time applications, and the others are used for offline applications. QRS detection methods are an essential field for wearable healthcare applications to reduce the data transmitting, speed processing time, and reduce the memory used. Linear filter, nonlinear processing, and decision are the three main stages that used for most QRS detection algorithm [23].

Pan and Tompkins 1985 [7] algorithm filtered the ECG signal to maximize the QRS frequency band and reduced the other frequencies. So, digital filters were designed for QRS-complex improvement. After that, was pre-processing the filtered signal to extract slope information. Then, two thresholds were applied to detect the QRS and search back the missing QRS based on the RR interval accepted ranges. The error detection for this method is moderate of (0.675%).

Xue and others 1992 [24] were developed an artificial neural network based on an adaptive whitening filter that updates the matched filter to improve the QRS detection. After squaring and moving the average for all samples. The method accuracy is 99.5%.

Moraes and others 2002 [25], moderate detection sensitivity was evaluated using two channels ECG detection method, two detections in parallel cross detection as mainly, and energy detection as secondary. The method sensitivity was 99.22%.

A complex detection for positive and negative slopes is using for two stages as pre-processing and decision then is made, this procedure was presented by Adnane and others 2009 [26]. Squaring, normalizing, and differentiation are used for the first stage before the decision rules, depending on RR durations. So, the complexity of the operation will increase the execution time and the detection error was 0.59%.

On the other hand, Zidelmal and others 2012 [27] were designed a discreet wavelet transform considering energy levels. It used the power spectrum of QRS for the normal and abnormal beats. The results showed a sensitivity of 99.64%.

Castells-Rufas and Carrabina 2015 [6] presented a novel nonlinear filter to minimal computational reason. A moderate accuracy for this technique, less computation to reduce the resource, and the detection error rate of 0.88%.

Shaik and others 2015 [28] proposed an adaptive threshold technique based on Short Time Fourier Transform with initial training and the detection error rate of 0.93%.

Excluding the derivative filter and based on new decision techniques Yakut and Bolat 2018 were proposed a new method [29]. The first stage is contained two filters, square and normalization. The second stage is the decision stage. A satisfying error detection rate of 0.33% is required more computation because it searches back the missing QRS based on normal durations and uses a complex calculation.

Chin and others 2019 [11] developed an efficient real-time QRS detector algorithm based on the Bayesian framework that contains a complex repeated multiply and accumulates calculations with detection error rate 0.29%.

Sharma and others 2019 [30] presented a tunable-Q wavelet transform. These methods consist of a complex operation with moderate detection errors of 0.29% for offline applications. The QRS localization can improve using the tunable-Q wavelet transform parameters.

Cai and Hu 2020 [31] proposed a Convolutional and Squeeze-and-Excitation networks (CNN), and hybrid Convolutional and Recurrent Neural Network (CRNN) based on deep learning methods. All ECG samples are processing to these neural network methods and so high neurons number increase the computation.

Zhang and others 2020 [32] were presented Kalman filter extract features for decrease computational cost, storage, fast response, and detection error rate of 1.387% for two adaptive threshold systems.

These methods are based on filters design [6, 7, 26, 32], Short Time Fourier Transform[28], Wavelet [27, 30], neural network (NN) [24, 31], energy detection [25], entropy [31], Bayesian framework [11] , and decision rules [29].

1.3.2 Heartbeat Classification

Diverse classification methods have been developed based on different concepts. Many methods have been proposed with high classification performance, but not easy to implement because of their high computation. Furthermore, each method depends on the application is designed, so some methods are used for real-time applications, and the others are used for offline applications. There are two main types of heartbeats classification techniques. The first type processes the raw ECG signal for a certain period (like 5 sec or 10 sec) and extracts the features according to this period. The second uses the beat or beats by beats from the ECG signal, and the extracted features depend on the beat's detection. The QRS-detection algorithms detect these beats. The arrhythmia classification algorithm based on QRS-detection is more popular than the ECG processing without beat detection [22].

Das 2014 [33] proposed system for classification the five AAMI main classes (N, V, S, F, and Q). S-transform based features along with temporal features and mixture of ST and WT based features along with temporal features are the method features extraction. High accuracy of 97.5% and moderate computation model used a Multilayer Perceptron Neural Network.

Sadrawi 2017 [34] proposed an Artificial Neural Network with entropy and fast Fourier transform classification method. The classifier has low complexity and moderate performance with 93.1% for VEB sensitivity.

Sannino and De Pietro 2018 [35] presented a high accuracy of (99.83%) and high complexity methods used deep neural networks consist of seven hidden layers. It classified normal and abnormal beats as an automatic classifier-based ECG after QRS detection.

Faust 2018 [36] designed a deep Recurrent Neural Network (DRNN) and Long Short-Term Memory (LSTM) classifier. A window with 100 beats used to segment the ECG signal after the QRS detection. The classification results were a high accuracy of (99.77%) and high complexity.

IZCI 2018 [37] developed an Empirical Mode Decomposition method for arrhythmia classification. The six classes are normal, left bundle branch block, right bundle branch block, premature ventricular contraction, paced beat and atrial premature beats. Low complexity and moderate performance with accuracy of 87% are the classification results.

Singh 2018 [38] presented a neural network used Long Short-Term Memory with Recurrent Neural Network classifier. Moderate accuracy of 88.1% and moderate complexity were the results for normal and abnormal classification.

Plawiak 2018 [22]presented a evolutionary neural method based frequency components of the power spectral density of the ECG signal. The ECG signal with 10 sec time is collected from the database for long time analysis. The classification accuracy was 95% for classification 13 heartbeat classes.

Marinho 2019 [39] presented different feature extraction and classification methods based on ECG. Four feature extraction techniques and four classification methods were evaluated. The method is classified the five AAMI main classes with an accuracy of 94.3.

Alfaras 2019 [10] designed an Echo State Network method based on single ECG lead. The method was a low computation and moderate accuracy of 97.7% to classify normal and supraventricular beats as (first-class SVEB+) and the ventricular ectopic and the fusion beats as (second-class VEB+).

Romdhane 2020 [4] proposed one-dimensional convolutional neural network for automatically feature extraction and classification. The ECG signal was segmented for each heartbeat based on a QRS detection algorithm. The five main classes for AAMI (N, S, V, Q, and F) are classified for a 98.41% overall accuracy.

Hua 2020 [40] presented a 1D Convolutional Neural Networks based on (R-R-R) ECG segmentation strategy for all samples of the R-before and R-after the current R peak. The classification accuracy for the fuve AAMI standard was 97.5%.

Atal 2020 [41] proposed an automatic arrhythmia classification based on features with Moderate accuracy of 93.19% and moderate complexity. A deep convolutional neural network with Bat-Rider optimization algorithm is used for arrhythmia classification.

Ullah 2020 [42] presented a two-dimensional convolutional neural networks classification method for eight heartbeat classes. The method was high accuracy of 99.11% and high complexity after transformed the ECG signal into two dimensional spectrograms.

Wang 2020 [43] proposed dual fully connected neural networks for classification the five AAMI main classes (N, V, S, F, and Q). A 105 features were extracted from the per-processing ECG signal as inputs for the neural networks. The method accuracy is 93.4% based on low computational process.

Yang 2020 [44] proposed a novel morphological feature for ECG signal for heartbeat classification based on neural network, SVM, and KNN classifiers. The overall accuracy for 15 heartbeats classification is 97.7%.

The most reviewed classification methods using the QRS detection algorithm for ECG-segmentation as in [4, 8, 10, 33-36, 38-41, 44] . In contrast, the methods in [22, 37] presented an algorithm based on period-time ECG-signal analysis classification without QRS detection.

1.3.3 Wearable System

In Zheng 2003 [45], a wearable mobihealth care system was presented for online diagnosis with alarm. New sensors and electrodes were used for the non-invasive method. It was diagnosed online with three alarm levels (low important, medium life-threatening, and high for emergency) and GPS location.

In J. J. Oresko 2010 [46], an assistive diagnosis solution based on ECG using smartphones like Holter portability for real-time processing capability. The sensors read the ECG and display it on the mobile. The mobile detected the QRS, RR interval, P duration, RP interval, QT interval, and QTr interval. Moreover, it was diagnosed the normal and premature ventricular contraction heartbeats.

In Jun Liu 2013 [47], a Multi-parameters monitoring system is designed for reading the ECG, respiratory condition, activity, and temperature. The sensing values were sent to mobile by Bluetooth to display the heart health index of measuring. Next, the mobile sent the information to the customer management centre via WIFI.

In D. Sopic 2018 [48], A random forest classification algorithm was presented for real-time Myocardial Infarction disease. The algorithm has high accuracy and low complexity. Furthermore, a wearable device was implemented for the proposed classifier with low energy consumption.

In Y. Xia 2018 [49], A wearable ECG classification and monitoring system was presented using a stacked denoising autoencoder. The ECG was sensed from sensors and sent via Bluetooth to the computer for classification. The classifier was based on deep neural networks for VEB and SVEB classes. The strategies for performing active learning were breaking ties and modified breaking ties. The MBADB was used for algorithm performance evaluation.

In A. Amirshahi 2019 [50], A real-time and ultra-low-power wearable device was designed based on a novel ECG classification algorithm. This algorithm was based on the third generation of spiking NN Spike-timing-dependent-plasticity, and reward-modulated spike-timing-dependent plasticity was employed to the model weights and trained. However, some neurons were trained to be sensitive to some pattern. Moreover, some neurons were not helped with the classification.

We can conclude the proposed system should has improvements over the previous systems by the following:

- The Pan and Tompkins algorithm [7] was used for QRS-detection by the existing devices. In contrast, the proposed QRS-detection algorithm should have higher performance and lowest computation than existing.
- Accurate classification and low computation are the performance advantages of the proposed method for both classification and detection.
- Reduce the computation of the classification and detection methods by sharing the QRS-shape extracted features.
- The features are extracted according to a simple mathematical calculation.

- The low computation method can be implemented in wearable devices and IoT.
- The device executes all processes except displaying the report using the mobile application. The processes include reading the ECG samples, detecting the QRS, classifying these heartbeats, sending the patient report, and storing the ECG samples with the report in a microSD-card.
- The device can work with internet connection (online) and without internet connection (offline).
- In the device, the ECG samples are stored using the microSD-card then it processed for the patient report.

1.4 Research Problems Statement

From the literature review for QRS-detection algorithms and heartbeats classification methods, the research problems statement as follows:

1. Wearable system:
    - The methods with high computation are performed on the workstation or cloud. However, these methods are unsuitable for low data rate internet applications and more resources from wearable devices for detection and classification.
    - The traditional systems transmit the overall ECG samples for the out-device process. So, it needs a reliable internet connection or analyzes the overall ECG samples for the in-device process without any reduction. Hence, it needs high resources device.
2. The QRS-Detection:
    - The reviewed QRS-detection methods stages are processed all ECG samples without reducing them, so improving the performance will add more complexity.

- The reviewed QRS-detection methods squaring all ECG samples and will add more computation. So, they did not deal with QRS polarity, and that will reduce the detection accuracy. Because of the squaring process, they did not deal with QRS polarity.
- The detection decision for the most existing methods is based on search back the missing QRS.

3. The MIT-BIH arrhythmia database:
    - The heartbeats numbers for the existing methods that used the MIT-BIH arrhythmia database are no standard. Different heartbeat numbers are calculated for the researchers depending on the difference in understanding the annotation file.
4. The normal and abnormal heartbeat classification:
    - The classification algorithms based on heartbeats detection are not reused the same QRS features from the detection stage in order to simplify and reduce the overall algorithm processes.
    - Most high-performance existing methods used the raw ECG signal instead of the features for detection and classification.
5. The 5-classes heartbeat classification, in addition to the previously stated in point (4):
    - Many methods have been proposed with high classification performance, but it is not easy to implement with their high computation. Therefore, the big challenge for wearable (low computation) applications is improving the performance without adding more complexity.

1.5 Research Objectives

The objectives of this work are to highlight the problem statement associated. The main goal of this thesis is to develop a wearable healthcare system with high accuracy and low computational with low cost operates in real time based on AI and IoT for heartbeats detection and classification. The contributions of this thesis are to improve the heartbeat detection and classification based on single-lead ECG signal with low computational methods. Furthermore, the methods are implemented in a wearable device. The main two stages are detection and classification. First, the ECG signal process for QRS-detection. The second, the heartbeat classification process. In this study, the focus is given more on a new approach of AI for both stages. The ANN is the primary classifier for both stages; the ANN hybrid with a decision tree for QRS-detection and improved based on new methods for heartbeat classification. Moreover, feature extractions from the QRS-shape and RR interval are studied to improve the detection and classification performance. The evaluation performance is based on the MBADB for detection and classification using MATLAB. The overall method is implemented in Node-MCU based on IoT for online and offline patient monitoring by mobile.

This system uses for real-time ECG monitoring as a Clinical Decision Support (CDS) system and offline for long-time ECG analysis. Moreover, this system provides the advantages of being able to integrate with other modern network communications. In addition, it has high system reliability, efficient performance, and low computation. In this context, the main objectives of this work are as follows:

1. Implement a CDS prototype wearable system for heartbeats detection and classification using Node-MCU with IoT based on the proposed heartbeats detection and classification methods.

2. Design and evaluate a QRS-detection algorithm based on low error detection, high accuracy, and low computation. The process is reduced to decrease the computation and improve performance by a novel technique for features extraction and hybrid classification based on ANN and decision trees considering the QRS polarity.
3. Verify and compare the heartbeats number of the MBADB used to evaluate the QRS-detection methods. Develop a MATLAB Waveform Database Toolbox (WFDB) function to standardize this number.
4. Design and evaluate a low computation and high accuracy classification method for normal and abnormal heartbeats based on new mixed and reused features.
5. Design and evaluate a high accuracy classification method for the 5-AAMI classes heartbeats based on a novel method named Selective-Mask Artificial Neural Network (SMANN) of low computational application.

1.6 Thesis Organization

The rest structure of the thesis is organized as follows:

- Chapter 2, “Principles of Wearable Systems Design based on IoT,” describes the wearable system design and architecture based on intelligent techniques.
- Chapter 3, “Design the Proposed Smart Wearable System and Its Implementation,” presents the proposed heartbeat detection and classification methods with the proposed wearable system based on these methods.
- Chapter 4, “Results and Discussions,” shows the proposed methods and wearable system results with their discussions.
- Chapter 5 ” Conclusions and Future Works.” The thesis’s future works and its conclusions are explained in this chapter.

Chapter 2: Principles of Wearable Systems Design based on IoT

Contents

Chapter Two:
Principles of Wearable Systems Design based on IoT

2.1 Introduction

The wearable systems are developed by the same factors that contributed to the transition's success from desktop computers to laptops and the new generation of smartphones. As a result of the advances in electronics and communications, wearable systems have improved performance and minimized the size. Moreover, the market demand for wearable technology is playing a significant role force for the development. As a consequence of this technical development, wearable technology applications will expand widely and improve life quality [51].

The wearable system should be designed based on a simple integrated sensor, and a small size can be worn. These systems are sensing the human body vital signs with storing options and are transmitting some sensing or analyzing data when needed. The sensors are placed on the human body in certain skin locations depending on the signs that are monitored, such as ECG, pulse meters or oximeters [51].

The challenge for wearable technology is designing an implementable and wearable system with low computational, low cost, and high reliability. Therefore, the wearable system consists of three main parts: *sensing*, *processing*, and application (*connecting*), as shown in Figure 2.1. The first part is sensing the signal and filtering the data after conditioning. The second part is processing these signals for features extraction and classification as a result of the monitoring operation. Finally, the results are transmitted or displayed to the patient, the doctor, or/and the family [51, 52]. The technology development in sensors, electronics, microcontrollers, and communication enables advancing and implementing wearable systems with advanced techniques [51]. The following sections are described these three parts in detail.

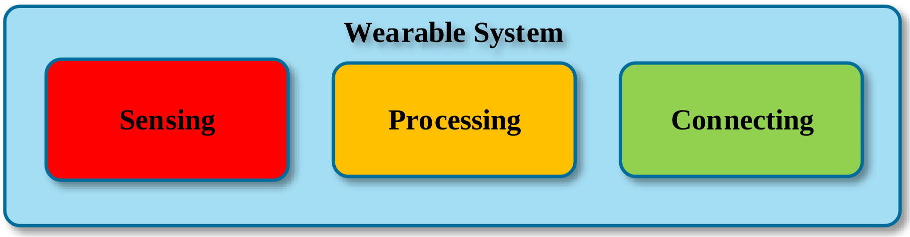

Figure 2.1 Wearable system architecture

2.2 Wearable System Sensors

The wearable sensors can be categorized into physiological sensors, biochemical sensors, and biomechanical sensors. The physiological sensors are sensing the body signal like ECG, pulse monitoring, oxygen saturation, thermal sensors, blood presser sensors, and gas sensors. The biochemical sensors like blood glucose recording, biomolecule recording, pH recording. The biomechanical sensors are sensing the body motion detection like accelerometers and gyroscopes. These sensor types are reading values for the related signs. The reading values can be noisy, so filters are proposed to smooth and reduce the noise for these signs. Some filter types are reducing the unwanted part of the signal to improving the wanted part. On the other hand, conditioning circuits are applied for each sensor type to amplifying the signal from very low voltage to suitable voltage. Moreover, they are isolating the sensor from the system to prevent damage to system stages [51].

As stated previously, there are numerous healthcare applications, and each application has specific sensors. So, different kinds of sensors are used according to the applications. The sensors related to the human body for healthcare applications are named biomedical sensors. Therefore, biomedical sensors are an essential kind of sensor. The sensors are transducer converts the sensed value to an electrical signal that carries the sensed information. They can be sensed physical, chemical or biological signs. In the biomedical field, sensors are electronic devices to transfer electrical or non-electrical measures into easily detectable electrical values. These values can be human physiological and pathological information [53].

In general, the main categories of biomedical sensors are physical sensors and chemical sensors. Physical sensors can be geometric, thermal, mechanic, electric, hydraulic, and optic sensors. The special two types of physical sensors earn notice according to biomedical applications. The first type is the electrical body sensors (electrodes); they perform a unique function because of the diagnostic applications. For example, the ECG is the most known sensor of this type to read the heart electrical signal. Consequently, the following section will explain the ECG in detail [54].

The second physical sensor type is the optical sensor that collects body information by employing light. For example, the pulse oximeter measures the oxygen saturation (SpO2) for the human body blood. Chemical sensors can be gas, electrochemical, and photometric sensors. This work is not be concerned with chemical sensors [54].

2.2.1 Electrocardiograph

The ECG is the process of sensing the heart’s electrical signal over time. For different biomedical applications like heart rate measuring, unnormal diagnosing, biometric identification, and movement recognition, the ECG is an efficient non-invasive tool. So, this signal shows the heart functionality for the doctors to diagnose the CVDs. The field for ECG signal processing developed significantly because of the seriousness of CVDs according to the high percentage of death [2].

The normal and abnormal patterns can be identified in the ECG signal by the doctor. It is acquired from particular ECG electrodes placed at pre-knowing locations on the patient body called the lead. Different ECG leads are required to monitor different areas of the heart. The 12-lead are the standard, and the limb leads are used for many applications. The ECG lead I, II, and III are the standard primary limb leads. The lead I for the right with left arms, lead II for the right arm with left leg, lead III for the left arm with left leg, where $ECG_{II} = ECG_{I} + ECG_{III}$ [55]. Real-time or long-time monitoring systems are concerned with a single-lead ECG signal to allow the patients to have a natural life [10].

The electrical signals in the human body are not exceeded one volt, and the ECG range voltages are from 0.5 to 4 mV. These millivolts are collected from the skin using the electrodes. The ECG signal frequency ranges are from 0.01 to 250 Hz. As previously described, the ECG signal is collected from specific body locations using a pair of electrodes for electrical contact with the skin surface. The electrodes are of two types: foam pad (disposable) and reusable. For allowing the patients to have a natural life, the small comfortable foam pad disposable electrodes are applied to the patient body for a long time or real-time monitoring [55] [56].

The disposable foam pad electrodes are preferred in long term cardiac monitoring applications thus from reliability and patient comfort viewpoints. A disposable foam pad adhesive ECG electrode is depicted in Figure 2.2. A male snap provided for connecting the lead wire is the silver colored center in front. The rear side of the connector is pre-gelled. The adhesive on the white foam on the rear side helps the electrode to be held at a fixed position on the skin [55].

The moving average is one of the most common filters for ECG signal pre-processing because it is the easiest digital filter to understand and use. It is a simple Low Pass FIR (Finite Impulse Response), as shown in Equation (2.1) for right and left sided moving average window. In spite of its simplicity, the moving average filter is optimal for a common task: reducing random noise while retaining a sharp step response and removing the baseline wandering, as shown in Figure 2.3. This makes it the premier filter for time domain encoded signals [57].

Figure 2.2 The disposable foam pad electrode

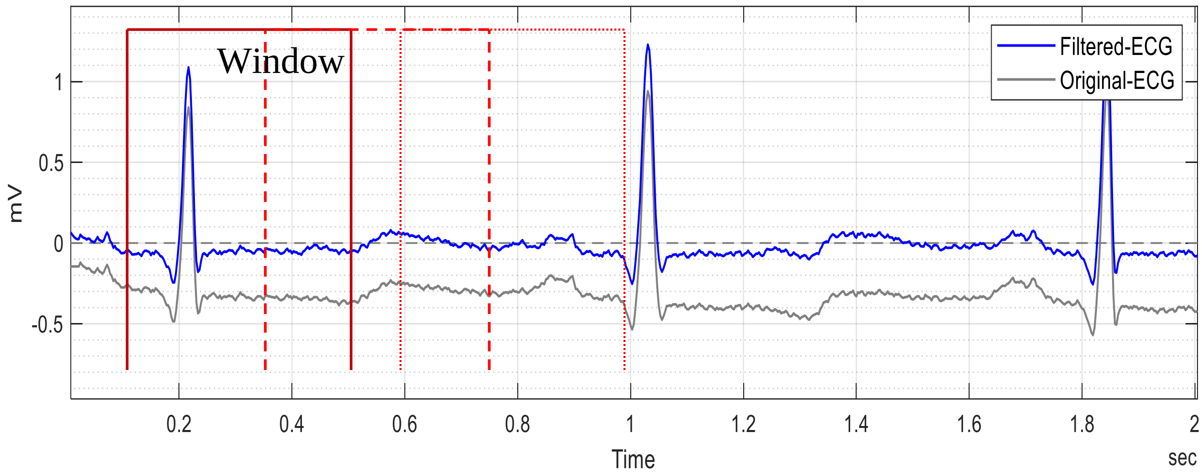

Figure 2.3 Filtering an ECG signal with moving average filter

$$FilteredSignal(n) = Signal(n) - \frac{1}{N} \sum_{i=-(N/2)}^{(N/2)} Signal(i+n) \qquad (2.1)$$

Where n: The sample number.

N: The number of samples for the filter window.

i: Index.

The typical cardiac cycle with a normal ECG signal is illustrated in Figure 2.4.. The heartbeat with normal rhythm consists of the waves P-QRS - T [2, 4, 5]. From the ECG cycle that is repeated continuously over time, the heart rate value can be calculated. Although each cycle is a heartbeat, the adult heartbeat range (heart rate) is from 60 to 100 heartbeats per minute for normal conditions. This value is variable according to different physiological conditions like stress, respiration, or age. Therefore, the heart performs unique patterns of electrical activity each time the cardiac muscles contract [55].

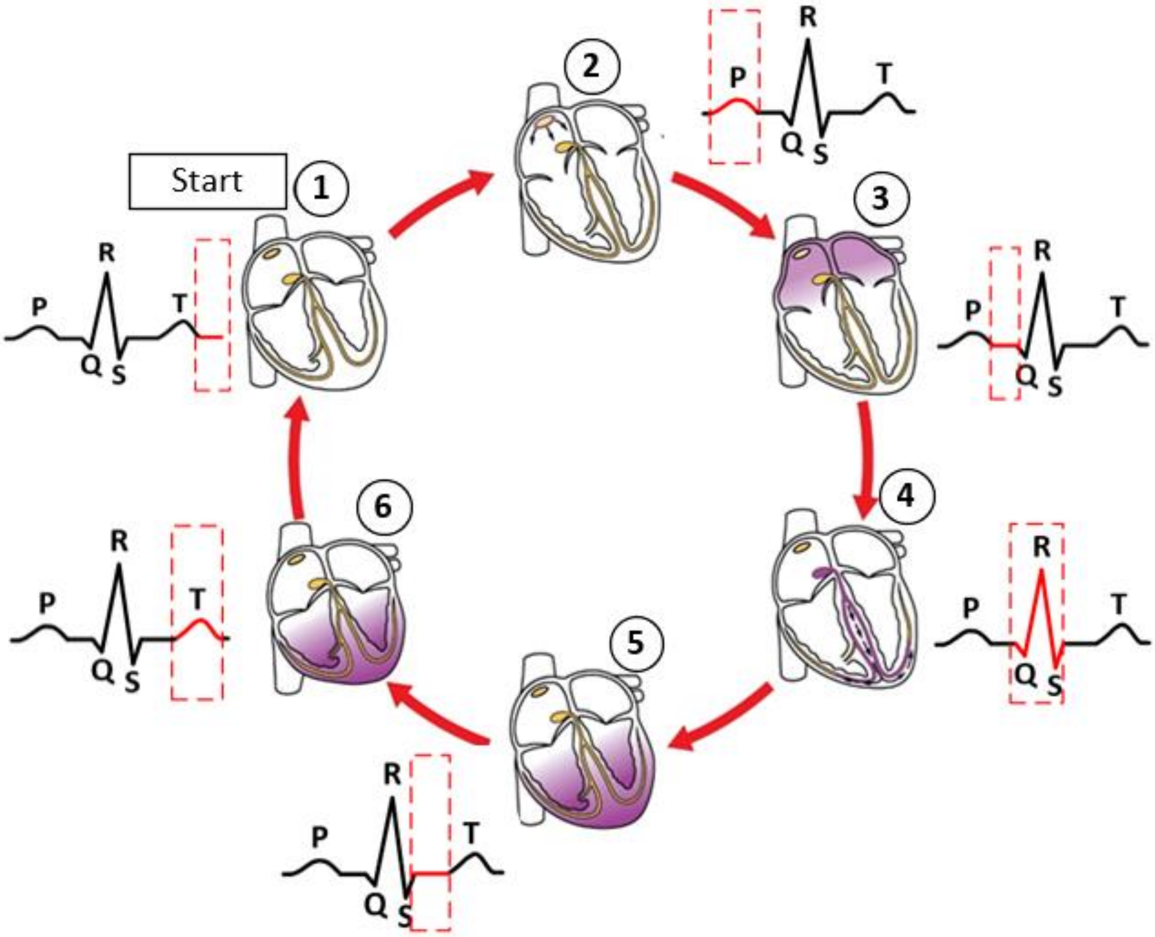

Figure 2.4 Cardiac cycle and ECG signal

The highest energy part for the ECG signal is the QRS-complex wave. Therefore, the QRS-complex detection is essential for most applications in ECG signal processing. However, the detection analysis is not easy because the noise affected the ECG signal and physiological variability for patients; moreover, the similarity between some cases of T wave with QRS-complex characteristics. Moreover, muscular noise, electrode motion effects, power-line interference, and baseline wandering are the noise sources that affect the ECG signals [6, 7].

After sensing, the ECG signal is pre-processing to reduce the noise and the artifacts. Therefore, the sensing stage consists of designing a corresponding filter for the specific ECG analysis applications. The filter improves the ECG wanted components based on frequency for the processing stage and reduces the influence of unwanted components. Then, one or more filters are utilized for the ECG signal with linear or nonlinear transformation to smooth the signal and reduce the noise. For real-time processing, the filters are applied to a window of samples [7].

The normal ECG rhythm is the regular class of normal heart activity. On the other hand, arrhythmia is (abnormal heart activity) too slow, too fast, or irregular heart activity. Arrhythmias main classes with the normal rhythm are:

1. Normal rhythm (N)
2. Supraventricular (S): Arrhythmias begin in the heart’s upper chambers (atria) with fast heart rate. Like Atrial flutter, Atrial fibrillation, and supraventricular tachycardia.
3. Ventricular (V): Arrhythmias begin in the heart’s lower chambers (ventricles). Fast heart rate. Like Ventricular tachycardia and Ventricular fibrillation.
4. Fusion (F): A hybrid complex beat combined from a supraventricular and a ventricular impulse.
5. Unknown (Q): the paced beats and unclassified beats are the unknown beats.

Arrhythmias are the most common causes of death among CVDs. Arrhythmias are a heartbeat abnormality with a too fast, too slow, or irregular rhythm and are detected and classified by ECG signals. So, accurate arrhythmias detection and classification have been of great concern in biomedical signal processing studies. [2-4].

The MIT-BIH arrhythmia database with variable ECG signals is used for testing and evaluating because it contains a variable ECG signal and noise. Furthermore, it is widely used from many other approaches for comparison purposes. This database contains 48 records with 30 minutes, two channels, 360 samples per second, and 11-bit resolution. In addition, the database contains positive and negative QRS, high and low QRS, baseline wander, power line interference, muscle noise, regular and irregular heartbeats, and normal and unnormal wave. All mentioned previously makes this database is suitable for evaluation reasons. Therefore, we used this database by taking the first ECG channel from the database [20].

The MIT-BIH arrhythmia database contains the primary arrhythmias classes in addition to the normal rhythm. Some of the ECG signals for this database from the specific records are summarized in figures (Figure 2.5 -Figure 2.9).

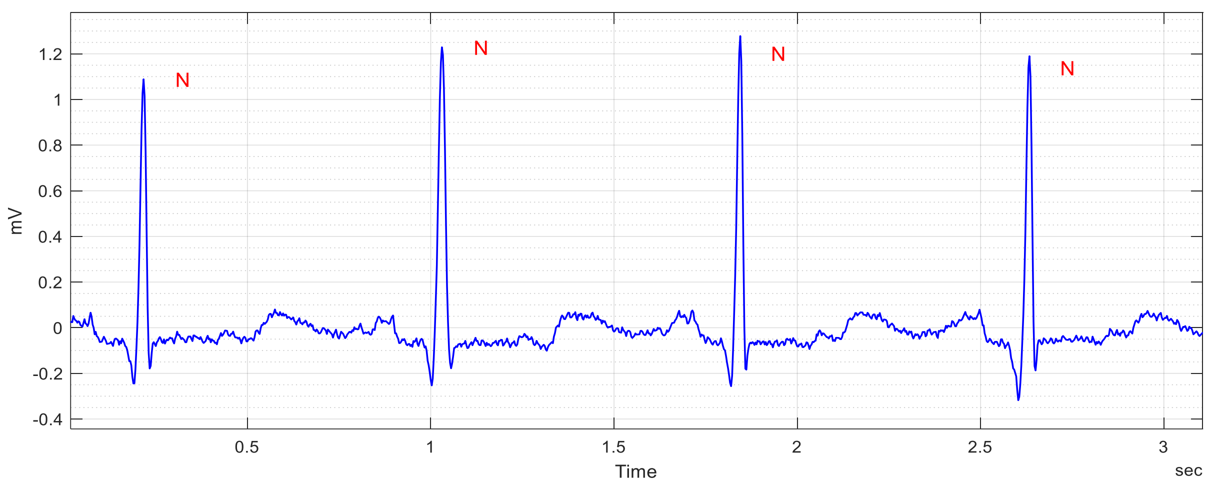

Figure 2.5 Normal rhythm from record 100

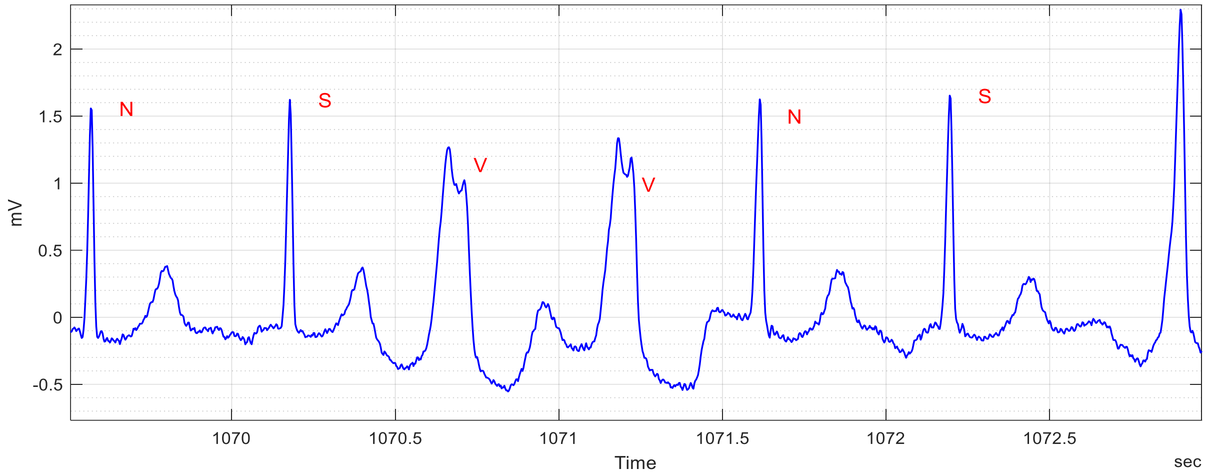

(a) Supraventricular premature from record 208

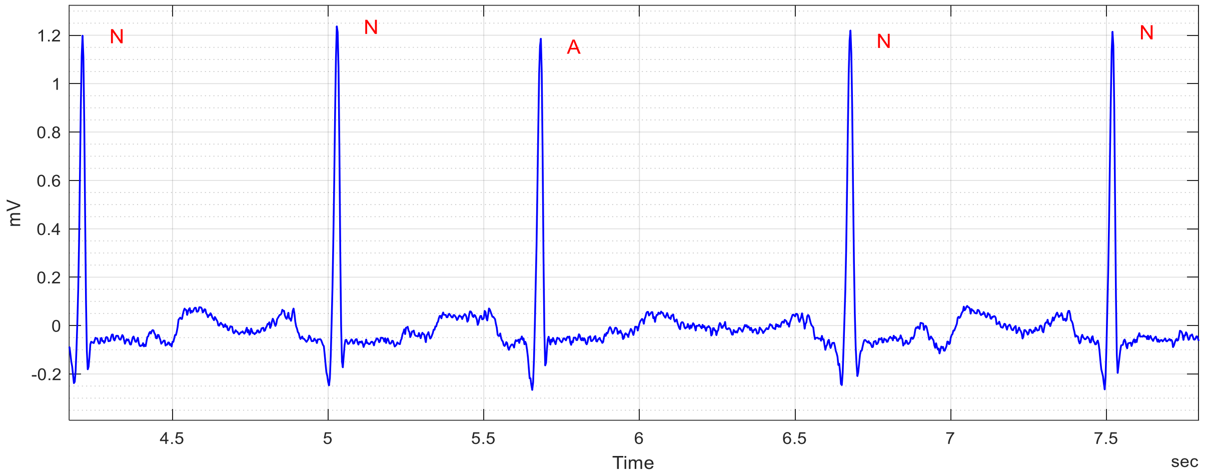

(b) Atrial premature from record 100

Figure 2.6 Supraventricular arrhythmia from records (a) 208 (b) 100

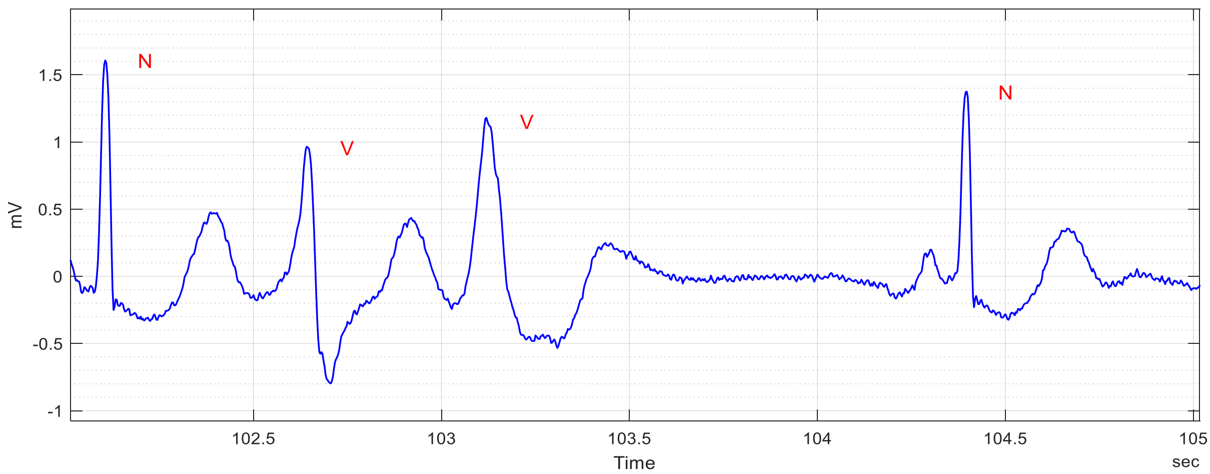

(a) Premature ventricular from record 207

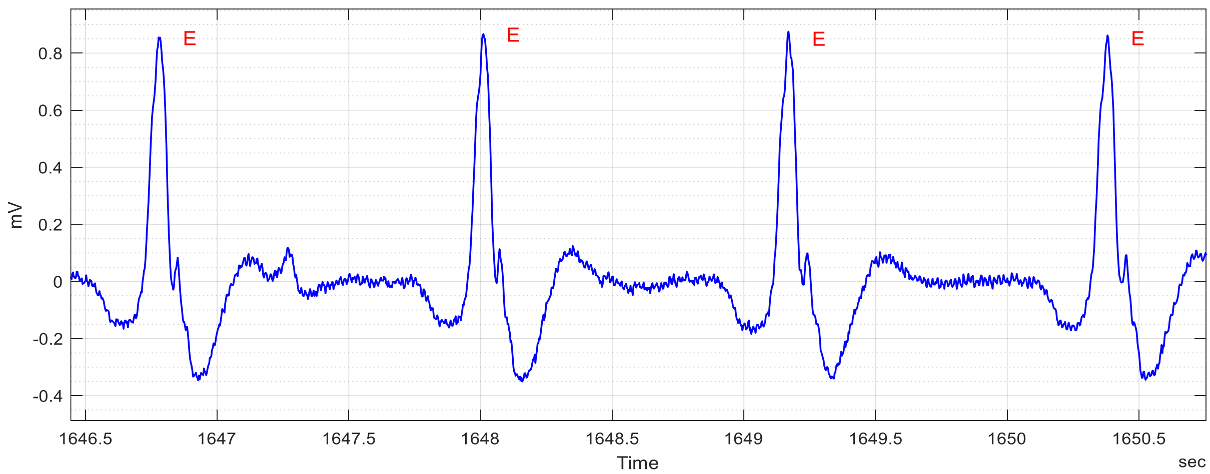

(b) Ventricular escape from record 207

Figure 2.7 Ventricular arrhythmia from record 207

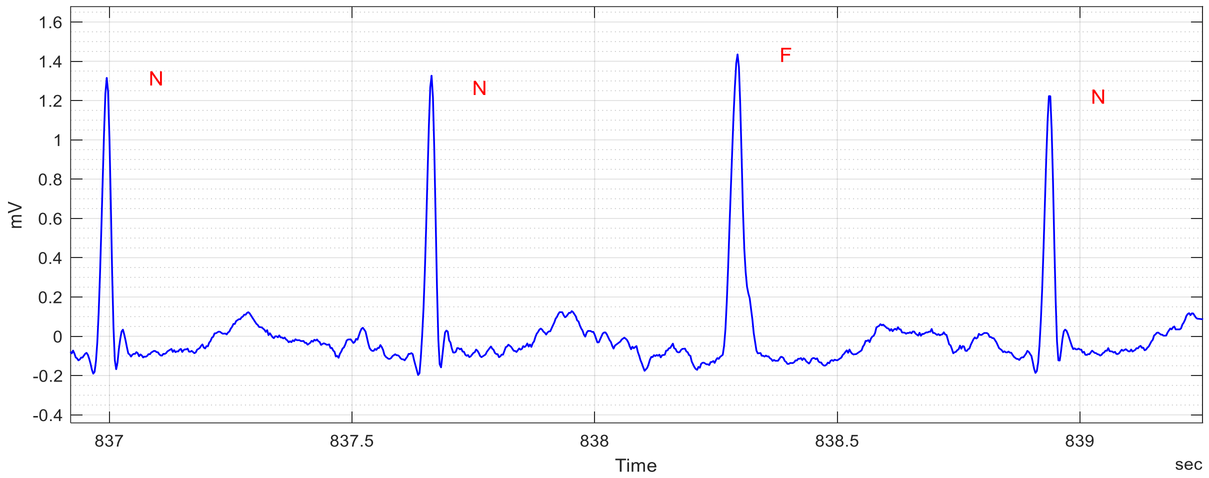

(a) Record 205

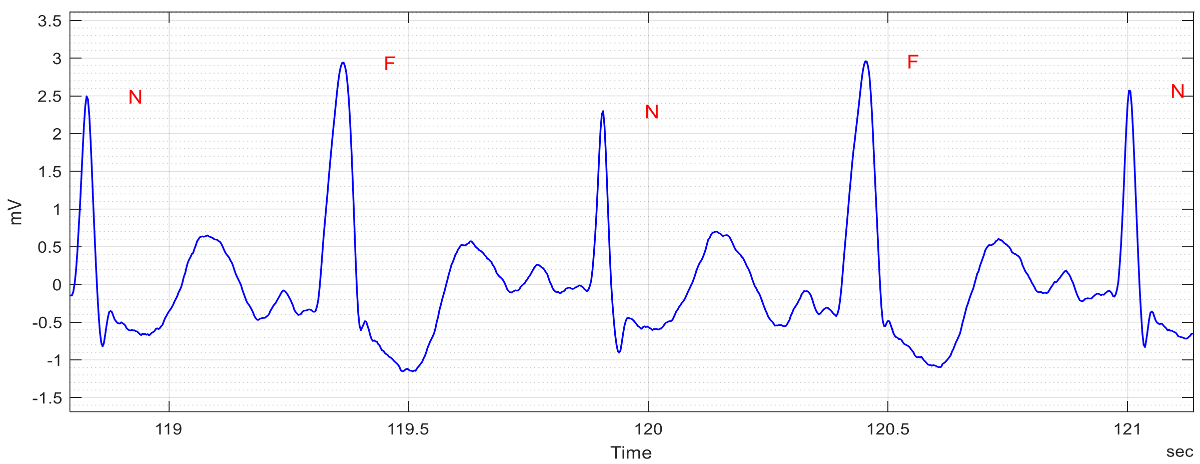

(b) Record 213

Figure 2.8 Fusion beat from records (a) 205 (b) 213

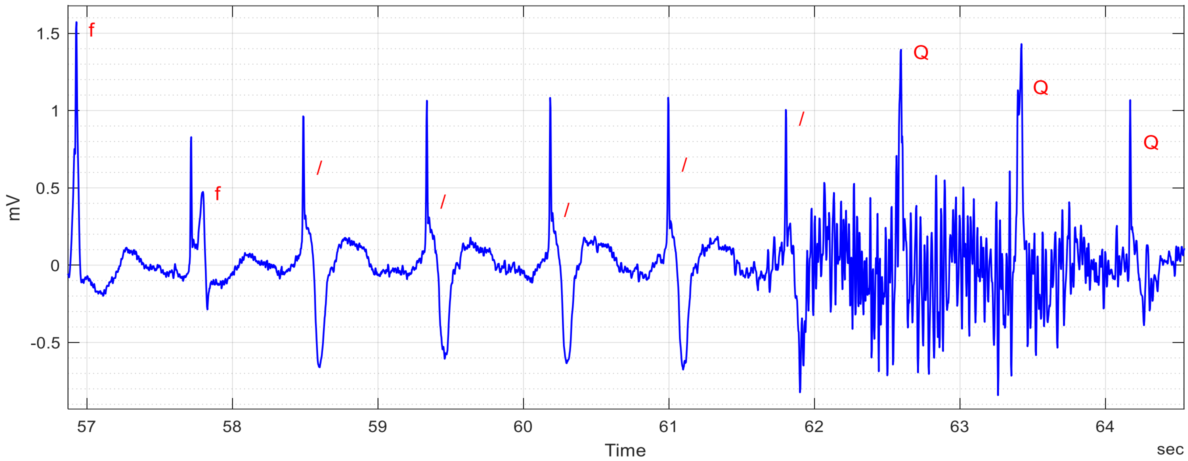

(a) record 104

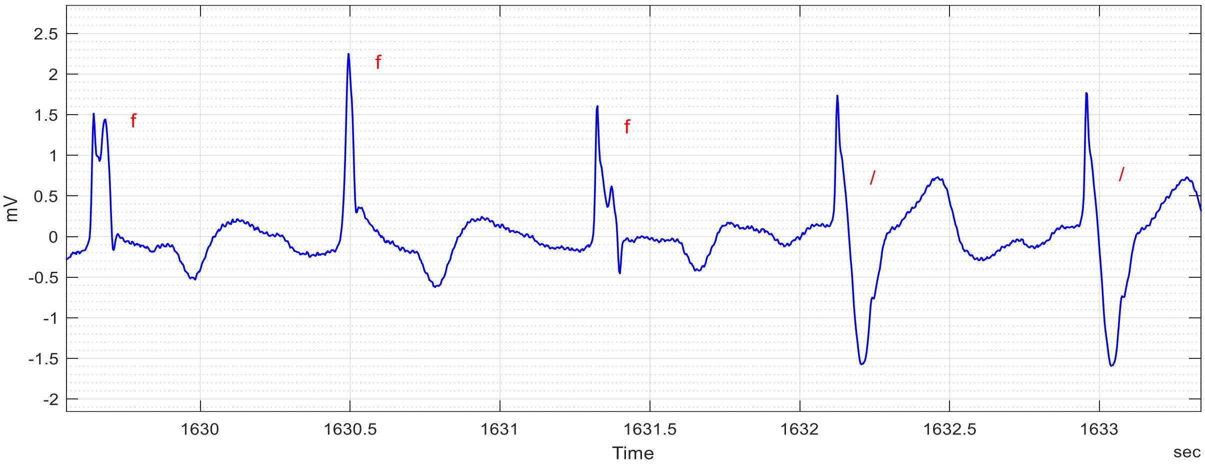

(b) record 217

Figure 2.9 Unknown beats from records (a) 104 (b) 217

2.3 Wearable System Processing

The second stage for the wearable system is processing the sensing data from the human. The microcontroller (MCU) or microprocessor performs the processing operation. The MCU will be described in the next subsection with processing techniques in ML such as ANN for ECG signals.

2.3.1 Microcontroller

The MCU is a single integrated circuit, and it contains a central processing unit (CPU), memory, buses, input/output, and clock. Many devices in different applications are utilized with the MCU. The typical MCU components are:

- CPU.
- RAM.
- ROM, EPROM, EEPROM, or flash memory.
- I/O interfaces.
- Clock generator.
- Analog-to-digital converters.
- Serial interfaces.

The MCU programming flexibility is the reason for integration with many applications. Small size, low cost, and low power consumption are the main constraints for the wearable system. These are features of the MCUs over many powerful and efficient processing units like field-programmable gate arrays (FPGA) and digital signal processors (DSP). Therefore, MCUs are processing the sensed signals in wearable systems and IoT applications. The programming languages for most MCU types are the assembly or C language [58].

The wearable system is the processing after collecting all data needed from the human body. In ECG signal processing, heartbeats detection is essential in most ECG applications. Furthermore, the classification of the heartbeat is an important topic in biomedical fields because it provides details regarding CVD [8]. Therefore, numerous studies for classification have been developed in recent decades. The ECG beats should be processed to find any cardiac anomalies. However, the long-time ECG signal processing from the hospital monitoring system or wearable healthcare for online monitoring is a big challenge for an individual, and it takes a very long time [9].

Automated arrhythmia classification provides excellent suitability for doctors and helps the patients for monitoring their conditions. Typically, it is not achievable in many regions because of financial and medical services issues.

Reducing the demand for physicians and care providers encourages the need for a low-cost, safe, and automatic framework for wearable healthcare monitoring devices [9]. On the other hand, real-time or long-time monitoring systems are concerned with a single-lead ECG signal to allow the patients to have a natural life [10]. There are many challenges for arrhythmia classification: the selected section may not show the arrhythmia, the ECG signal is not constant like the ECG signal variability depending on age or gender, large data may cause classification errors, and the noise for ECG signal [9].

2.3.2 Machine Learning

Heartbeat can be detected and classified from the ECG signal in a complex way because of the ECG signal variability and the noise with the artifact. As previously described in “Literature Review”, the processing operation for the heartbeat detection and classification based on ECG signal is utilized as one of the ML techniques included in the AI field. These techniques are:

- artificial neural network [34] [43],
- neural network ensembles [59],
- multilayer perceptron neural network [33],
- echo state network [10],
- empirical mode decomposition [37].
- short-term long memory with recurrent neural network [38],
- one-dimensional convolutional neural network [4, 40, 60],
- two-dimensional convolutional neural networks [42],
- deep neural networks [35],
- and deep-recurrent-neural-network with long short-term memory [36].

2.3.2.1 Artificial Neural Networks (ANNs)

ANNs are essential to machine learning ML techniques for classification and recognition problems such as heartbeat classification [14, 15]. ML is a part of Artificial Intelligence (AI) that makes computers for programming themselves according to the input data to solve a problem. It attempts to provide computers with cognitive abilities in order to train them to learn and solve issues like human brain intelligence. However, artificial intelligence cannot duplicate human intellect, but computers can only be taught to do certain human brain functions [16, 61, 62].

Researchers have discovered that unique mechanisms are founded on human brain intelligence based on decades of scientific and philosophical study. The brain operations are inspired to create machines for simulation of these mechanisms. On the other hand, AI systems are not integrated with all or most of the brain mechanisms. What was previously done in the name of advancing machine intelligence can now be attributed to the groundbreaking usage of so-called Artificial Neural Networks (ANNs) [16, 61, 62].

The brain is the complex and vital human part which is performed the human's overall functions as a central processing unit (CPU). It contains billions of neurons. A neuron is a cell that transmits nerve impulses (electrochemical signals) information. Thus, the brain is a complex neurons network that processes information by a complex connection of neurons. Until recently, it has been difficult to comprehend the brain processes, but with advances in computer technology, it can now build artificial neural networks [16].

The field of ML is a sub-discipline of AI that assists in teaching computers how to program themselves depending on the input data. Data-based issue resolution is possible with machine learning, which enables AI to make use of large datasets. In other words, ANNs are machine learning algorithms in action. The concept of the relationship between AI, ML, and ANN is as shown in Figure 2.10.

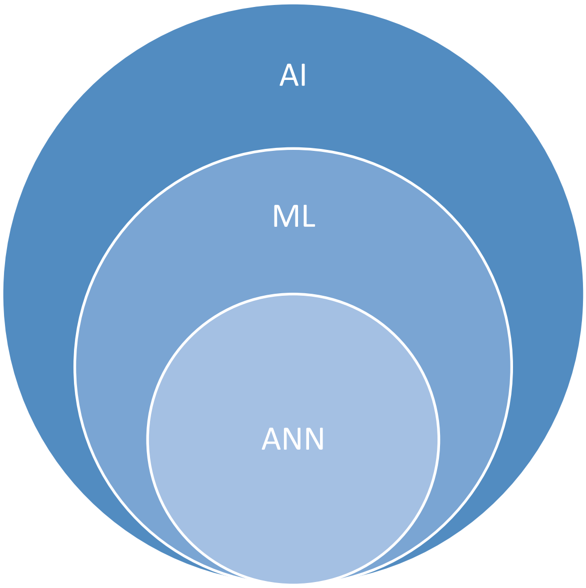

Figure 2.10 The AI, ML, and ANN

The term "deep learning" describes a sophisticated collection of neural networks with many layers of processing. For example, it is common for image recognition, image classification, and handwriting identification to employ models of this kind. The simple element for the neural networks that process the data is named neurons. It performs the summing, nonlinear mapping, and some cases as threshold units. The neurons are parallel operations and are organized in layers. Neurons are connected together through a weight value [16].

2.3.2.2 Inspiration for Neural Networks

The human brain is the inspiration for artificial neural networks. The brain processes the information through the neurons that are connected in a complex way. Therefore, the electrical signals are processing by the neurons networks in a logical operation. The simple neuron structure is illustrated in Figure 2.11.

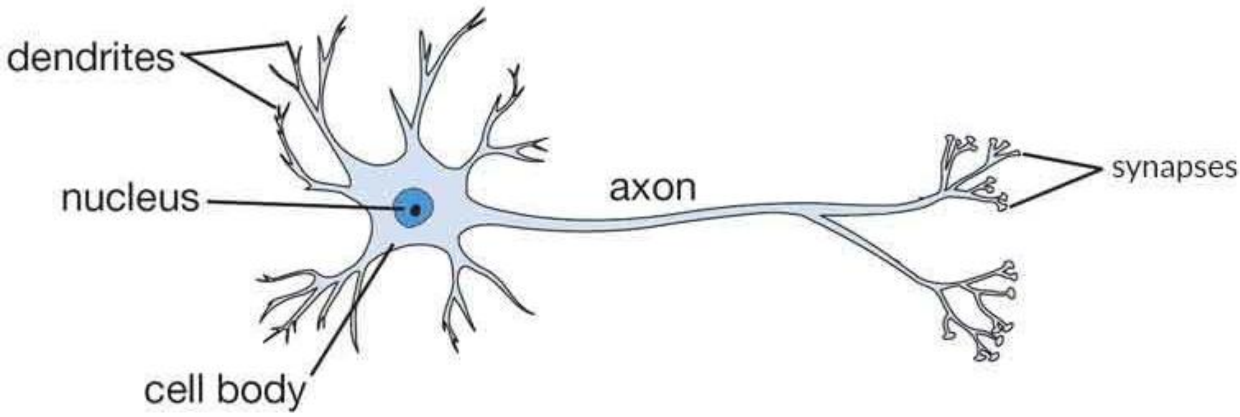

Figure 2.11 The neuron structure

The main parts of the neuron are:

- ***Dendrites*** are the input of the neuron that is connected to the axon of the other neuron.
- ***Cell body*** interprets the dendrite input and then uses this information to decide on an action.
- ***Axon*** is the output of the neuron that is connected to the dendrite of the other neuron.

The connection between axon and dendrite is called a synapse. It is the location of the neurons to transmit the signal to the adjacent neuron. Thus, the interconnection weight is in the synapse. The ANN is a huge parallel computing network that contains massive interconnections with simple processing operations.

The neurons are the central processing unit for the ANN as the biological neuron networks. It performs a simple mathematical operation from multi inputs to produces a single output. Each input and neurons connection have weight, and each neuron has a bias, so the output is the sum for the multi weighted inputs and the bias after a simple operation. The simple neuron operation is depending on a function called the activation function [16].

The following terms are associated with ANN:

- Input layer
- Hidden layer
- Output layer
- Weights
- Bias
- Activation functions

A single layer for multi inputs data is the first layer. Next, single-layer or multi-layers is processing the inputs data as middle layers. Finally, a single-output layer is an output for the ANN. The processing operation for the overall layers of the ANN is based on the weights, bias, and activation functions furthermore the network topology [16, 61, 62]. The architecture of a single hidden layer ANN is shown in Figure 2.12.

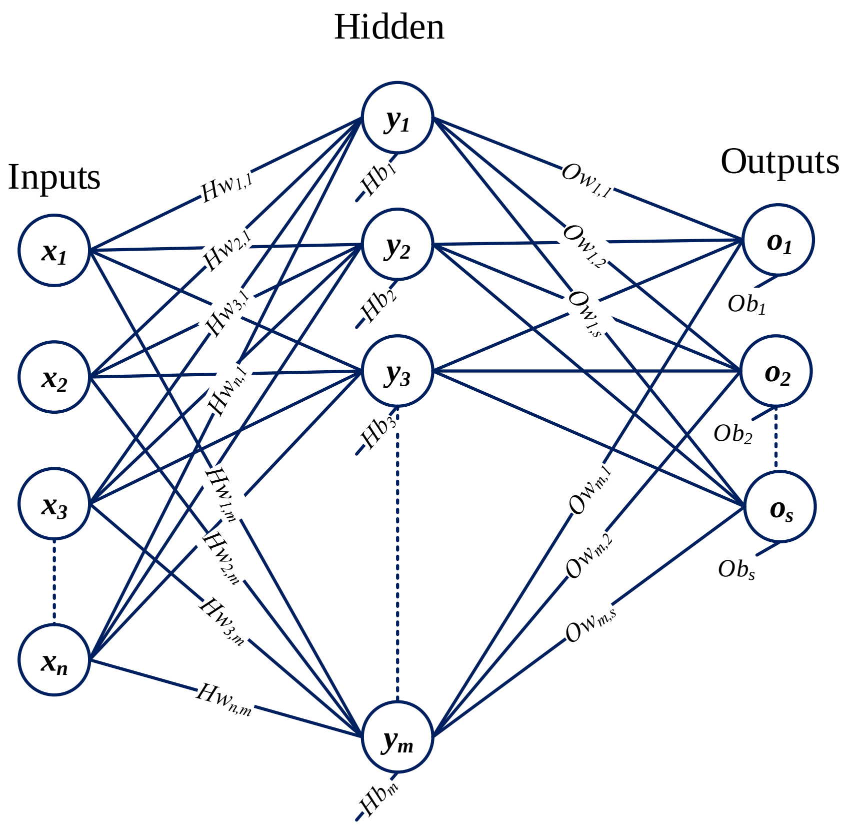

Figure 2.12 ANN with a single hidden layer

The neuron inputs are multiplied by values called weights, so each input is weighted by this value. So, the weights are weighted the neuron inputs. Thus, weights are the most important parameter for the ANN. The weights control how strongly one neuron influences the other. For a single neuron, the inputs (*x*), output (*y*), bias (*b*), and weights (*w*), Equation (2.2) is described ANN output. So, for a single neuron with multi inputs, multi weights (each input has a weight), single output, and single bias. The summation operation for the inputs and weights is simple matrix multiplication [62].

$$y_j = f\left(b_j + \sum_{i=1}^{n}(x_i \times w_i)\right) \qquad (2.2)$$

Where *b*: the neuron bias

f: Activation function

x: the input

w: the neuron weight

y: the output for the neuron

n: the total number of inputs for the neuron

The bias is the value to adjust the neuron output with the weighted inputs before the activation function. For example, for multi hidden layers network, the output for the first hidden layer will be the input for the second hidden layer and so on [16, 61, 62]. The general neuron model is illustrated in Figure 2.13

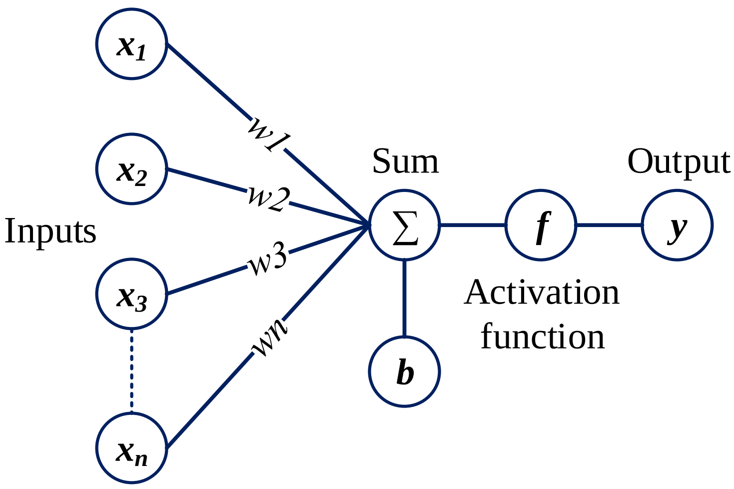

Figure 2.13 General model of ANN

The critical component of neural network architecture is the activation function. The selection of the activation functions may significantly affect network performance and capabilities. So, the neural network applied variable activation functions for each network layer. The neural network applied variable activation functions for each network layer. The hidden layer's activation function controls how effectively the neural network learns. The output layer's activation function defines the classes to be classified. The activation functions applied include threshold, hard limiter, sigmoid, Hyperbolic Tangent (Tanh), Rectified Linear Unit (ReLU), and piecewise linear [62]. Different types of activation functions will be described with figures and equations in Table 2.1.

Table 2.1 Activation functions

Plot	**Name and Function**	
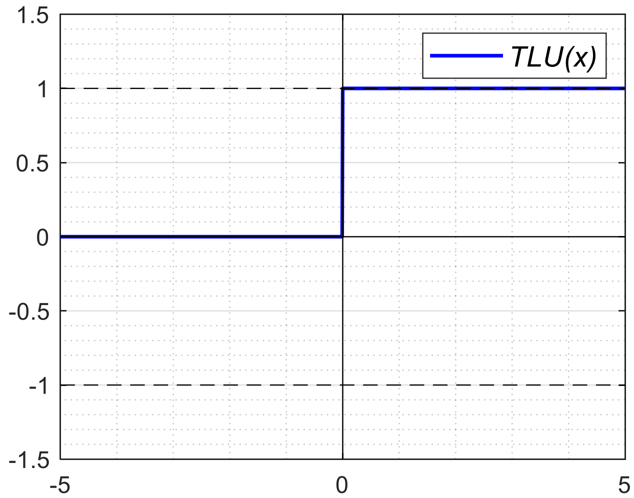	Name: Threshold Logic Unit (TLU)	
	Function: $y = \begin{Bmatrix} 1 & x > 0 \\ 0 & x \leq 0 \end{Bmatrix}$	(2.3)

<table>
<tr><td rowspan="2">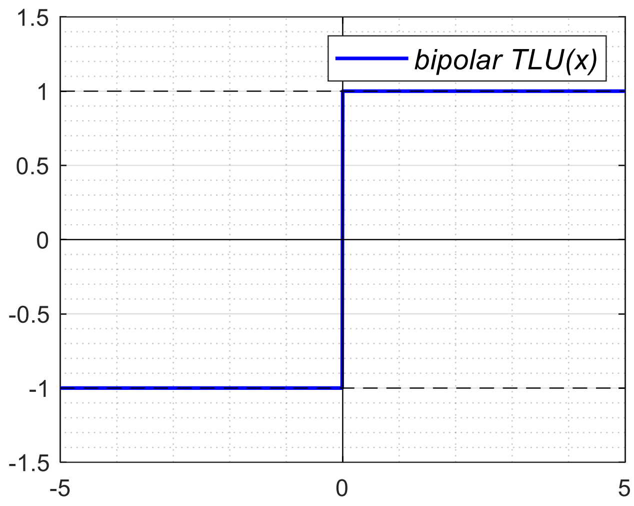
</td><td colspan="2">Name:
Bipolar Threshold Logic Unit
(TLU)</td></tr>
<tr><td>Function:
$y = \begin{Bmatrix} 1 & x > 0 \\ -1 & x \leq 0 \end{Bmatrix}$</td><td>(2.4)</td></tr>
<tr><td rowspan="2">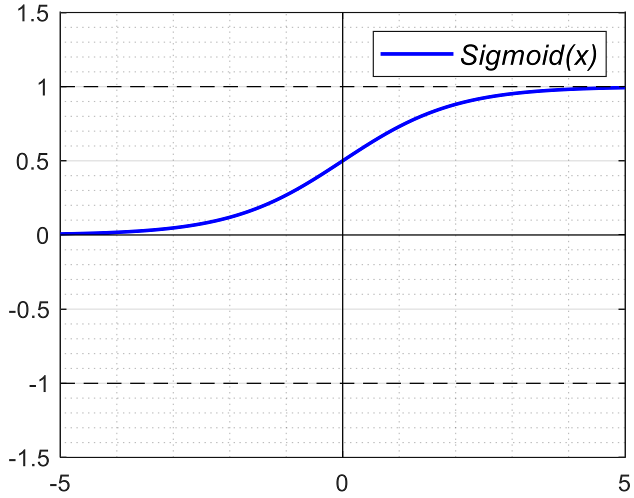
</td><td colspan="2">Name:
Sigmoidal</td></tr>
<tr><td>Function:
$y = \frac{1}{1 + e^{-x}}$</td><td>(2.5)</td></tr>
<tr><td rowspan="2">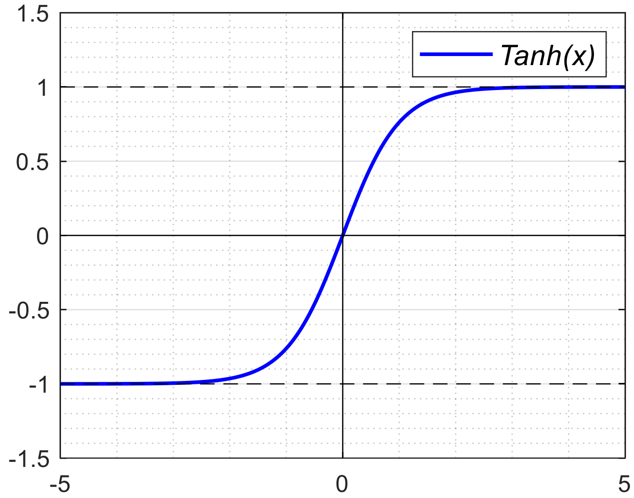
</td><td colspan="2">Name:
Hyperbolic Tangent (Tanh)</td></tr>
<tr><td>Function:
$y = Tanh(x)$
$= \frac{e^{x} - e^{-x}}{e^{x} + e^{-x}}$</td><td>(2.6)</td></tr>
</table>

<table>
<tr><td rowspan="2">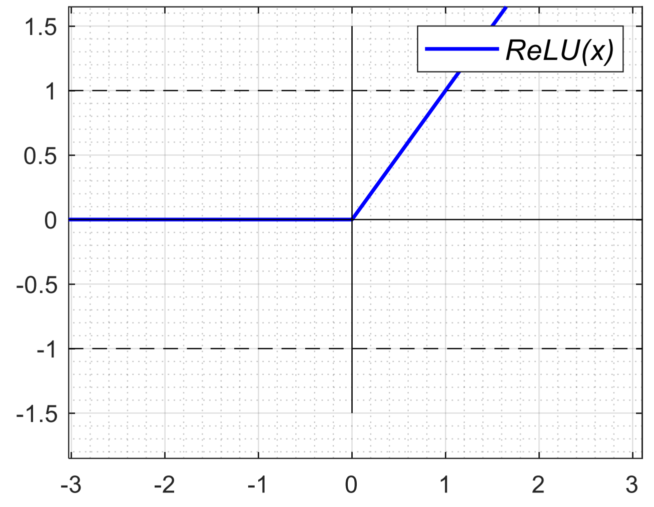
</td><td colspan="2">Name:
Rectified Linear Unit (ReLU)</td></tr>
<tr><td>Function:
$$y = \begin{Bmatrix} x & x > 0 \\ 0 & x \leq 0 \end{Bmatrix}$$</td><td>(2.7)</td></tr>
</table>

2.3.2.3 Training

Training the network is to adjust (modify) the weights and biases for each layer in the network to perform a particular task with more performance using two main methods called supervised learning and unsupervised learning [16]. ANN can be designed using network growing based on trial and error [63, 64],

a. Supervised learning

The network is training by inputs and the desired output for these inputs. According to the network response, the weights of each layer are adjusted to approximate actual and desired outputs [16, 61, 62]. Supervised learning is illustrated in Figure 2.14.

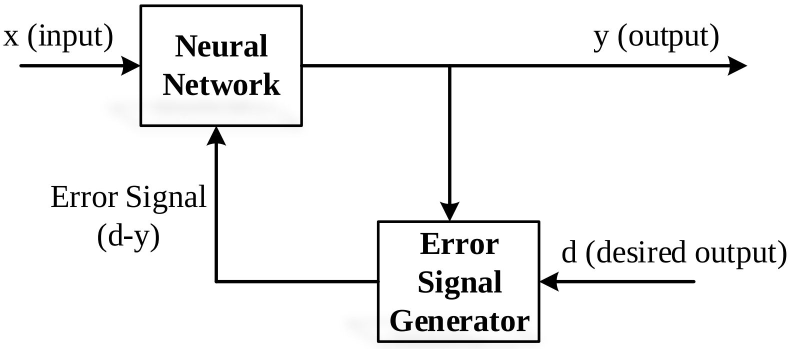

Figure 2.14 supervised learning

b. unsupervised learning

The network is training by inputs only. According to these inputs, the network evaluates the weights for each layer to produce the same output for the trained inputs. This operation occurs without any external assistance based on the inputs only [16, 61, 62]. Unsupervised learning is illustrated in Figure 2.15.

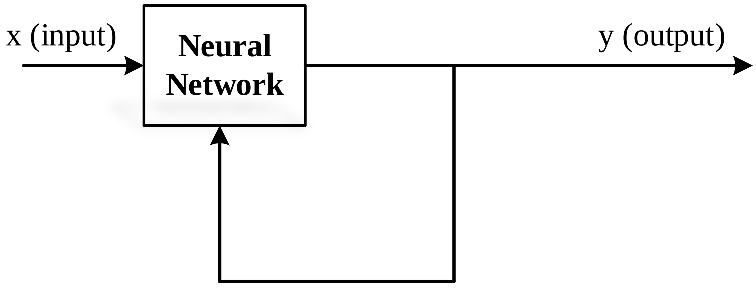

Figure 2.15 unsupervised learning

2.3.2.4 Feedforward and backpropagation

a. Feedforward

The Feedforward propagation is the data flowing from the inputs to the output through the hidden layers. The processes for each layer are calculated using Equations (2.8)-(2.11) to evaluate the output from the inputs, weights, biases, and activation functions. The neural network can have one or more hidden layers according to the network design.

b. Backpropagation

The activation function partial derivatives for all neurons are used to determine the gradient for weights in the backpropagation direction. Thus, the backpropagation process starts from the output to the inputs through the hidden layers. For every weight change, the gradient predicts how quickly the error will be decreased or increased. During backpropagation, the weights are adjusted until the error is reduced to the point where it matches the learning rate [16, 61, 62].

The feedforward and update weights and biases are included in the backpropagation algorithm. The activation functions can be used in the standard backpropagation algorithm given here [61]. The algorithm is as follows:

The backpropagation algorithm

Step 0. Initialize weights. (Set to small random values).

Step 1. While stopping condition is false, do Steps 2-9.

Step 2. For each training pair, do Steps 3-8.

Feedforward:

Step 3. Each input unit (x_i , $i = 1, \ldots , n$) receives input signal x; and broadcasts this signal to all units in the next layer (the hidden units).

Step 4. Each hidden unit (y_j , $j = 1, \ldots , m$) sums its weighted input signals,

$$y_{net(j)} = Hb_j + \sum_{i=1}^{n} \left(x_i \times Hw_{i,j} \right) \tag{2.8}$$

applies its activation function to compute its output signal, (for the tanh activation function applying Equation (2.6))

$$y_j = f\left(y_{net(j)} \right) \tag{2.9}$$

and sends this signal to all units in the next layer (output units).

Step 5. Each output unit (o_l, $l = l, \ldots , s$) sums its weighted input signals,

$$o_{net(l)} = Ob_l + \sum_{j=1}^{m} \left(x_j \times Ow_{j,l}\right) \tag{2.10}$$

applies its activation function to compute its output signal,

$$o_l = f\left(o_{net(l)}\right) \tag{2.11}$$

Backpropagation:

Step 6. Each output unit (o_l, $l = 1, \ldots, s$) receives a desired (target) d_l pattern corresponding to the input training pattern o_l, computes its error information term ,

$$O\delta_l = (d_l - o_l) f'\left(o_{net(l)}\right) \tag{2.12}$$

calculates its weight correction term (used to update O$w_{j,l}$ later),

$$\Delta Ow_{j,l} = \alpha \times O\delta_l \times y_j \tag{2.13}$$

calculates its bias correction term (used to update Ob_l later),

$$\Delta Ob_l = \alpha \times O\delta_l \tag{2.14}$$

and sends $O\delta_l$ to units in the previous layer.

Step 7. Each hidden unit (y_j, $j = 1, \ldots, m$) sums its delta inputs (from units in the next layer),

$$H\delta_j = \sum_{l=1}^{s} O\delta_l \times Ow_{j,l} \tag{2.15}$$

multiplies by the derivative of its activation function to calculate its error information term,

$$\delta_j = H\delta_j \times f'\left(H\delta_j\right) \tag{2.16}$$

calculates its weight correction term (used to update $Hw_{i,j}$ later),

$$\Delta Hw_{i,j} = \alpha \times \delta_j \times x_i \tag{2.17}$$

and calculates its bias correction term (used to update Hb_j later),

$$\Delta Hb_j = \alpha \times \delta_j \tag{2.18}$$

Update weights and biases:

Step 8. Each output unit (o_l, $l = 1, \ldots, s$) updates its bias and weights ($j = 1, \ldots, m$):

$$Ow_{j,l}(new) = Ow_{j,l}(old) + \Delta Ow_{j,l} \tag{2.19}$$

Each hidden unit (y_j, $j = 1, \ldots, m$) updates its bias and weights ($i = 1, \ldots, n$):

$$Hw_{i,j}(new) = Hw_{i,j}(old) + \Delta Hw_{i,j} \tag{2.20}$$

Step 8. Test stopping condition

Where

i: 1, 2, ……n no. of inputs (features)

j: 1, 2, ……m no. of hidden neurons

l: 1, 2, ……s no. of output neurons

α: learning rate

x_i: input layer from ($i=1$,…., n)

y_i: hidden layer from ($j=1$,…., m)

o_i: output layer from ($l=1$,…., s)

d_l: desired (target) output from ($l=1$,…., s)

$Hw_{i,j}$: hidden layer weights

$Hb_{i,j}$: hidden layer biases

$Ow_{i,j}$: output layer weights

$Ob_{i,j}$: output layer biases

$y_{net(j)}$: hidden layer net

$o_{net(l)}$: output layer net

$O\delta_l$: output error information term

$\Delta Ow_{j,l}$: output weight correction term

ΔOb_l: output bias correction term

$H\delta_j$: hidden error information term

$\Delta Hw_{j,l}$: hidden weight correction term

ΔHb_j: hidden bias correction term

f: the activation function

f': the activation function derivative

2.3.2.5 Classification

ANNs are essential to machine learning ML techniques for classification and recognition problems such as heartbeat classification. The classification is a concept for supervised learning, classifies a collection of data into predefined groups or classes. The classification approach is solved many complex computing problems, such as face detection, speech and handwriting recognition, and emails spam. The classification can be one of the following types [16, 65, 66]:

- Binary: to classify a binary class for two problems classes called binary classification, like (yes or no) and (true or false) problems.
- Multi-class: to classify multiple classes for more than two classes for the same type called multi-class classification, like face detection for a specific face from multiple faces.
- Multi-Label: to classify multiple label classes for two or more than two label classes called multi-label class classification, like image object detection for a specific object from the same image.

2.3.2.6 Confusion Matrix

The confusion matrix is the summarized results that are shown in a table for the classification method. The true classes and the predicted classes are the axes of the confusion matrix. For these axes, there are numbers of values corresponding to the number of the classification classes. So, the confusion matrix for the binary classification has two by two matrix, as shown in Figure 2.16. For example, the first class is named positive, and the second one is named negative. The columns present the true classes, and the rows present the predicted classes. This table is filled with results values for the classification operation [16, 65, 66].

TruePositive (TP) is the right prediction for the positive-class; the positive is predicted as positive.

TrueNegative (TN) is the right prediction for the negative-class; the negative is predicted as negative.

FalsePositive (FP) is the wrong prediction for the positive-class; the positive is predicted as negative.

FalseNegative (FN) is the wrong prediction for the negative-class; the negative is predicted as positive.

		True classes	
		Positive	Negative
Predicted classes	Positive	TP	FP
	Negative	FN	TN

Figure 2.16 Binary classification confusion matrix

Table 2.2 The Parameters effects for the classification performance

Parameters	Better classification
TP	↑
FP	↓
FN	↓
TN	↑

In machine learning, the classification results in the confusion matrix evaluate the method performance because the confusion matrix describes and summarizes the classification results in a simple and efficient way. Therefore, the performance is evaluated by the following measures from the confusion matrix parameters [65, 66]:

- Accuracy (Acc): the ratio for the correct prediction to the overall prediction. It measures the classification performance for the overall classes.

$$Acc\,\% = \frac{TP + TN}{TP + TN + FP + FN} \times 100 = \frac{Correct}{Total} \times 100 \quad (2.21)$$

- Sensitivity (Se): the ratio of the all right positive prediction was right predicted as positive. Also called True Positive Rate (TPR) or recall. It measures the classification performance for one class (positive).

$$(Se)\% = \frac{TP}{TP + FN} \times 100 \quad (2.22)$$

- Positive_Predicitvity (PP): the ratio of the right positive prediction to the total positive prediction. Also called precision. It measures the classification performance for one class (positive).

$$(PP)\% = \frac{TP}{TP + FP} \times 100 \quad (2.23)$$

- Detection_Error_Rate (DER): the ratio of the all wrong prediction to the total true positive. It measures the classification performance for one class (positive).

$$(DER)\% = \frac{FP + FN}{TP} \times 100 \qquad (2.24)$$

Table 2.3 The measures effects for the classification performance

Measures	Better classification
Acc	↑
Se	↑
PP	↑
DER	↓

For multi-class classifiers, the confusion matrix of the 3-class classification is shown in Figure 2.17. The three classes are class A, B, and C. So, the AA is the true A as predicted A (true A), the AB is true A as predicted B (false B), the BA is true B as predicted A (false A), BB is the true B as predicted B (true B), and so on.

The parameters TP, TN, FP, and FN for the three classes can be calculated by each class individually. For example, for class A, the confusion matrix parameters can be calculated as follows. The performance measures can simply calculate from these parameters.

$$TP = AA$$

$$TN = \mathrm{BB} + \mathrm{CB} + \mathrm{BC} + \mathrm{CC}$$

$$FP = \mathrm{BA} + \mathrm{CA}$$

$$FN = \mathrm{AB} + \mathrm{AC}$$

		True classes		
		A	B	C
Predicted classes	A	AA	BA	CA
	B	AB	BB	CB
	C	AC	BC	CC

Figure 2.17 Three class classification confusion matrix

2.4 Wearable System Connection based on IoT

Wearable devices connect through a network to the internet for monitoring and controlling in the way of the Internet of Things (IoT). IoT refers to technology, standards, and programs that vary widely used for many applications. The basic concept, things are connected in a network through the internet. The things are objects with IoT devices connected to the internet, as shown in Figure 2.18. The core concepts and ideas of IoT are based on both data and things. With electrical components and software, IoT devices and assets may receive, sort, and share data [67].

Figure 2.18 The IoT concept

A network of things is connected through wired or wireless to collect, control, and transfer data; these things are any physical devices that can connect. IoT is enhanced human life at home or work by integrating with other devices through the internet, such as wearable devices, phones, computers, cars. The worldwide number of devices connected to IoT is growing exponentially. The advanced technologies in electronics, communication, ML, AI, and IoT lead to connecting devices like computers, smartphones, and wearables to other devices that were not connected to the internet to monitor and control [67].

The IoT can be achieved from four main parts: devices, connection, process, and user interface [67]:

- The devices are collecting the data from the surrounding by sensors. These sensors are sensing simple and complex data according to the applications. A single sensor or multiple sensors are used for each device. For example, multiple sensors like GPS, camera, accelerometer, fingerprint, proximity, and heart rate are inside the smartphone to collect the data for many reasons to improve the mobile benefit.

- These devices are connected through wired or wireless networks like Wi-Fi, Bluetooth, mobile, LAN, and Ethernet. The networks with different properties, such as range, data rate, and power consumption, are the IoT designer's selecting constraints.
- The collecting data are stores and processed after or before transmission. The process can be inside the device before transmission for low computation algorithms or for low data rate networks. In contrast, it can be on the cloud after the transmission for high computational complex algorithms. So, the data process is performed using techniques like simple mathematical operations or AI systems.
- The user interface is the last part for the IoT systems to display or control the collecting data after the process. The data can be displayed using text messages, email, or other mobile or computer IoT applications. In addition, the IoT system can control the devices automatically or manually based on the process operation.

The IoT systems are dominated by many applications such as smart homes, wearables, Smart Cities, Transportation, and Medical and Healthcare. For example, the IoT devices advantage like smart healthcare systems assist doctors in monitoring patients in a real-time or long-time way. Therefore, the monitoring process for some cases can be at home to reduce the cost for patient monitoring inside the hospital [67].

IoT technology is widely used in healthcare since it is a crucial part of delivering good health. Doctors may use the Internet of Things to assist patients. Ageing patients may benefit from health monitoring systems that are both simple and small since they can decrease the distance between them and the doctor. The healthcare industry will greatly benefit from the IoT since it enables the doctor to target every patient individually, collect their health data, and then prescribe each patient with their unique treatment strategy. Healthcare providers may monitor patients' vital signs in real-time with assists of wearable devices. However, these devices are required a continuous connection to the internet [67].

The IoT and AI technologies coordination is leading to better healthcare services. With these advanced tools, it is feasible to track and study various diseases and processes in detail. Bringing together experience from personal and professional life while using modern diagnostics, collecting, and analysis techniques will benefit the medical field [67].

As mentioned before, variable wireless technologies are utilized to provide support for the many application areas of wearable devices like Wi-Fi and Bluetooth. One of the most widely used communication standards is Wireless Fidelity (Wi-Fi) which is used for large scale applications in different areas. The IEEE standard is 802.11, working at 2.4 GH and 5 GH with a 6-600 Mbps data rate, summarized in Table 2.4. The Wi-Fi has a large domain, high data rate and can be integrated with many systems [68].

The technology of wireless networking Wi-Fi allows devices like computers, smartphones, wearable, and other compatible devices to access the internet. Moreover, these devices can be connected with each other to transfer the data between devices. A wireless router is used to connect to the internet. When the device connects to Wi-Fi, it connects to a wireless router connecting Wi-Fi-enabled devices to the Internet [68].

The internet of things (IoT) play a significant to improve many applications; healthcare applications are at the top of these applications [11]. On the other hand, this field seems to be saturated because many methods are proposed. Despite that, the development of wearable devices and the healthcare system make a new challenge to increase the algorithm efficiency, performance, and portability [6, 12]. Moreover, it reduces memory storage and transmits low-rate data for wearable devices [7]. Many advanced techniques and tools are still not used for future improvement [13].

The technology of wearable devices has attracted the attention of academics and healthcare providers over the past years. The reasons for wearable device development are due to the enormous advantages such as real-time or long-time home monitoring [18]. Moreover, the wearable devices technological progress made in communication like IoT and electronics like the reliable microcontrollers. Since the IoT features, it is a promising technology for many applications; one of these applications is healthcare to improve the quality of life and save human life. The IoT is a new context of modern wireless telecommunications based on interaction and cooperation using a unique address between various objects like sensors, actuators, devices, etc., for common goals. Therefore, healthcare application is one of the most applications which playing the leading roles in the near future for the IoT [19].

Table 2.4 Some Wi-Fi generations

Standard	**Frequency** GHz	**Max Data rate** Mbit/s	**Modulation**	**Adopted**
802.11	2.4	2	DSSS	1997
802.11b	2.4	11	DSSS	1999
802.11a	5	54	OFDM	1999
802.11g	2.4	54	OFDM	2003
Wi Fi 4 (802.11n)	2.4/5	600	OFDM &MIMO	2008

The advantages of Wi-Fi are wireless ethernet, extended access, cost reduction, mobility, and flexibility. In addition, many devices are integrated with Wi-Fi in different applications such as control and process devices for industrial, emergency and disaster monitoring, mobile tracking, surveillance cameras, and other devices communication [68].

Chapter 3: Design the Proposed Smart Wearable System and Its Implementation

Contents

Chapter Three:
Design the Proposed Smart Wearable System and Its Implementation

3.1 Introduction

This chapter presents the thesis objectives as shown in the block diagram depicted in Figure 3.1. Each objective will be described in this chapter subsection. This figure will be in front of each subsection to indicate the corresponding objective for this subsection. The objectives are integrated by each other to achieve the aim of this work. The aim is to develop a high accuracy real-time low computational wearable healthcare system based on AI and IoT for heartbeats detection and classification. In addition, research papers have been published or have been accepted for publishing after accomplishing the main specific objectives.

To achieve the thesis aim: ***First,*** a CDS prototype wearable system for heartbeats detection and classification using Node-MCU with IoT is implemented based on the proposed QRS-detection algorithm (2), the verified heartbeats (3), and classification method for the 5-classes (5). ***Second,*** a QRS-detection algorithm based on low error detection, high accuracy, and low computation is designed. ***Third,*** the heartbeats number of the MBADB is standardized after developing a MATLAB Waveform Database Toolbox (WFDB) new function. So, the heartbeats are detected and evaluated based on the standard number. The detected heartbeats will be used in the next objectives for classification. ***Fourth,*** a low computation and high accuracy classification method for normal and abnormal heartbeats is developed based on new mixed and reused features. ***Fifth,*** a high accuracy classification method for the 5-AAMI classes heartbeats according to a novel method named Selective-Mask Artificial Neural Network (SMANN) for low computational application is designed.

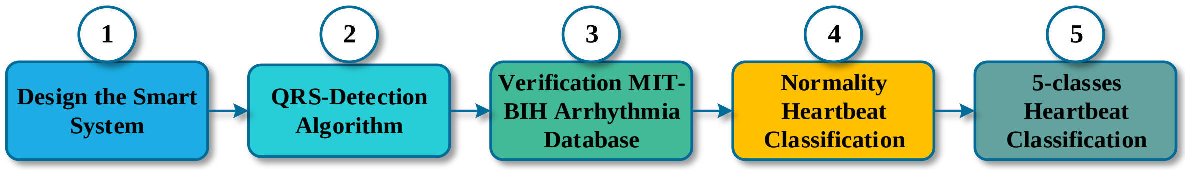

Figure 3.1 Research Objectives

3.2 Design and Implementation of Smart Wearable System based on IoT

A wearable system is designed and implemented after the software evaluation using the Node-MCU and the same database to evaluate the resources, speed, and performance. The overall proposed wearable system based on IoT is shown in Figure 3.2.

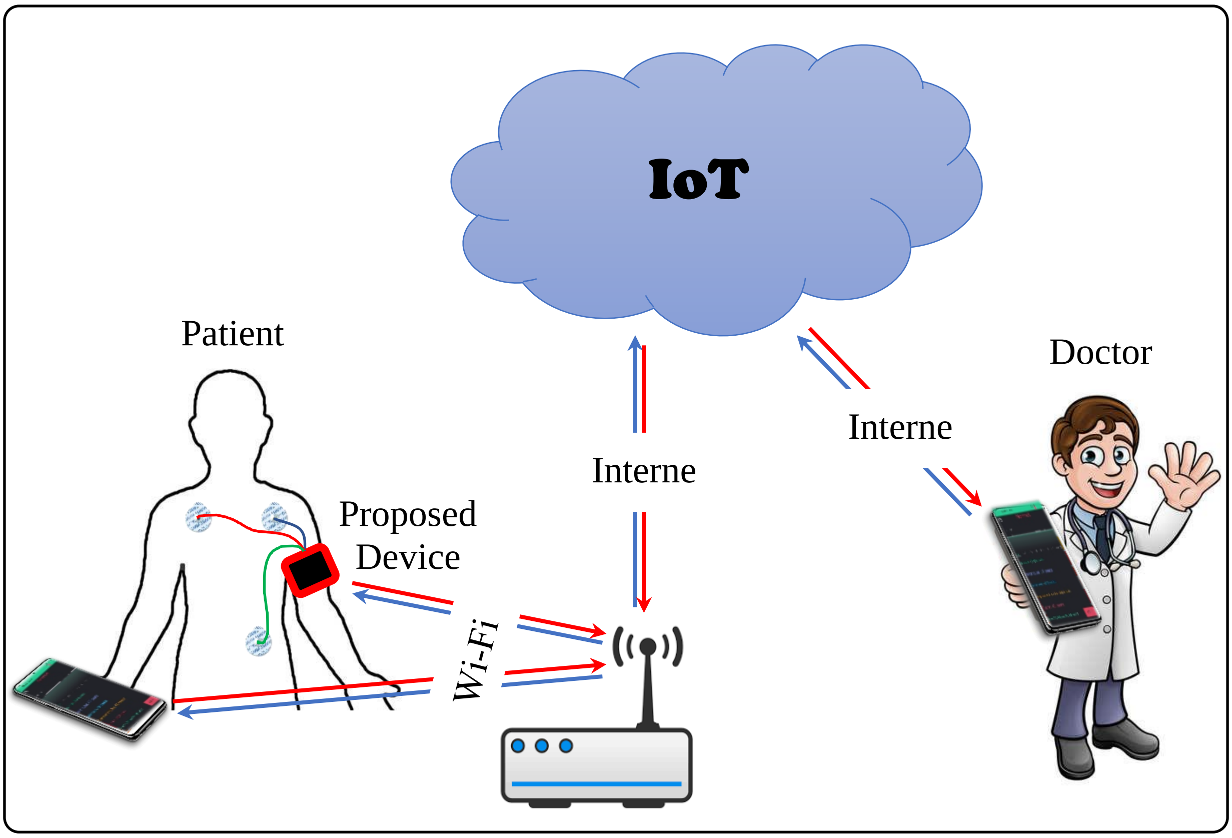

Figure 3.2 The proposed wearable system based on IoT

In this subsection, the system design will be described in detail, and the results for evaluation with discussions will be presented in the next chapter with the same subsection sequence.

3.2.1 Hardware Implementation

The system on a chip Node MCU is an IoT open-source platform running the ESP8266 Wi-Fi low-cost microchip. The ESP8266 supports the full MCU capability with the full transmission control protocol and internet protocol (TCP/IP). It was based on the ESP-12 module, which allows the MCU to connect a network using the TCP/IP protocol.

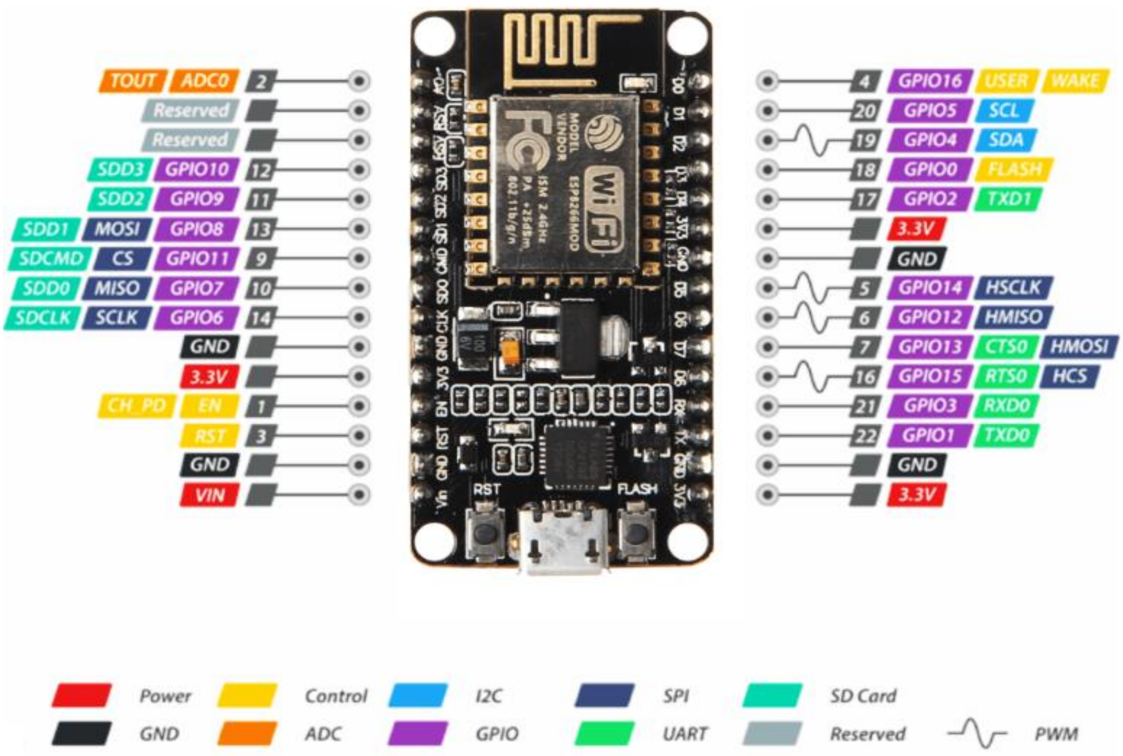

Figure 3.3 Mode MCU pinout

The Node-MCU (ESP8266) stands for Microcontroller Unit firmware development hardware. It is used for IoT projects because of the high performance and deep sleep with the following specifications:

- 32-bit MCU

- Voltage 3.3V
- Input Voltage is between 5-12V
- Memory is 4 MB
- S-RAM is 64 KB
- Speed is 80 MHz
- USBTTL
- PCBAntenna

The pinout of the Mode MCU are:

- Power Pins One pin (in) with three 3.3V.
- GND is ground pin.
- I2C are connecting pins.
- GPIO 17 pins are for functions.
- ADC analogue to digital pin Channel.
- UART pins are 2 UART.
- SPI pins slave and master modes.
- SDIO pins features are Input/Output Interface (SDIO).
- PWM pulse width modulation.
- Control pins control the MCU.

The IoT technology connects physical objects through the digital world. The electronics companies are developing their products for integrated with the new technology requirement. For example, the semiconductor company (Espressif Systems) designed new small size for low price MCU with embedded Wi-Fi named ESP8266. It is produced for (monitoring or/and controlling) systems based on IoT. The following significant applications are:

- Home Appliances
- Home Automation

- Smart Plug and lights
- Mesh Network
- Industrial Wireless Control
- Baby Monitors
- IP Cameras
- Sensor Networks
- Wearable Electronics
- Wi-Fi Location-aware Devices
- Security ID Tags
- Wi-Fi Position System Beacons

The prototype system (using Olimex- EKG and Node-MCU) at run time with the mobile application and computer shows in Figure 3.4. For hardware evaluation, the data are used from the same 103,192 beats, and overall processing data are displayed by the computer using the serial port. At the same time, the diagnostic report (patient report) is uploaded to the mobile application through the IoT. The patient report consists of the detection and classification information. The report summarized the patient's ECG heart rate (HR), average HR, maximum and minimum (HR), the beats count of each one for the five diagnostic types (N, V, S, F, and Q), and the current beat class. At the same time, the patient report and the ECG original samples are stored in the device using the microSD-card for backup and offline analysis. The mobile application displays the patient report in real-time and controls the ON/OFF device through the IoT connection. Furthermore, actual cases are connected to the system using the Olimex- EKG, and the patient report results are promising for real-time heartbeats detection and classification.

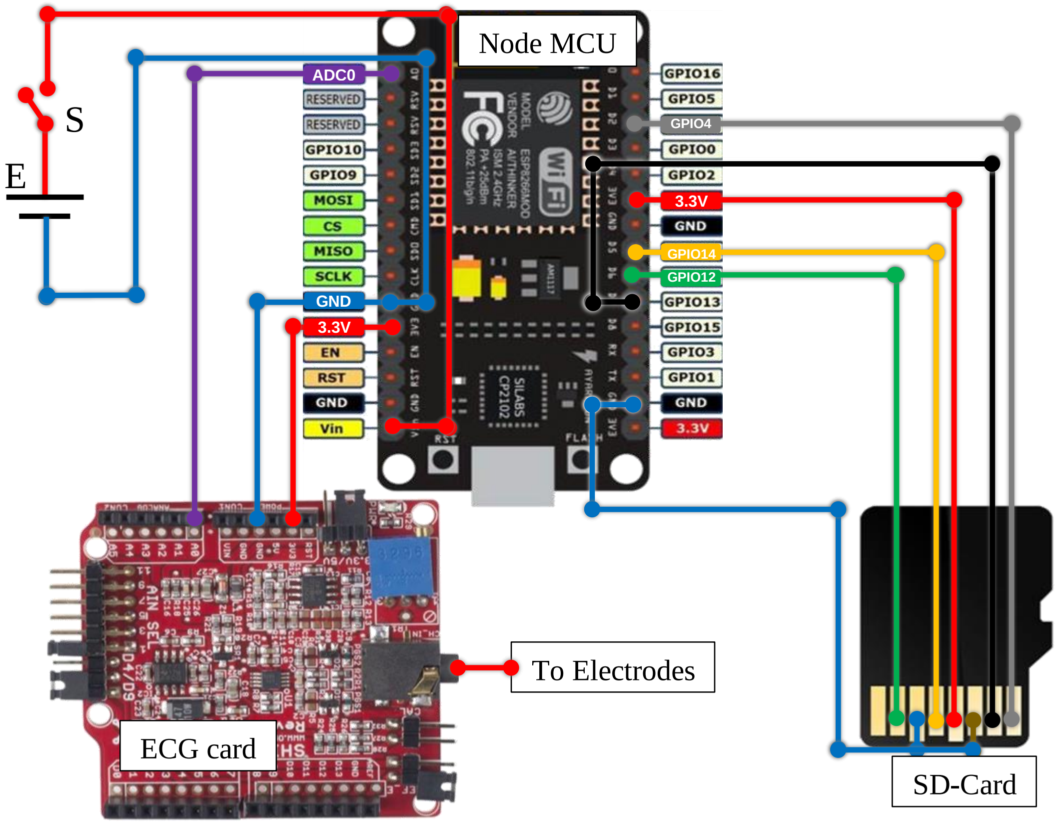
Node MCU
S
E
ADC0
RESERVED
RESERVED
GPIO10
GPIO9
MOSI
CS
MISO
SCLK
GND
3.3V
EN
RST
GND
Vin
GPIO16
GPIO5
GPIO4
GPIO0
GPIO2
3.3V
GND
GPIO14
GPIO12
GPIO13
GPIO15
GPIO3
GPIO1
GND
3.3V
To Electrodes
ECG card
SD-Card

(a)

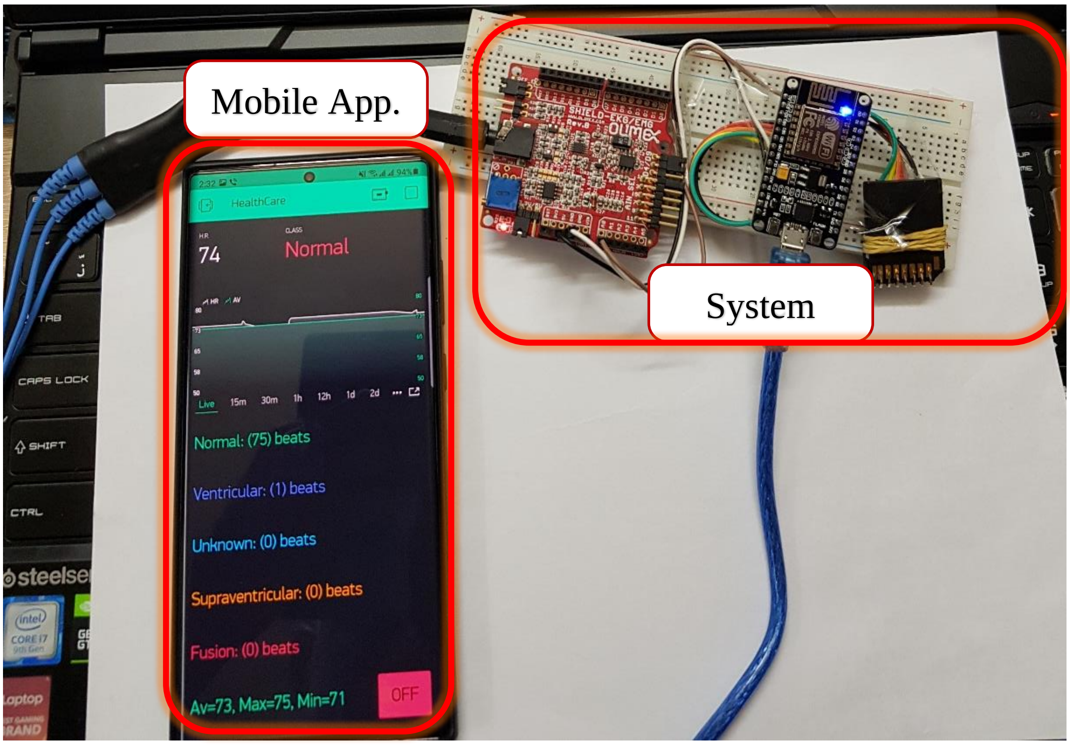
Mobile App.
System
HealthCare
74
Normal
Normal: (75) beats
Ventricular: (1) beats
Unknown: (0) beats
Supraventricular: (0) beats
Fusion: (0) beats
Av=73, Max=75, Min=71
OFF

(b)

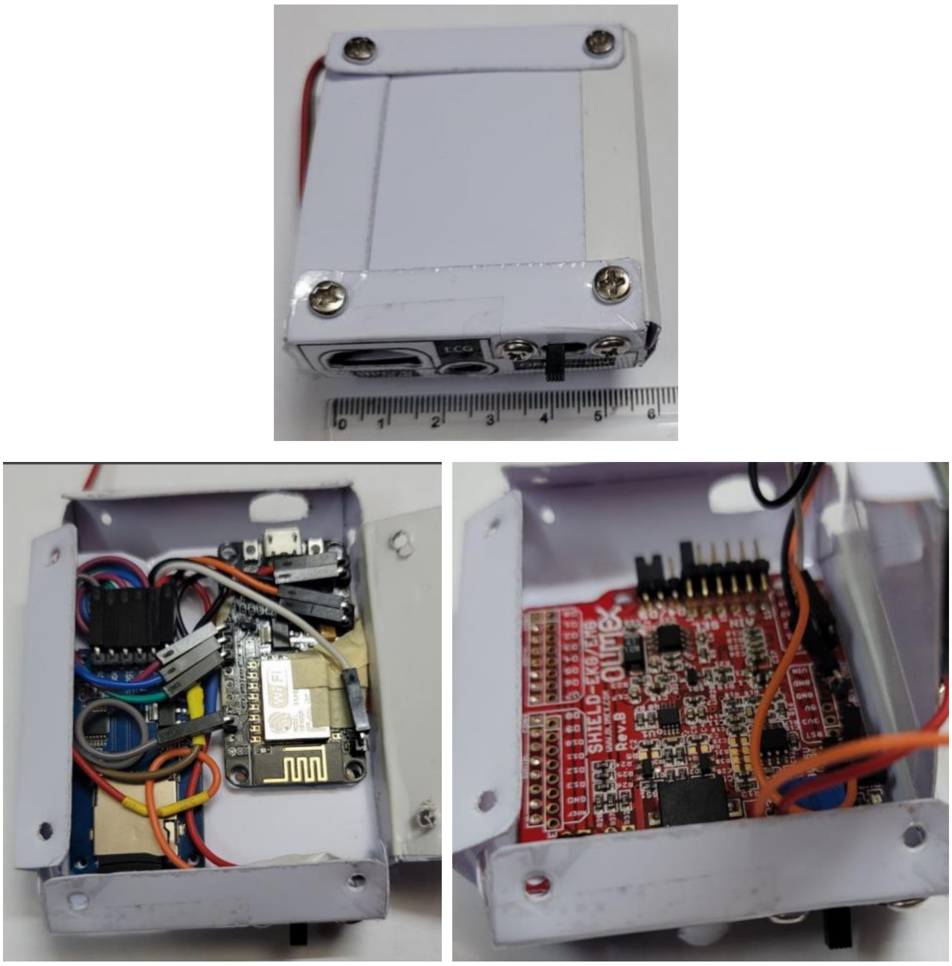

(c)

(d)

Figure 3.4 The prototype system (a) circuit (b) implementation (c) device (d) wearable.

3.2.2 System Characteristics

The proposed system based on the new method has several distinct characteristics:

a. The same features for the QRS-detection are reused for classification because it contains the most beats shape features.
b. The SMANN implementation is easy with multi masks (matrices); it is like the ANN with a new dimension for selective inputs.
c. The features are extracted according to a simple mathematical calculation, as shown in the previous equations.
d. Low computation device is implemented in wearable devices and IoT.
e. The device executes all processes except displaying the report using the mobile application. The processes include reading the ECG samples, detecting the QRS, classifying these heartbeats, sending the patient report, and storing the ECG samples with the report in a microSD-card. The device can work with and without an internet connection because the internet is used to display the patient report for real-time monitoring, and the device performs all other processes, as shown in Figure 3.5.
f. The device executes all processes except displaying the report using the mobile application. The processes include reading the ECG samples, detecting the QRS, classifying these heartbeats, sending the patient report, and storing the ECG samples with the report in a microSD-card.
g. The device can easily connect to the internet using Wi-Fi.
h. It works online for real-time patient monitoring and CDS using IoT.
i. It works offline for data logging using a microSD-card for storing the patient data. Therefore, it can work without the internet as a Holter with more features for CDS.
j. According to the Node-MCU specification and the low computational algorithm for detection and classification, it is a low power device.

The flowchart is shown in Figure 3.5, and the system performs the following operation steps:

a. The device and the mobile start connection to the internet.
b. The device starts operation from the mobile application.
c. The ECG card reads the ECG signal using the Olimex- EKG by the analogue port (A0) for Node-MCU.
d. MCU filters the ECG signal and stores the original ECG signal in the microSD-card.
e. MCU applies the equations to extract the (14) QRS-shape features.
f. MCU detect the QRS after perform the tree and ANN.
g. MCU applies the equations to extract the (4) between-RR features.
h. MCU applies the equations to extract the (6) RR-interval features.
i. MCU processes some of the (24) features based on the knowledge base to select the corresponding mask.
j. MCU applies the selective mask of SMANN to heartbeat classification of the 24 features.
k. The outputs are the QRS, class, and other information. This information is the patient's report.
l. The report sends to the mobile application using IoT and stores in the microSD-card.

3.2.3 System Operation

The patient report displays the detection and classification information for real-time monitoring, as shown in Figure 3.6. The report shows the following:

1. It displays the patient current heart rate.
2. It displays the patient current heartbeat class based on the five AAMI classes.

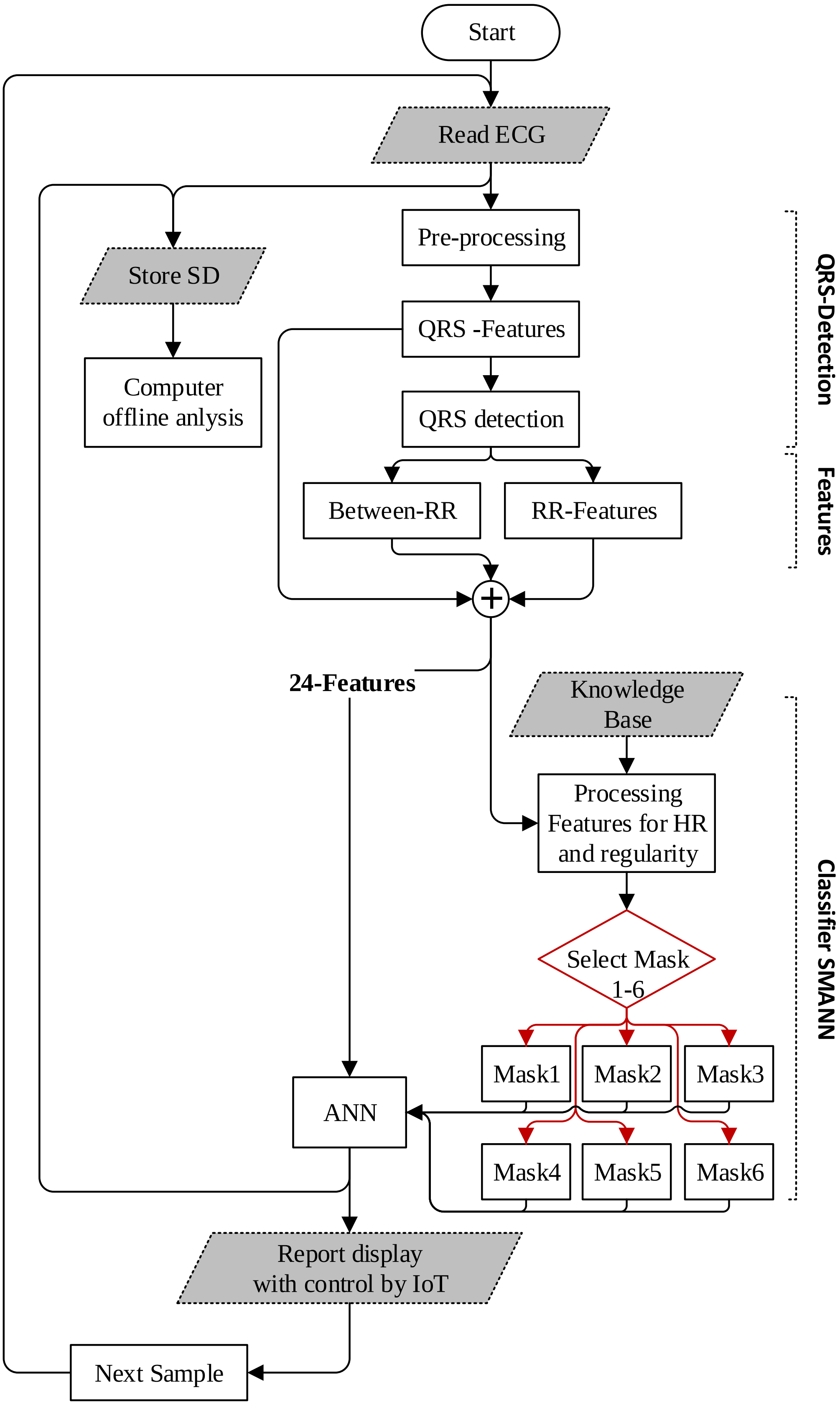

Figure 3.5 System flowchart

3. It displays the average heart rate, maximum heart rate, and minimum heart rate
4. It shows the historical chart for the current and the average heart rate based on multi periods.
5. It counts for the normal heartbeat.
6. It counts for the ventricular heartbeat.
7. It counts for the unknown heartbeat.
8. It counts for the superventricular heartbeat.
9. It counts for the fusion heartbeat.
10. It controls the ON/OFF device.

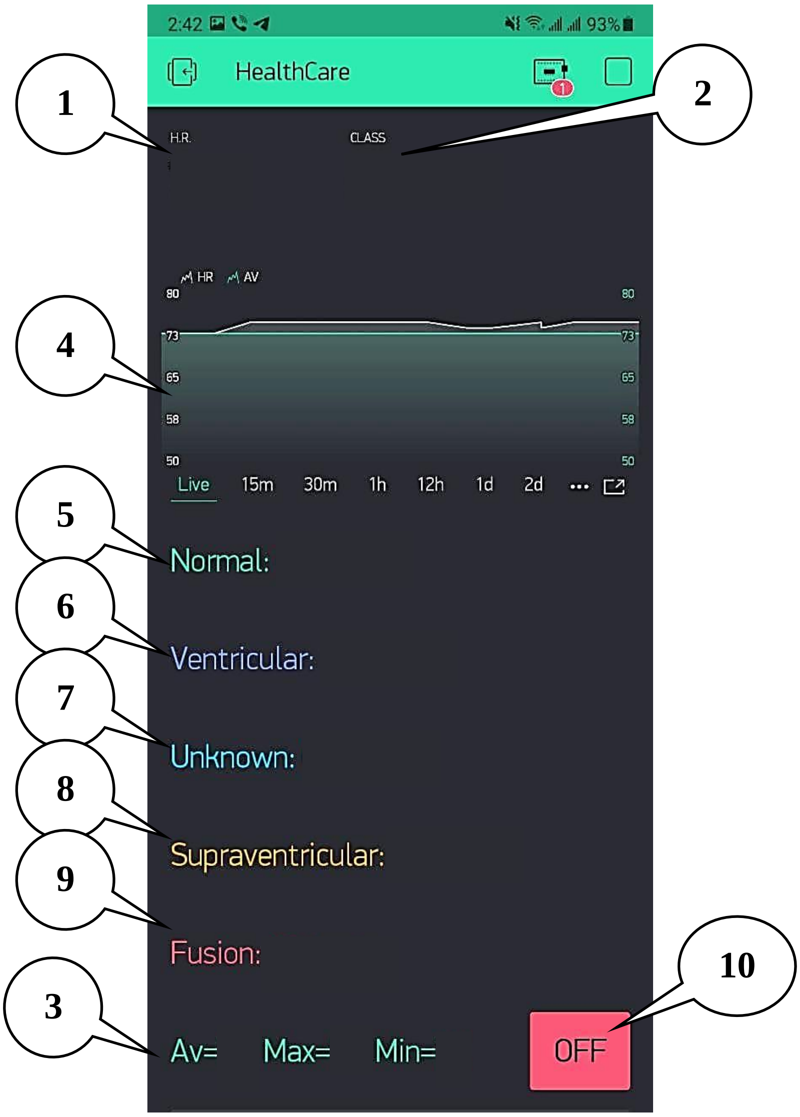

Figure 3.6 The mobile application

3.3 QRS-Detection Proposed Algorithm

The proposed QRS-detection algorithm is a simple, real-time, high-performance based on a novel technique for features extraction and hybrid classification by ANN and decision trees, as shown in part (2) of Figure 3.1. In this work, five stages algorithm is designed for low computational wearable healthcare applications. The first stage is filtering the original ECG signal to reduce the noise and baseline wandering. After that, a maximum or minimum moving window for positive or negative peaks respectively searches R-peaks for any expected value and finds the Q and S corresponding to this R-peak. Only these values from all ECG samples are passed to the next stage for feature extraction to reduce the algorithm computation. Stage four is excluded any unlikely points using the mean of the slope and level based on a simple decision tree. Finally, artificial neural networks are designed to classify the rest point for QRS detection using ANNs for each peak polarity to improve the network's performance by separating the data as a positive or negative peak. In this subsection, the algorithm design will be described in detail, and the results for evaluation with discussions will be presented in the next chapter with the same subsection sequence. The QRS detection algorithm block diagram is shown in Figure 3.7.

The algorithm based on five-stage is designed to improve the QRS-detection to be implemented for real-time wearable applications. ECG signal filtering uses a simple moving average filter without more filters to reduce the noise and baseline wander. The second stage is searching the window for the R-peak, Q, and S using the window for maximum and minimum values. These QRS points pass to stage three to extract features that are used for the next stages. Stage four is a simple decision using one of the features to pass any QRS near expected for the final decision stage based on a neural network. Stage five is the final stage that is using the overall features to inspect the QRS for detection purposes. Each algorithm stage is explained in the following subsections.

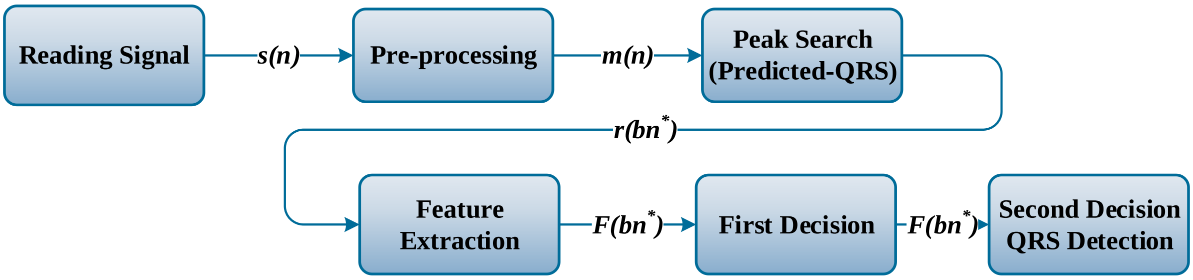

Figure 3.7 The proposed QRS-detection algorithm block diagram

Where n: the sample number

bn^*: the predicted beat number

3.3.1 Pre-processing

The original ECG signal $s(n)$ suffers baseline wander, power line interference, electrode, and muscle noise. A moving average with an N window filters the signal to remove the noise, and the signal becomes smooth, as shown in Figure 3.9. This algorithm used a moving average window with N=150 samples for ECG at a sampling rate of 360 samples per second (convenient design, best accuracy with low delay). The moving average filter for 150 samples window is shown in Equation (3.1).

$$m(n) = s(n) - \frac{1}{150}\sum_{i=1}^{150} s(n - 75 + i) \tag{3.1}$$

3.3.2 Peak Search

The major point for the detection algorithm is finding R-peak. Searching the filtered signal $m(n)$ for maximum or minimum value using N=90 single window for the signal rate 360 sample per second (depending on the maximum

QRS width for the normal case is 150ms) to find the positive-peak or negative-peak as present in Equation (3.2). Where the absolute value of the max is greater than the absolute of the min, the peak is positive and vice versa. These two types of peaks values will be as predicted R-peak. After that, search the Q and S points related to the predicted R-peak to get the predicted QRS (QRS*) three points and eliminate the residual points (the signal samples that are not an R, Q, or S points). Therefore, the only signal points that pass to the next stage are QRS*.

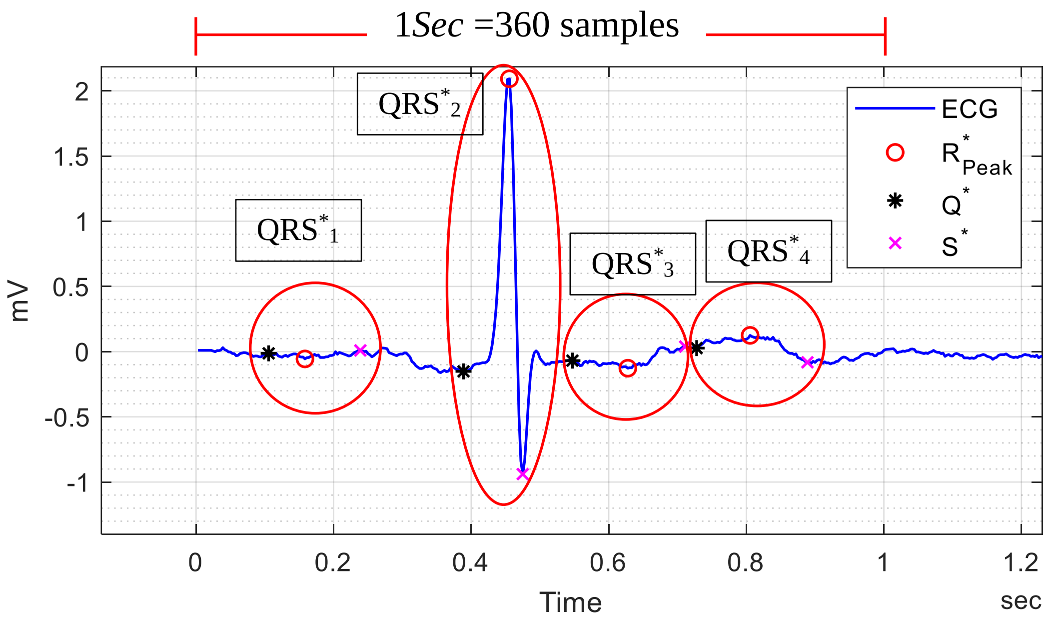

Figure 3.8 The average QRS* for 1 sec time and 360 samples

For 360 samples, an average of 4 QRS* (predicted) can be found. So, that will reduce the original samples to three pairs for each QRS* (4×6=24 values), as shown in Figure 3.8. Only 24 (bn^*) values as predicted beats are used after this stage instead of 360 (n) samples to reduce computation. The rest of the samples is eliminated because it is far away to be QRS points. So, the computation for the next stages will be less than the traditional methods. On the other hand, the traditional methods process all ECG samples and add more complexity. The QRS-predicted points and the max or min values for the moving window are shown in Figure 3.10 and Figure 3.11.

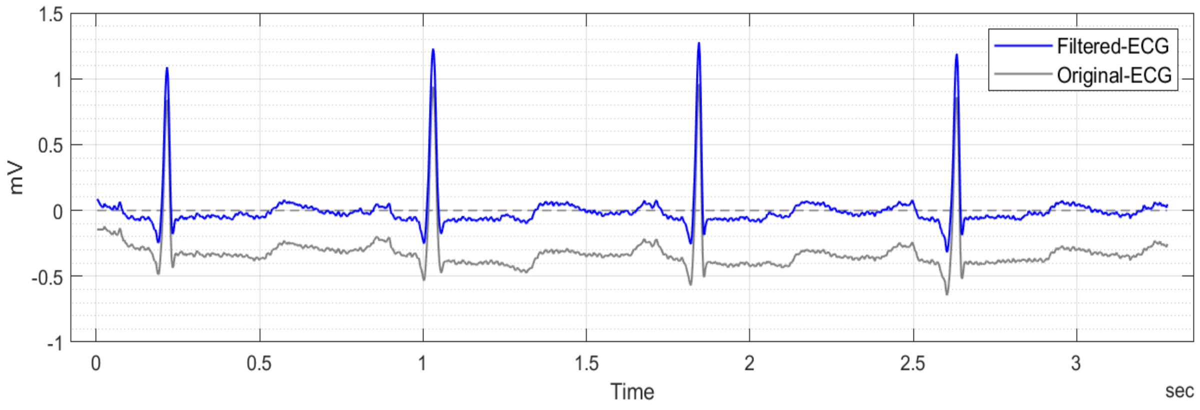

Figure 3.9 The original and filtered signals

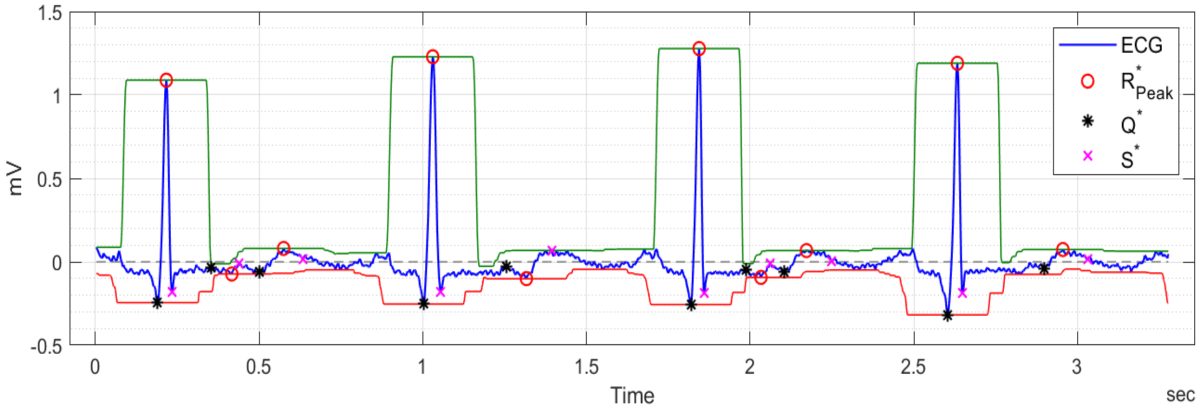

Figure 3.10 Predicted QRS (QRS*) and the min-max window

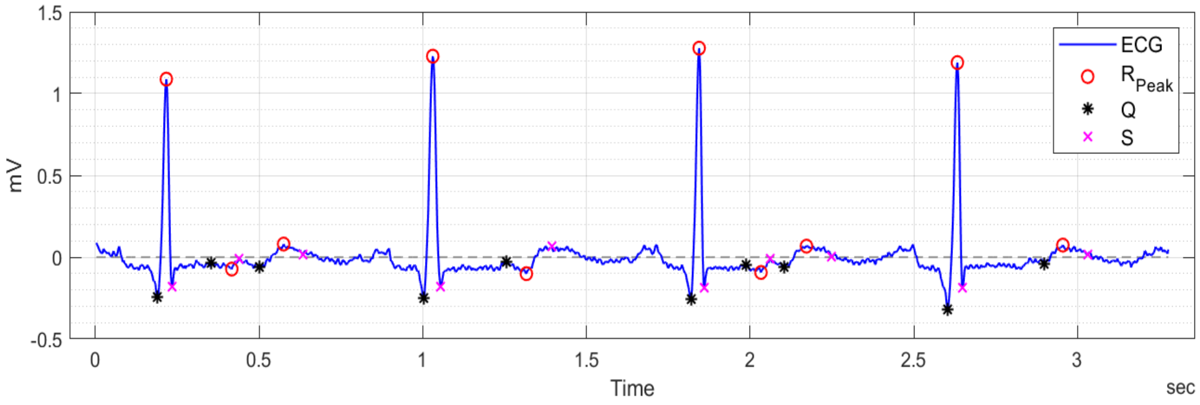

Figure 3.11 Predicted QRS (QRS*)

$$r(bn^*) = \begin{Bmatrix} +\ QRS^* & (m(n) = max)\ \&\ (|max| > |min|) \\ -\ QRS^* & (m(n) = min)\ \&\ (|max| < |min|) \\ - & otherwise \end{Bmatrix} \quad (3.2)$$

Where: r (1-3, bn^*): x-axis values

r (4-6, bn^*): y-axis values

The r(t) contains x-values and y-values for the three QRS points for positive or negative waves to increase the accuracy using separate wave values for each QRS polarity. This technique is used to speed the algorithm and eliminate the useless signal samples for the detection process. In contrast, traditional methods square the samples which add more computation and decrease the performance.

3.3.3 Feature Extraction (Slope-Level)

The features are extracted from the current QRS* and some relations with the preceding QRS* points. After finding all predicted points that could be actual or detected QRS, these points contain enough information that is used to detect the correct QRS points. The slope is the most feature used for detection in many algorithms. Moreover, the proposed algorithm extracts more features like the slope from QR, the slope from RS, the level from Q to R and the level from R to S, and the time for QR, RS, and QS. These features will improve detection performance. In contrast, the existing methods based on threshold detection are used the slope feature only.

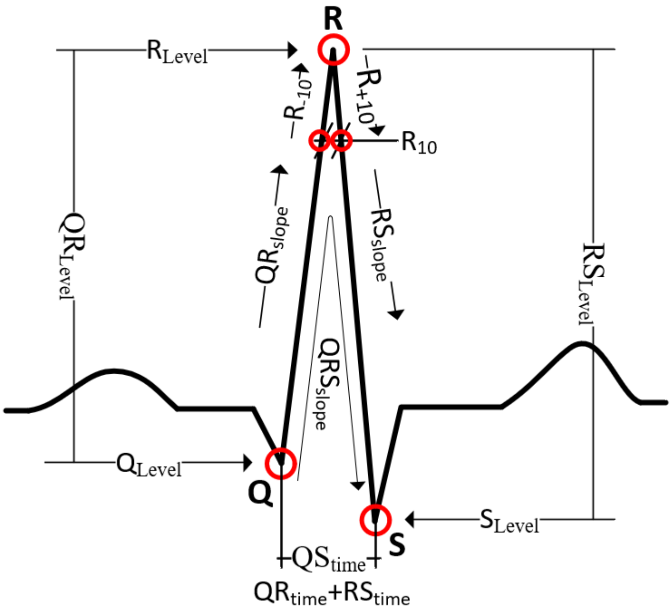

Figure 3.12 The features of QRS*

From the three QRS* pair (x, y) points, fourteen features are extracted, shown in Figure 3.12, after testing these features to improve the accuracy of the classification process. These fourteen features started from $F_1\,(bn^*)$ to $F_{14}\,(bn^*)$, and its calculation equations are:

- $F_{1\text{-}3}$: Q, R, and S levels (y-values for each of the three points)

$$F_1(bn^*) = r(4, bn^*) \tag{3.3}$$

$$F_2(bn^*) = r(5, bn^*) \tag{3.4}$$

$$F_3(bn^*) = r(6, bn^*) \tag{3.5}$$

- $F_{4\text{-}5}$: R-10_slope and R+10_slope (the slope of fixed time from R point to bn^*-10 and bn^*+10)

$$F_4(bn^*) = \frac{r(5, bn^*) - r(5, bn^* - 10)}{10} \tag{3.6}$$

$$F_5(bn^*) = \frac{r(5, bn^* + 10) - r(5, bn^*)}{10} \tag{3.7}$$

- F_6: QRS_level = QR_level + RS_level (y- value from R point to Q + from R point to S)

$$F_6(bn^*) = \left(r(5, bn^*) - r(4, bn^*)\right) + \left(r(5, bn^*) - r(6, bn^*)\right) \tag{3.8}$$

- F_7: *QRS_slope= QR_slope +RS_slope* (the slope value from Q point to R + the slope from S point to R)

$$F_7(bn^*) = \left(\frac{r(5, bn^*) - r(4, bn^*)}{r(2, bn^*) - r(1, bn^*)} - \frac{r(6, bn^*) - r(5, bn^*)}{r(3, bn^*) - r(2, bn^*)}\right) \tag{3.9}$$

- $F_{8\text{-}9}$: *QR_time* and *RS_time* (the x_values from Q point to R point and from R point to S point)

$$F_8(bn^*) = r(2, bn^*) - r(1, bn^*) \tag{3.10}$$

$$F_9(bn^*) = r(3, bn^*) - r(2, bn^*) \tag{3.11}$$

- F_{10}: QRS_{dec} =*QRS_level* × *QRS_slope* (Equation (3.8) and Equation (3.9) are used for the first decision stage)

$$F_{10}(bn^*) = F_6(bn^*) \times F_7(bn^*) \tag{3.12}$$

- F_{11}: *QS_time* (the x_values from Q point to S point)

$$F_{11}(bn^*) = F_8(bn^*) + F_9(bn^*) = r(3, bn^*) - r(1, bn^*) \tag{3.13}$$

- F_{12}: *m_QRS*$_{dec}$: The mean for 15 values of the QRS_{dec} used as a threshold for the first decision stage start at five values for initializing algorithm.

$$F_{12}(bn^*) = \frac{1}{15} \sum_{i=-7}^{7} F_{10}(bn^* - i) \tag{3.14}$$

- F_{13}: The mean for three values of the QRS_{dec} (current, previews, and next values) that is used to eliminate noise detection.

$$F_{13}(bn^*) = \frac{1}{3} \sum_{i=-1}^{1} F_{10}(bn^* - i) \tag{3.15}$$

- F_{14}: The mean for three values of the *QRS_level* (current, previews, and next values) that is used to eliminate noise detection.

$$F_{14}(bn^*) = \frac{1}{3} \sum_{i=-1}^{1} F_6(bn^* - i) \tag{3.16}$$

Where bn^*: predicted beat number

The features are normalized using Equation (3.17) because these features are calculated from a variable ECG signal. In addition, the amplitude of ECG signals changed depending on device connectivity, personal age, and some heart diseases. Each feature is calculated for their max and min value to normalize the features values between (-1, 1) using the *mapminmax* MATLAB function.

$$F_i(bn^*) = \frac{2 \times (F_i(bn^*) - F_{i_{min}})}{F_{i_{max}} - F_{i_{min}}} - 1 \qquad (3.17)$$

3.3.4 First Decision

The QRS level and slope are the most features that can be used to separate the QRS predicted or detected. So that each predicted (QRS*) level and slope named (QRSdec) that achieve the lowest mean of the QRS* level and slope named (m_QRSdec) can be QRS and pass to the next stage. On the other hand, the QRS* level and slope (QRSdec) that not achieving the condition are eliminated and excluded to be QRS. This stage is such a threshold in the other algorithm. The first condition is illustrated in Equation (3.18).

$$F(bn^*) = \begin{Bmatrix} F(bn^*) & QRS_{dec} > (0.2 \times m\_QRS_{dec}) \\ deleteF(bn^*) & QRS_{dec} \leq (0.2 \times m\_QRS_{dec}) \end{Bmatrix} \qquad (3.18)$$

Where *F(bn*)*: the features that pass the first condition.

The simple decision tree is using one feature (m_QRSdec) to select the QRS* that passes the lowest threshold condition and excludes the QRS* that not passes the condition. The excluded QRS* values are far away to be actual points. So, increasing the algorithm speed is done by reducing the number of values that are processing to the final stage using a simple decision stage.

3.3.5 Second Decision (QRS Detection)

A simple two-layer feed-forward Artificial Neural Network (ANN) is designed with multi Tanh hidden neurons and single linear output neurons. The network is trained with the backpropagation algorithm for 70% training data and 30% testing data. ANN is designed using network growing based on trial and error, started at one hidden neuron. After that, adding more neurons to reach twice the input number for the hidden layer to improve the classifier performance (results are shown in the next chapter and Appendix C). Also, for two decision classifiers, a single output neuron is used. On the other hand, for each QRS* positive and QRS* negative, a particular full neural network is designed to improve the accuracy without adding more complexity. So, the algorithm computation will be simple than the existing methods.

The classifier is designed using twenty-eight neurons in the hidden layers and a single output neuron, as shown in Figure 3.13. The features are feed to the first layer, which contains twenty-eight neurons fully connected and applies the Equations (2.8), (2.9), (2.10), and (2.11) for (*i*: 1, 2, ……14 no. of inputs and *j*: 1, 2, ……28 no. of hidden neurons)

The 28 hidden neurons output are calculated by Equation (2.8) and Equation (2.9). Then the net value for the output neuron is determined using Equation (2.10). The output for Equation (2.11) is QRS final detection; if the value is 1, the QRS detection is true and 0 for not a QRS detection.

From the these equations, the multiplication occurs in the ANN for low numbers of neurons (28 neurons only), Equation (2.8) and Equation (2.10). Moreover, the number of values that processing is less than the original samples. Therefore, the proposed algorithm is low computation. The QRS detection and the original R-peak annotation file is shown in Figure 3.14 as a final result for these stages. The overall algorithm flowchart and a sample ECG detection signal are described in Figure 3.15.

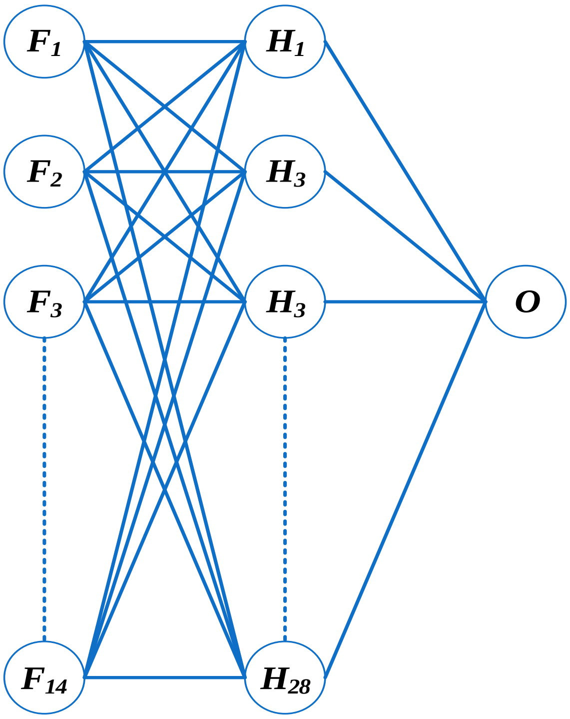

Figure 3.13 The designed ANN

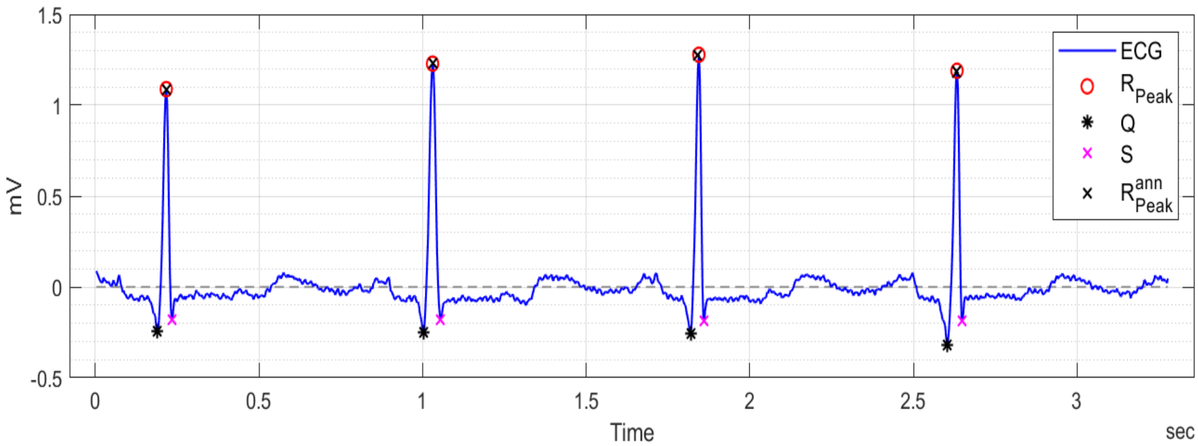

Figure 3.14 The detected QRS and R-peak from the annotation file

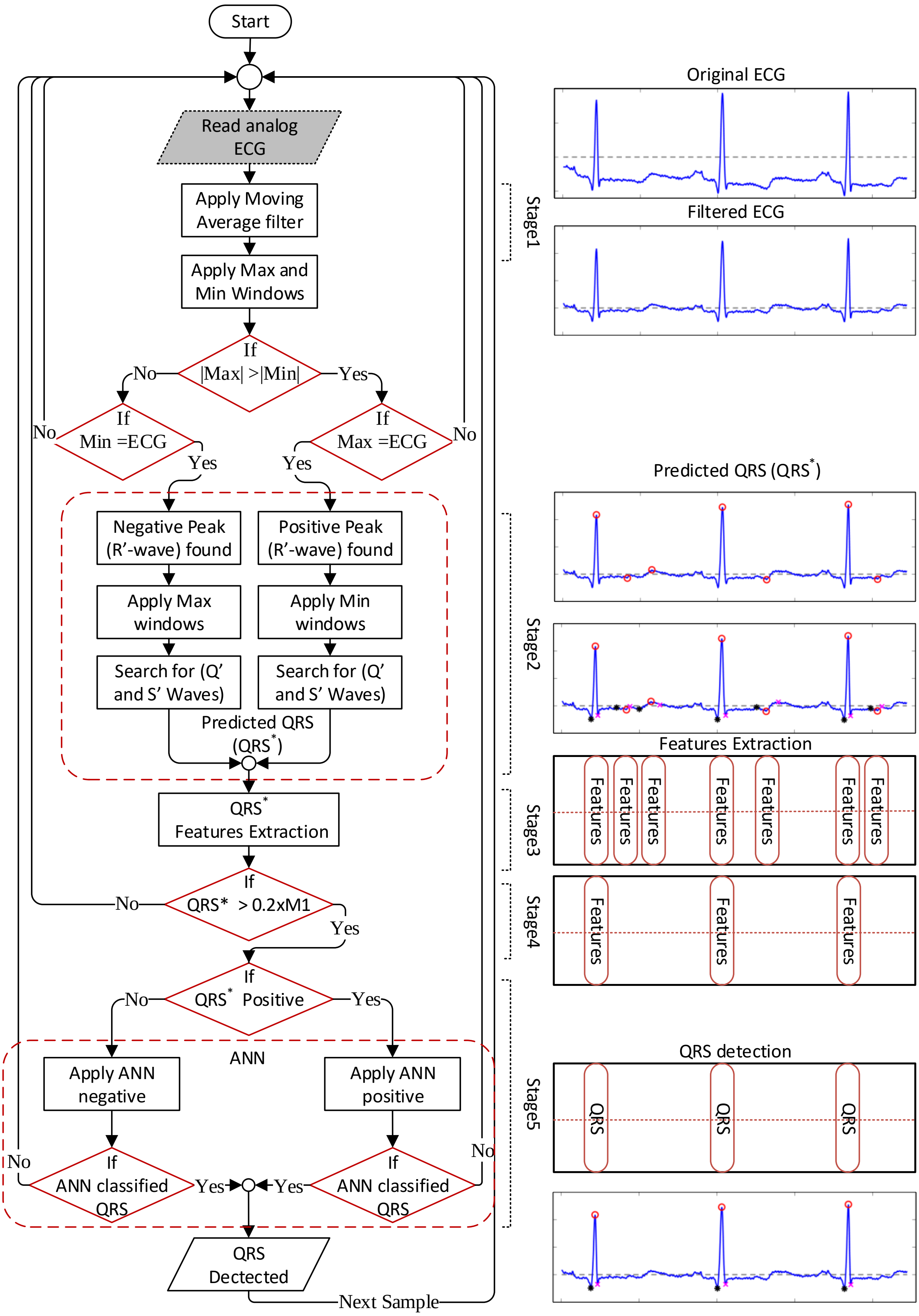

Figure 3.15 The overall algorithm flowchart

3.4 Verification of MIT-BIH Arrhythmia Database

The ECG signal processing methods are tested and evaluated based on different databases. The most ECG database used by many researchers is the MIT-BIH arrhythmia database. The QRS-detection algorithms are essential for ECG signal analysis to detect the beats for the ECG signal. There is no standard number of beats for this database that are used from numerous researches. Different heartbeat numbers are calculated for the researchers depending on the difference in understanding the annotation file.

The heartbeat numbers for existing methods are studied and compared to find the correct number that should be used. Then, a simple function is proposed to standardized the beats number for any ECG PhysioNet database for improving the Waveform Database Toolbox (WFDB) for the MATLAB program. This function is based on the annotation's description from the databases and can be added to the Toolbox. The function is removed the non-beats annotation without any errors. In this subsection, the database verification and the function design will be described in detail. The results for evaluation with discussions will be presented in the next chapter with the same subsection sequence.

The MIT-BIH has comprised variable ECG signals with a variable: noise, artifacts, beat types, and wave shapes. A 48-records with two channels for each ECG signal and an annotation file is included. These signals are recording from 25 men and 22 women for a half-hour period at 360 samples per second. The database has been annotated with 112,647 annotations, and these annotations have been verified. It has been labelled into two main annotation categories: the beats and the non-beats. The beat annotations for the MBADB consist of 15 subtypes, and the non-beats annotations consist of 24 subtypes, as shown in Table 3.1 [20].

The beat type consists of 14 classified beats types and one unclassified beats type. The beats annotations are occurring for any type of QRS wave in the

ECG signal. Therefore, this database is widely used for testing, performance evaluating, and learning for QRS-detection methods. In general, the databases are used to evaluate any new algorithm's performance before implementing it in devices for many applications. So, any errors for this evaluation will cause an error in the device measure. Furthermore, in biomedical applications like QRS-detection, which is substantial for many ECG monitoring devices, the detecting errors for these devices may affect doctor's diagnosis and the treatment that depend on these devices. So, verifying the database for these applications will improve the doctor's decision.

Until now, more than two thousand works cited the MIT-BIH Arrhythmia Database. It is unique in terms of arrhythmia classification, since it offers five arrhythmia standards groups. The QRS detection methods are essential for most of the cited works, including arrhythmia detection, classification, and diagnosing applications. Depending on this database, many QRS detection algorithms have been developed, tested, and evaluated. The QRS detection algorithms are according to the beats annotations in the database signals for testing and evaluation. These beats are used as learning data for the methods depending on the learning technique.

Many researchers used MATLAB for algorithm implementation based on the Waveform Database (WFDB) Toolbox. This Toolbox consists of the functions that are used for reading, writing, and signals processing the files of PhysioNet databases. The MIT-BIH arrhythmia is one of the PhysioNet databases which contains data and annotations files. The WFDB is used to extract the ECG signals and these annotations from the MBADB for all records. It can extract one type of beats or non-beats annotations or extract all annotations without any filter. So, it is not easy to extract all beat annotations only, which is leads to errors from reading the non-beat annotations. When reviewing the existing methods that used the MIT-BIH arrhythmia database, not all these methods are considered the same number of beats for the same database records.

Also, this difference affects even slightly the evaluation results that used to compare the performance of the methods.

Table 3.1 The beat and non-beat for the MIT-BIH arrhythmia database

Beat annotations		**Non-beat annotations**	
Code	**Description**	**Code**	**Description**
N	Normal beat	[	Start of ventricular flutter/fibrillation
L	Left bundle branch block beat	!	Ventricular flutter wave
R	Right bundle branch block beat	]	End of ventricular flutter/fibrillation
A	Atrial premature beat	x	Non-conducted P-wave (blocked APC)
a	Aberrated atrial premature beat	(N	Normal sinus rhythm
J	Nodal (junctional) premature beat	(P	Paced rhythm
S	Supraventricular premature or ectopic beat (atrial or nodal)	(B	Ventricular bigeminy
V	Premature ventricular contraction	(VT	Ventricular tachycardia
F	A fusion of ventricular and normal beat	(T	Ventricular trigeminy
e	Atrial escape beat	(SVTA	Supraventricular tachyarrhythmia
j	Nodal (junctional) escape beat	(IVR	Idioventricular rhythm
E	Ventricular escape beat	(NOD	Nodal (A-V junctional) rhythm
/	Paced beat	(AFIB	Atrial fibrillation
f	A fusion of paced and normal beat	(AFL	Atrial flutter
Q	Unclassifiable beat	(VFL	Ventricular flutter
		(AB	Atrial bigeminy
		(PREX	Pre-excitation (WPW)
		(BII	2° heart block
		(SBR	Sinus bradycardia
		|	Isolated QRS-like artifact
		~	Change in signal quality
		":TS	Tape slippage
		":PSE	Pause
		":MISSB	Missed beat

This work will study the reasons for reading different numbers of beats and methods comparison with correction and verification. Furthermore, a new function is designed to extract the correct beats and remove the non-beats annotations from the original database files based on WFDB Toolbox for MATLAB.

3.4.1 MIT-BIH Arrhythmia Database

The MBADB is one of the most substantial ECG databases. Contrasting database signals, noise, and artifacts make it suitable for testing and evaluation. Moreover, the verified annotations files contain the beats and non-beats types, as shown in Table 3.2 and Table 3.3. These tables show the MBADB annotations for each record based on the PhysioNet annotations descriptions for beats and non-beats annotations. There are more than these annotation types, which are shown in other databases.

3.4.2 Heartbeats Filter Function

In this thesis, a new MATLAB function named Beat Function (BF) is designed to filter the annotations file for any PhysioNet databases included the MIT-BIH arrhythmia. The function removes the non-beat annotation shown in Table 3.3 so, the annotations file will contain the beat annotation only, as shown in Table 3.2. On the other hand, the existing MATLAB-WFDB function (rdann) reading the annotations file can read all annotations or one annotation. So, rdann cannot filter the annotation by beats or non-beats type; for this reason, the function with new features was proposed to filter the data correctly without any errors.

This function is simple, but it is essential to standardize the beats number for any researcher that are used PhysioNet databases. This function can be added to the MATLAB-WFDB toolbox to simply filtered the annotations files by removing the non-beat annotations precisely with the standard values. The function read and search all annotations data files for each record, as shown in Figure 3.16. If the annotation is one of the non-beat types, this annotation will be

Table 3.2 MBADB beat annotations

Record No.	Total Anno-tations	N	L	R	A	a	J	S	V	F	e	j	E	/	f	Q	Total Beats
100	2274	2239			33				1								2273
101	1874	1860			3											2	1865
102	2192	99							4					2028	56		2187
103	2091	2082			2												2084
104	2311	163							2					1380	666	18	2229
105	2691	2526							41							5	2572
106	2098	1507							520								2027
107	2140								59					2078			2137
108	1824	1739			4				17	2		1					1763
109	2535		2492						38	2							2532
111	2133		2123						1								2124
112	2550	2537			2												2539
113	1796	1789				6											1795
114	1890	1820			10		2		43	4							1879
115	1962	1953															1953
116	2421	2302			1				109								2412
117	1539	1534			1												1535
118	2301			2166	96				16								2278
119	2094	1543							444								1987
121	1876	1861			1				1								1863
122	2479	2476															2476
123	1519	1515							3								1518
124	1634			1531	2		29		47	5		5					1619
200	2792	1743			30				826	2							2601
201	2039	1625			30	97	1		198	2		10					1963
202	2146	2061			36	19			19	1							2136
203	3108	2529				2			444	1						4	2980
205	2672	2571			3				71	11							2656
207	2385		1457	86	107				105				105				1860
208	3040	1586						2	992	373						2	2955
209	3052	2621			383				1								3005
210	2685	2423				22			194	10			1				2650
212	2763	923		1825													2748
213	3294	2641			25	3			220	362							3251
214	2297		2003						256	1						2	2262
215	3400	3195			3				164	1							3363
217	2280	244							162					1542	260		2208
219	2312	2082			7				64	1							2154
220	2069	1954			94												2048
221	2462	2031							396								2427
222	2634	2062			208		1					212					2483
223	2643	2029			72	1			473	14	16						2605
228	2141	1688			3				362								2053
230	2466	2255							1								2256
231	2011	314		1254	1				2								1571
232	1816			397	1382							1					1780
233	3152	2230			7				831	11							3079
234	2764	2700					50		3								2753
Total	112647	75052	8075	7259	2546	150	83	2	7130	803	16	229	106	7028	982	33	109,494

Table 3.3 MBADB non-beat annotations

Rec No.	Total Annotation	[	!	]	x	(N	(P	(B	(VT	(T	(SVTA	(IVR	(NOD	(AFIB	(AFL	(VFL	(AB	(PREX	(BII	(SBR	—	~	":TS	":PSE	":MISSB	Total Non-Beats
100	2274					1																				1
101	1874					1															4	4				9
102	2192					2	3																			5
103	2091					1																6				7
104	2311					22	23															37				82
105	2691					1															30	88				119
106	2098					21		18	1	1												30				71
107	2140						1															2				3
108	1824				11	1															8	41				61
109	2535					1																2				3
111	2133					1																8				9
112	2550					1																10				11
113	1796					1																				1
114	1890					2					1										1	7				11
115	1962					1															6	2				9
116	2421					1																8				9
117	1539					1																3				4
118	2301				10	1																12				23
119	2094					49		37		17												4				107
121	1876					1																12				13
122	2479					1															2					3
123	1519					1																				1
124	1634					6				2		3	2									2				15
200	2792					70		71	7													43				191
201	2039				37	16				12	1		3	3								4				76
202	2146					3								4	1						2					10
203	3108								21	1				21	2						26	57				128
205	2672					7			6												1	2				16
207	2385	6	472	6		10		4	2		1	1				6					2	15				525
208	3040					27				26											8	24				85
209	3052					11					10										7	19				47
210	2685							5	2	1				9							1	17				35
212	2763					1															1	13				15
213	3294					22		19	2																	43
214	2297					13			2	10											5	4	1			35
215	3400					3			2													30	2			37
217	2280						33	9	1					24							1	4				72
219	2312				133	8		2		1				10										3	1	158
220	2069					9					8											4				21
221	2462							1	2	8				12								12				35
222	2634					32					4		31	24	42		3					15				151
223	2643					11		7	7	3												10				38
228	2141					21		20													24	20	3			88
230	2466					104												103			1	2				210
231	2011				2	6													5						427	440
232	1816																			1		35				36
233	3152					36		28	6	1											2					73
234	2764					2					1											8				11
Total	112,647	6	472	6	193	530	60	221	61	83	26	4	36	107	45	6	3	103	5	1	132	616	6	3	428	3153

removed from the annotation data. Also, it has to be used for any PhysioNet database to extract the beat annotation by removing the non-beat annotations used to prepare the data for many applications, including QRS-detection methods.

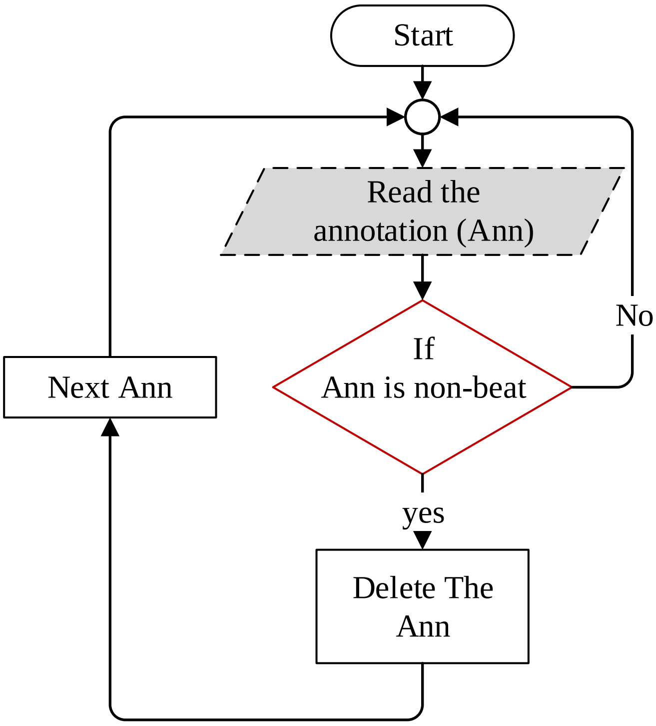

Figure 3.16 The BF flowchart for filtering the annotations file

3.5 Normality Heartbeat Classification Proposed Method

In this method, three stages algorithm is designed and evaluated for low computation applications. The first stage is filtering the original ECG signal, features extraction for QRS, and QRS-detection. In the second stage, the new features are extracted from RR-interval and added to the same QRS-detection features. Finally, A simple ANN is designed to classify the beats for two classes (normal and abnormal) based on the QRS shape used for detection and the RR-interval features. In this subsection, the method design will be described in detail, and the results for evaluation with discussions will be presented in the next chapter with the same subsection sequence.

High accuracy and low computational algorithm to classify the normal and abnormal heartbeats are designed and evaluated. The normal and abnormal heartbeats are classified because the 15 beats can be divided into normal and abnormal beats for the patient's monitoring system. So, diagnosing the normality will eliminate the abnormal case for a beat's classifier or physiologist.

The heartbeats normality classification for the real-time diagnostic is the proposed algorithm's main objective using information acquired from extract features as a substitute for raw ECG signals. The same features extracted from QRS- detection (subsection 3.3.3) will be used for classification in addition to RR-interval features. Therefore, the heartbeats are detected using an appropriate (fast, real-time, low computation, high accuracy) QRS-complex detection algorithm.

The proposed method has three main parts: detection, features extraction, and classification, as shown in Figure 3.17. First, the detection prepared the ECG signal by filters and QRS-detection. Second, the features are extracted from the RR-interval in addition to the QRS-shape from the QRS-detection. Finally, an ANN is designed to classify the normality of heartbeat with a low computational model. The following subsection describes these parts in detail.

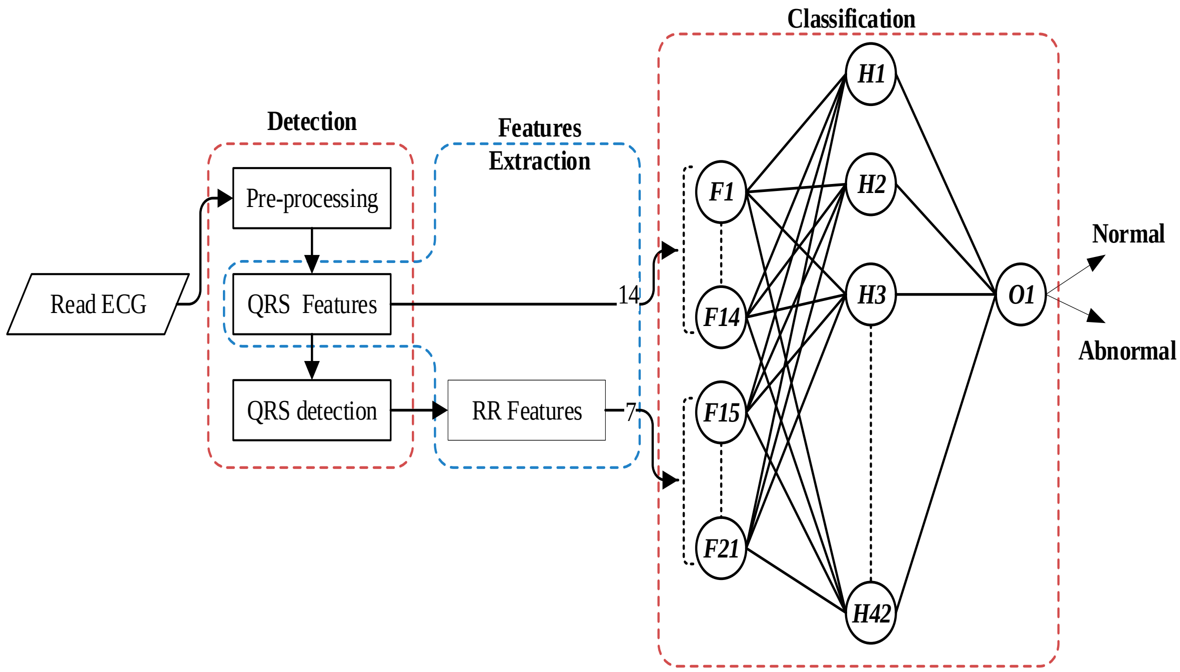

Figure 3.17 The proposed normality classification method

3.5.1 Detection

A QRS-detection algorithm is applied to detect the heartbeats for the ECG signal. Fast speed, low computational, and high accuracy are the algorithm constraints. The QRS-detection algorithm in section 3.3 was used for this work because the detection features are mixed with the classification stage's new features. The ECG signal is filtered to eliminate the baseline wander, power line interference, and other noise. A 150 samples window with a moving average filtered the ECG signal to remove the noise and smooth the signal, as shown in Equation (3.1). This window size is selected for the signal with 360 samples per second. Finally, the output of this stage is the QRS detected and the 14 QRS-shape features that are extracted from the detection algorithm as explained in Equations (3.3) to (3.16).

3.5.2 Features Extraction

The most important part of any classifier is the features extracted in order to enhance the classification performance. A new mixture features method is applied to achieve the purpose of the classifier for the ECG signal. The QRS complex is the highest energy part of the ECG signal for any signal processing operations. So, the features extracted from the QRS complex are reused. The heartbeat regularity can be found from the R-peaks for the QRS complex. The interval or duration RR (between two R-peaks) from the ECG signal can also show the heartbeats' normality based on the RR interval's neighbour beats. The average heartbeats calculate the heart rate for a certain time and can indicate the beats' normality. The heart rate range for the normal case is between 60-120 beats per min.

The mixture features are divides into the two-part. First, the QRS-shape has most features for the ECG signal; fourteen features are extracted from the QRS- shape. Second, the RR-interval is shown the regularity of the heartbeat. For each heartbeat, the algorithm determines the RR-before, RR-after, RR-after-average, and RR-before-average.

The first fourteen features are extracted from the QRS complex; these are the same features used from the QRS detection algorithm. It contains the most features for the QRS complex that can be used for the next stage to classify the heartbeat together with the RR interval features. Features 1-14 are extracted from the level, slope, and time for the QRS-complex. The equations for these features are described in Equations (3.3) to (3.16) of the QRS-detection algorithm. The RR-interval features (F_{15} – F_{21}) are calculated from Equations (3.19)-(3.25), and Figure 3.18 shows these features.

- F_{15}: RR before

$$F_{15}(bn) = \left(t_{R(bn)} - t_{R(bn-1)}\right) \tag{3.19}$$

- F_{16}: RR after

$$F_{16}(bn) = \left(t_{R(bn+1)} - t_{R(bn)}\right) \tag{3.20}$$

- F_{17}: The average of F_{15}

$$F_{17}(bn) = \frac{1}{3}\sum_{i=1}^{3} F_{15}(bn - i + 2) \tag{3.21}$$

- F_{18}: The average of F_{16}

$$F_{18}(bn) = \frac{1}{7}\sum_{i=1}^{7} F_{16}(bn - i + 4) \tag{3.22}$$

- F_{19}: The different RR after the average

$$F_{19}(bn) = F_{16}(bn) - F_{17}(bn) \tag{3.23}$$

- F_{20}: ECG signal level before 50 samples from Q point

$$F_{20}(bn) = m(t_{Q(bn)} - 50/f_s) \tag{3.24}$$

- f_{21}: ECG signal level after 50 samples from S point

$$F_{21}(bn) = m(t_{S(bn)} + 50/f_s) \tag{3.25}$$

Where: *bn*: The beat number

t_Q: The time of Q wave for the (*bn*) beat

t_R: The time of R wave for the (*bn*) beat

t_S: The time of S wave for the (*bn*) beat

f_s: The sampling frequency

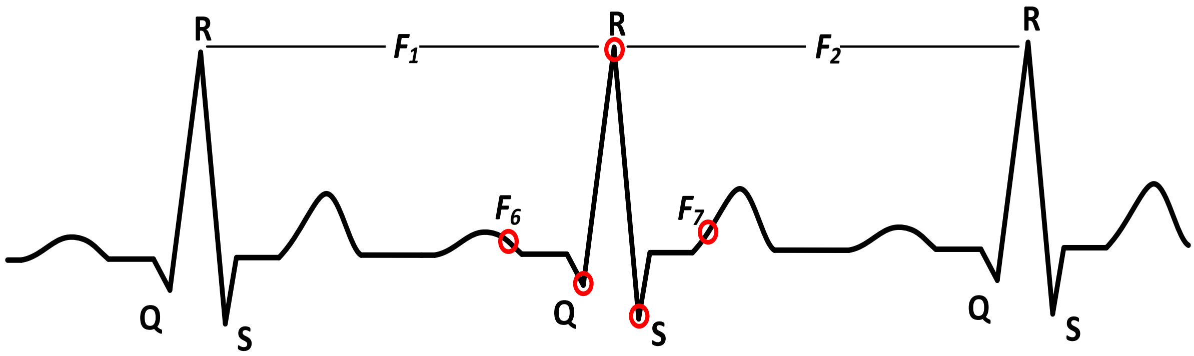

Figure 3.18 The RR-interval features.

3.5.3 Normality Heartbeat Classification

A feed-forward artificial neural network (ANN) is designed based on 42 hidden neurons as a first layer. The second layer is a single output neuron for the two classes, normal and abnormal. The output activation is a linear function, and the activations of the hidden neurons are Tanh. The database is divided into 70% of training data and 30% testing data. Then, the proposed ANN is trained using bayesian regularization backpropagation for better performance. Finally, the 42 neurons are selected as twice the number of the input features to classify performance improvement.

The classifier is designed using 42 neurons in the hidden layers and a single output neuron, as shown in Figure 3.17. The features are feed to the first layer, which contains 42 neurons fully connected and applies the Equations (2.8), (2.9), (2.10), and (2.11) for (i: 1, 2, ……21 no. of inputs and j: 1, 2, ……42 no. of hidden neurons)

The outputs of the hidden neurons are calculated from Equations (2.8) and (2.9), then the classifier output is calculated from Equations (2.10) and (2.11) to find the final class for normal and abnormal beats. The single hidden layer with a low number of hidden neurons (42); therefore, the classifier is low computational based on the low number of multiplications for this process.

3.6 Five Classes Heartbeat Classification Proposed Method

In this subsection, a method for 5-classes heartbeat classification based on a novel method named SMANN design will be described in detail. The results for evaluation with discussions will be presented in the next chapter with the same subsection sequence.

The ECG signal is an essential biomedical human body signal that shows heart activity and can diagnose CVDs. Therefore, many researchers investigate heartbeats detection and classification based on ECG to achieve a high-performance method. However, the main problem with improving performance is increasing the computation, such as in many existing methods. In this work, a novel artificial neural network (ANN) method named Selective-Mask Artificial Neural Network (SMANN) is proposed to improve the performance with low computational processes. Furthermore, A new mixture of features from reused the QRS-detection stage features and the others features from the RR-interval and between-RR are used to decrease the computation for features extraction.

Many methods have been proposed with high classification performance, but it is not easy to implement with their high computation. The big challenge for wearable (low computation) applications is improving the performance without adding more complexity. ANN is an essential machine learning technique for classification and recognition problems. Adding more hidden layers, extracting new features, and increasing the number of neurons per layer are fundamental ways to improve the classification for the ANN. On the other hand, this improvement will add more computation with more complexity for the classifier. The main objective is designing and implementing a wearable device for heartbeats detection and classification at real-time monitoring and diagnosis using a SMANN. The method is a high accuracy, low computation, and implementable. The SMANN will give the ANN a new dimension (selective or parallel) instead of the serial dimension for deep learning methods. SMANN does not consist of multi-layers like deep learning, high multiplication processes like convolutional, or tree with ANN used multi-design networks for each tree branch. Furthermore, this method is differed from ensemble neural networks by using a single network with multi masks, and the inputs for each mask are divided based on its properties. On the other hand, the ensemble using multi networks for any inputs.

The proposed method can be divided into three main parts: QRS-detection, Features extraction, and heartbeat classification, as shown in Figure 3.19. The QRS-detection prepares the ECG signal by filters and heartbeats detection. The features are extracted from the QRS morphology, the between-RR, and the RR-interval. A new classification method is proposed based on ANN, and it is SMANN.

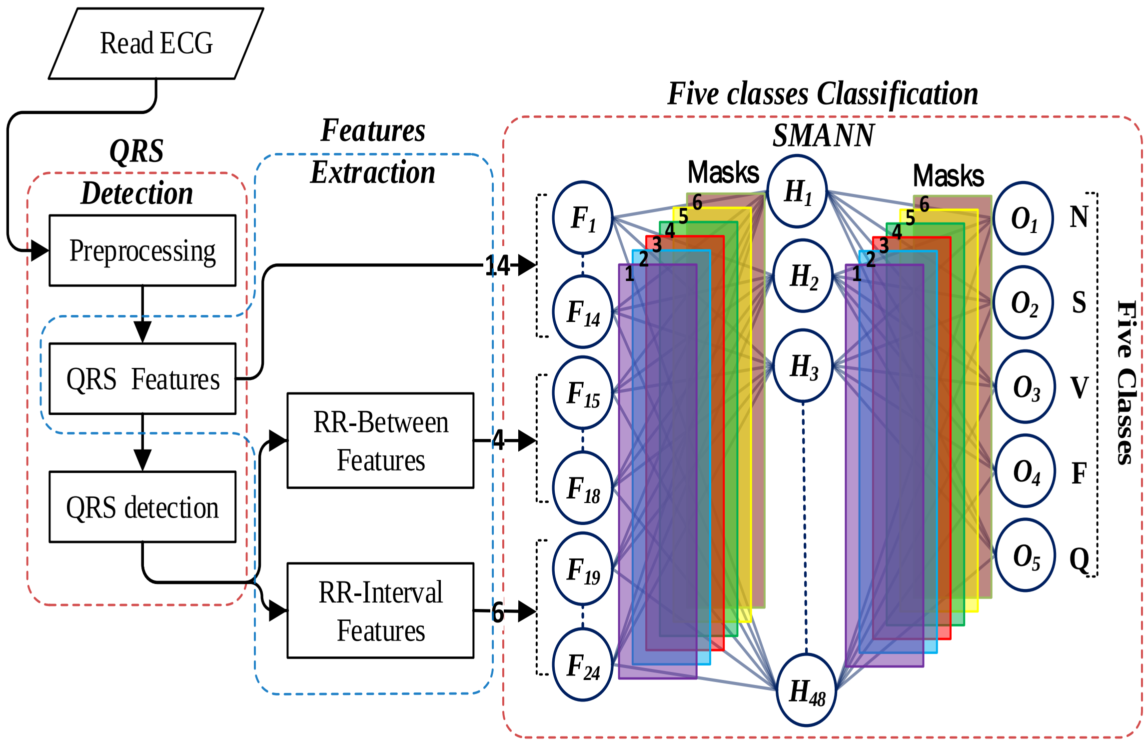

Figure 3.19 The proposed five classes classification method

3.6.1 QRS-Detection

The QRS-detection algorithm from section 3.2 is used for pre-processing and heartbeat detection. This algorithm is real-time, low computation, and high accuracy. In addition, the extracted features from this stage are reused mixed with the new features to reduce the processing for features extraction. Moreover, a (150 samples) moving average window filters the ECG signal to remove the noise and smooth the signal, as shown in Equation (3.1).

3.6.2 The Features Extraction

A new mixed features method is applied to achieve the purpose of the heartbeat classifier because the essential part of any classifier is the features extracted to enhance the performance. The features are divided into three-part. First, the QRS-complex has the most features for the ECG signal because, in the ECG signal processing operations, the QRS-complex is the highest energy part for the ECG signal. These are fourteen features extracted from the QRS shape using the QRS-detection algorithm in section 3.3 Second, the between-RR features are extracted four features from the ECG signal nearby the QRS-complex. The between-RR features are calculated from Equations (3.26) to (3.29), and Figure 3.20 shows these features.

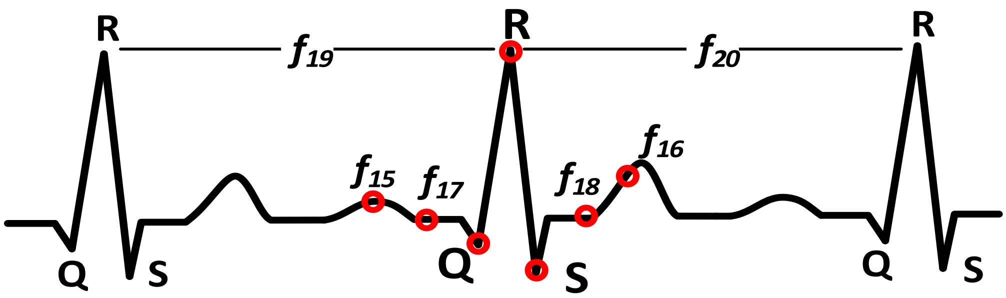

Figure 3.20 The between-RR and RR-interval features

- F_{15}: ECG signal level before 50 samples from Q

$$F_{15}(bn) = m(t_{Q(bn)} - (50/f_s)) \tag{3.26}$$

- F_{16}: ECG signal level after 50 samples from S

$$F_{16}(bn) = m(t_{S(bn)} + (50/f_s)) \tag{3.27}$$

- F_{17}: ECG signal level before 20 samples from Q

$$F_{17}(bn) = m(t_{Q(bn)} - (20/f_s)) \tag{3.28}$$

- F_{18}: ECG signal level after 20 samples from S

$$F_{18}(bn) = m(t_{S(bn)} + (20/f_s)) \tag{3.29}$$

Third, the RR-interval features are shown the regularity of the heartbeat and the heart rate. It determines the RR-before, RR-after, RR-after-average, RR-before-average, different RR, and the heart rate as six RR-interval features. The RR-interval features are calculated from Equations (3.30) to (3.35), and Figure 3.20 shows these features.

- F_{19}: RR before

$$F_{19}(bn) = \left(t_{R(bn)} - t_{R(bn-1)}\right) \tag{3.30}$$

- F_{20}: RR after

$$F_{20}(bn) = \left(t_{R(bn+1)} - t_{R(bn)}\right) \tag{3.31}$$

- F_{21}: The average of F_{19}

$$F_{21}(bn) = \frac{1}{7}\sum_{i=1}^{7} F_{19}\,(bn - i + 4) \tag{3.32}$$

- F_{22}: The average of F_{20}

$$F_{22}(bn) = \frac{1}{5}\sum_{i=1}^{5} F_{20}(bn - i + 3) \tag{3.33}$$

- F_{23}: The different RR after the average

$$F_{23}(bn) = |F_{20}(bn) - F_{21}(bn)| \tag{3.34}$$

- F_{24}: The average heart rate

$$F_{24}(bn) = 60\Big/\left(\frac{1}{3}\sum_{i=1}^{3} F_{20}(bn - i + 2)\right) \tag{3.35}$$

Where: *bn*: The heartbeat number.
t_Q: The Q wave time for the (*bn*) heartbeat.
t_R: The R wave time for the (*bn*) heartbeat.
t_S: The S wave time for the (*bn*) heartbeat.
f_s: The sampling frequency.

3.6.3 Five Classes Heartbeat Classification

The human brain solves many problems using a logical operation depending on select the region of the problem to be solved with more performance. The selection starts with a simple (yes or no), (right or left), (positive or negative), (true or false), or (grey or colour) moving with more selection for high order (complex) problems. For example, in image processing applications, the problem can be selected from two images: grey or colour. If the image is grey, the selection will be in the range of grey solution; if not, the selection will be in the range of colour solution. Adding more selection for this example by image size (small or large) so the range of solution will be four types (grey small, grey large, colour small, or colour large). More selection that gives more performance.

This logical brain operation can be used in machine learning to improve performance by using the selective operation to separate the problem and its solutions. The ANN is one of the essential machine learning techniques for classification and recognition problems. A new method has been proposed based on a multi ANN. The novel ANN proposed method named Selective-Mask ANN (SMANN) depends on the selection for the problem range to find the solution in this range. So, the input data are divided into multi-range based on a knowledge base.

The ANN weights and biases matrices are produced from training the network by the database. Different features were extracted from the database using different methods. These features are the inputs for training the ANN to classify these inputs. After training, the network weights and biases matrices are applied for all input features from the database. Single weights and biases matrices are produced from training for each network layer and applied for classification. Adding more features, using a new technique for extracting these features, and changing the network design, like adding more layers, are the procedure to improve the network performance. All these procedures are increasing the computation with improving the performance.

A knowledge base is created depending on the dominant inputs to divide the data with the same properties. This knowledge base is a starting basis for the ANN before the supervision learning or training. So, the ANN will not start to learn from zero. In the ECG signal, the heart rate and the heartbeat regularity are the two most properties that can divide the data into subtypes. The subtypes of heartbeats regularity are: regular and irregular, and subtypes of heartrate are: normal, low, and high. The normal heart rate is from 60-120 bpm, the low heart rate is lowest than 60 bpm, and the high heart rate is the highest than 120 bpm. Figure 3 shows six ranges for the ECG database: regular- (normal, low, high), irregular- (normal, low, high). The beats numbers in Figure 3.21 are represented the beats according to the MBADB records for each subtype.

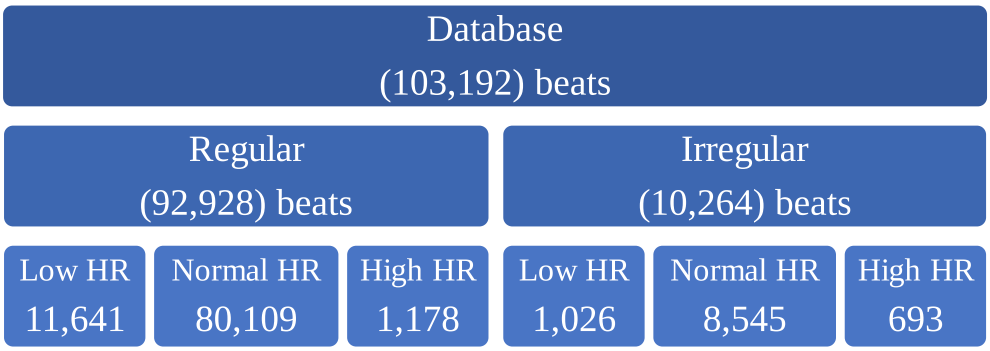

Figure 3.21 The MBADB subtypes

The weight and bias matrices for the ANN can be called the mask for this network. The SMANN is produced multi masks for the same problem and same ANN design based on separating the features extracted from the database by the dominant properties to be selective. It applies each mask for the inputs (features) based on the selective property. Figure 3.22 shows a general diagram of the SMANN method for a single hidden layer and can be expanded for more hidden layers.

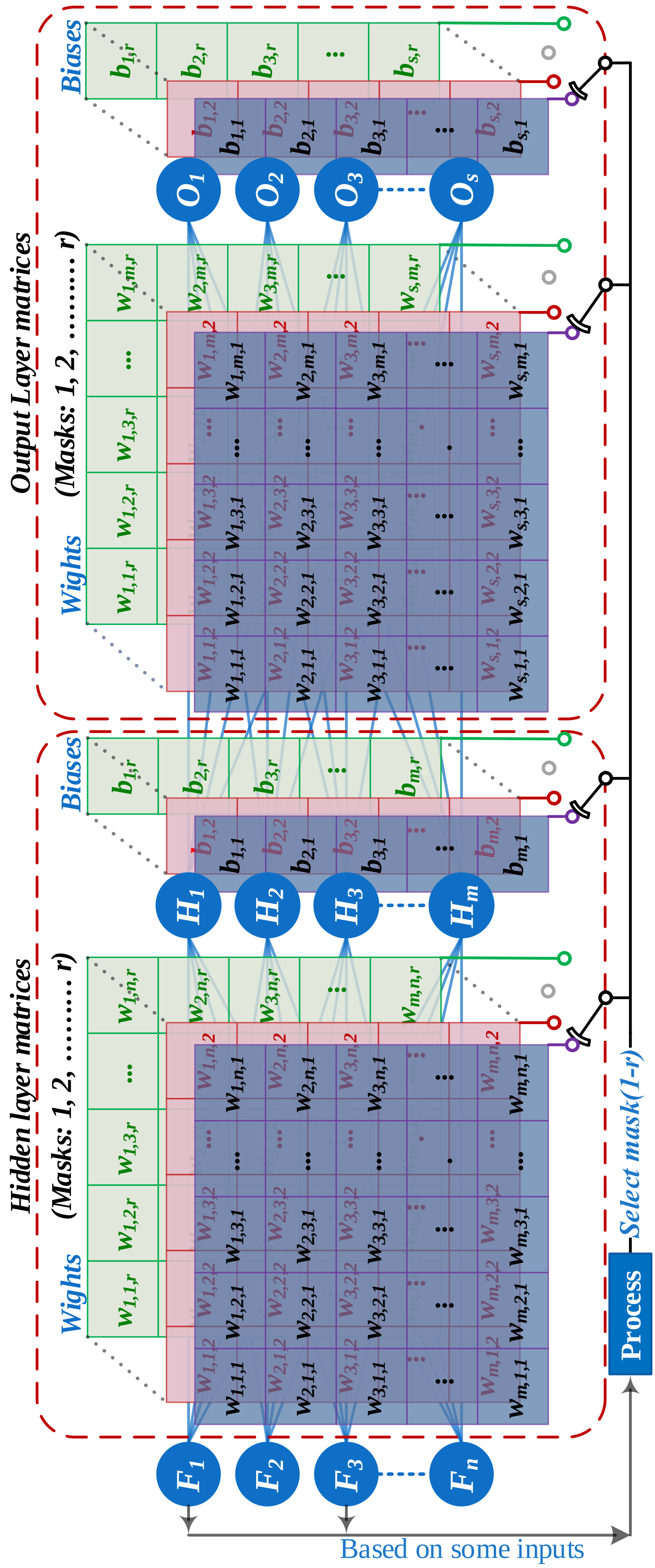

Figure 3.22 General diagram of a SMANN for a single-layer

The SMANN can be defined as a fixed layers ANN design with multi masks (weights and biases matrices) for each layer. The mask is a two-dimension matrix for weights and a one-dimension matrix for biases, as shown in Figure 3.22 with a different colour. The SMANN has several distinct characteristics:

- The mask dimension (hidden mask (m, n) or output mask (s, m)) for each layer is fixed for all inputs.
- The number of hidden layers design should be constant.
- Based on the SMANN designer:
  - For all selective properties, the number of inputs (n), hidden neurons (m), and outputs (s) can be fixed using fixed masks.
  - Some inputs, hidden, and outputs neurons can be eliminated using zeros values for rows or columns of weight and bias matrix corresponding to the selective mask for any selective property.

In this work, a feed-forward SMANN is designed with a single hidden layer. The hidden layer has 48 hidden neurons (m) and 24 input features (n). Also, the number of masks is 6 (r): regular-normal, regular-low, regular-high, irregular-normal, irregular-low, and irregular-high. The outputs are five classes: N, S, V, F, and Q.

$$H_{net(j)} = (Hb_j + \sum_{i=1}^{24(n)} Hw_{i,j,k} \times F_i\ ) \tag{3.36}$$

$$H_j = \ Tanh\left(H_{net(j)}\right) \tag{3.37}$$

For all (*j: 1-48 (m)*) hidden neurons using one of the selective masks (*k: 1,2, or 6 (r)*).

$$Onet_l = Ob_l + \sum_{j=1}^{48(m)} Ow_{\,l,j,k} \times H_j \tag{3.38}$$

$$O_l = \begin{cases} 1 & Onet_l > 0 \\ 0 & Onet_l \le 0 \end{cases} \tag{3.39}$$

For all (*l: 1-5 (s)*) output neurons using one of the selective masks (*k: 1,2, or 6 (r)*).

Where: *i*: 1, 2, …… 48 (*m*-Hidden neurons)

j: 1, 2, …… 24 (*n*-Input Features)

k:1, 2, …… 6 (*r*-Selective Masks)

l:1, 2, …… 5 (*s*-Outputs Classes)

H_{net}: Hidden layer net.

Hb: Hidden layer bias.

Hw: Hidden layer weight.

H: Output for the Hidden layer.

O_{net}: Output layer net.

Ob: Output layer bias.

Ot: Output layer weight.

O: Output.

Table 3.4 The Five classes and their corresponding outputs

O_1	**O_2**	**O_3**	**O_4**	**O_5**	**Class**
1	0	0	0	0	N
0	1	0	0	0	S
0	0	1	0	0	V
0	0	0	1	0	F
0	0	0	0	1	Q

A two-layer feed-forward network is used with Tanh hidden and SoftMax output neurons. The equations are calculated for (i) inputs from (1) to (n=24), (j) hidden neurons from (1 to m=48), (k) selective masks from (1 to r=6), and (l) output classes from (1 to s=5). The outputs of the hidden neurons are calculated from Equations (3.36) and (3.37), then the classifier output is calculated from Equations (3.38) and (3.39) to find the final classes from one of the five beats types. All equations are calculated for a single mask (k: 1,2, or 6 (r)) at a time, depending on the selective input features properties. The (k) value is a constant for each selective input; the (i) and (j) are all values to calculate the overall network equations to find the SMANN output for a single mask with constant (k). For this design, the classifier is low computational based on the low process.

Chapter 4: Results and Discussions

Contents

Chapter Four:
Results and Discussions

4.1 Introduction

The results and discussions for the thesis objectives are presented in this chapter. The results for each objective are described in the same sequence as the previous chapter. Therefore, the subsection presents results and discussions for a specific objective. The results are connected by each other to achieve a high accuracy real-time low computational wearable healthcare system based on AI and IoT for heartbeats detection and classification.

First, design and implement a prototype wearable system that achieves low computation and high accuracy for the QRS-detection and classification using Node-MCU with IoT. ***Second***, a QRS-detection algorithm based on low error detection, high accuracy, and low computation was evaluated based on the MBADB. Furthermore, the algorithm evaluation was tested based on the QT database. The results for evaluation are presented for both databases. ***Third,*** the MBADB heartbeats number and the MATLAB Waveform Database Toolbox (WFDB) function results are described in order to standardize the heartbeat used for the detection algorithm. Moreover, these heartbeat results are used for the rest of the methods. ***Fourth,*** the low computation and high accuracy classification algorithm results for normal and abnormal heartbeats based on new mixed and reused features are presented after the method evaluation based on the MBADB. ***Fifth,*** the high accuracy classification method results for the 5-AAMI classes heartbeats according to SMANN for low computational application are described according to method evaluation based on the MBADB.

4.2 The Smart Wearable System based on IoT Results and Discussions

The five classes classification method consists of the QRS-detection algorithm and the developed SMANN classification method for five classes. Therefore, the five classes method is the overall algorithm that was implemented in the wearable device as a prototype. The overall algorithm as shown in Figure 3.5 was evaluated in the next subsection (4.6) using the MATLAB 2020b program. The high performance and the low computational are the overall algorithm features for heartbeat detection and classification to five main classes. As a result, the wearable system implements the five classes heartbeat classification method that contains the QRS-detection algorithm.

The overall algorithm was programmed into the microcontroller (node-MCU) using The Arduino Integrated Development Environment (Arduino-IDE). The IDE software is an open-source application based on C and C++ programming to write the programming codes and upload these codes to any compatible boards after verifying and compiling these codes. The node-MCU is one of the compatible boards that can be programmed using Arduino-IDE. Furthermore, the implementation code lines are fit into the Microcontroller because the same mask dimension is using in each layer. In other words, the implementation for the ANN is a simple with selective mask according to the input properties. Consequently, for each selective input, the code will select the mask for this input. Thus, the code line is a simple ANN code with multi masks based on the selective input properties.

In order to evaluate the performance of the wearable system, two procedures were applied. ***First***, the system was evaluated and tested according to the identical data records used in the previous subsection for evaluating the five classes heartbeat classification method. ***Second***, the actual ECG signal reads from a human body by the ECG card.

First:

The first evaluation procedure applied the ECG signal for the lead-II from the MBADB to compare these results with the MATLAB evaluation and the valid results from the annotation file. Therefore, the node-MCU read the ECG signal directly without using the ECG card. Then, in order to add the execution time for the program of the analogue-read command, the program contains the analogue-read command code without using the value for the first procedure.

The system (node-MCU) analyzed the ECG samples by executing the heartbeat detection and classification programming algorithm. The system connected to the computer through the serial connection. The computer serial port for the Arduino-IDE displayed the running progress and the algorithm outputs are shown in Figure 4.1. The outputs are:

- The ECG samples.
- The non-QRS values.
- The detected QRS values and features for ANN.
- The QRS polarity was positive or negative.
- The classification QRS features.
- The classification outputs values.
- The class for the QRS.
- The following report:
    - Current heart rate.
    - Current heartbeat class.
    - Count of each class.
    - Average heart rate.
    - Maximum heart rate.
    - Minimum heart rate.

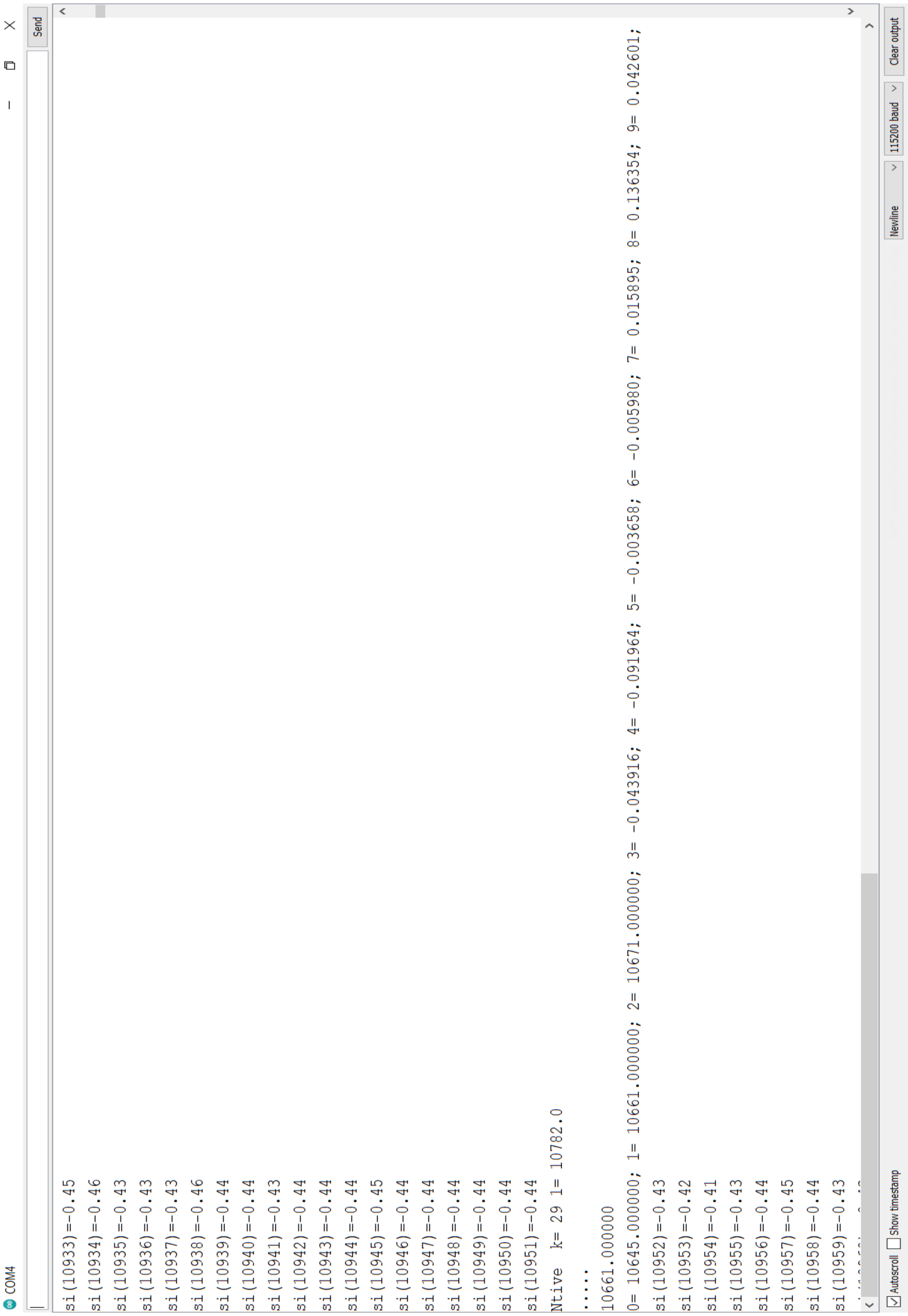
COM4
Send
si(10933)=-0.45
si(10934)=-0.46
si(10935)=-0.43
si(10936)=-0.43
si(10937)=-0.43
si(10938)=-0.46
si(10939)=-0.44
si(10940)=-0.44
si(10941)=-0.43
si(10942)=-0.44
si(10943)=-0.44
si(10944)=-0.44
si(10945)=-0.45
si(10946)=-0.44
si(10947)=-0.44
si(10948)=-0.44
si(10949)=-0.44
si(10950)=-0.44
si(10951)=-0.44
Ntive k= 29 1= 10782.0
.....
10661.000000
0= 10645.000000; 1= 10661.000000; 2= 10671.000000; 3= -0.043916; 4= -0.091964; 5= -0.003658; 6= -0.005980; 7= 0.015895; 8= 0.136354; 9= 0.042601;
si(10952)=-0.43
si(10953)=-0.42
si(10954)=-0.41
si(10955)=-0.43
si(10956)=-0.44
si(10957)=-0.45
si(10958)=-0.44
si(10959)=-0.43
Autoscroll
Show timestamp
Newline
115200 baud
Clear output

(a)

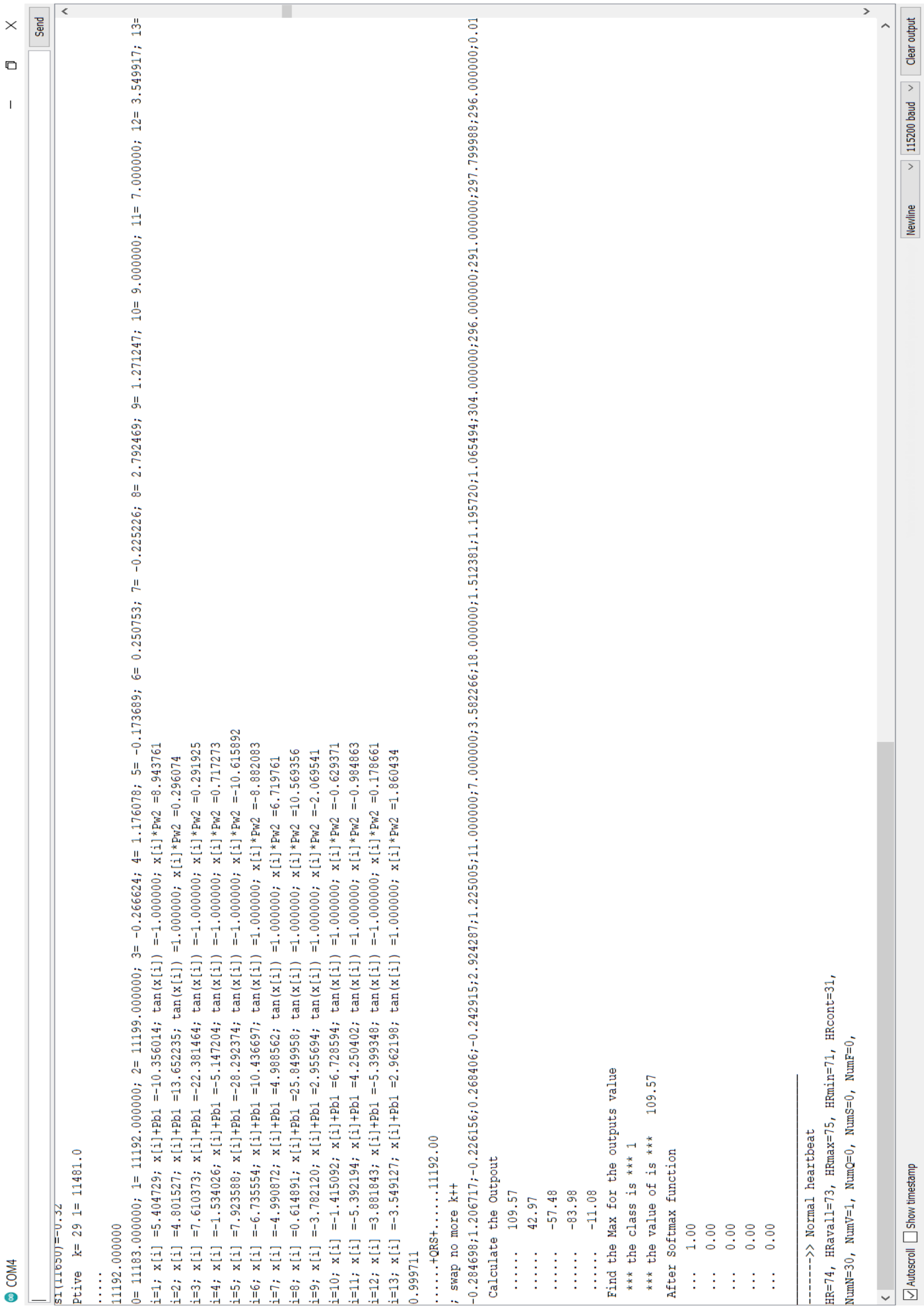

(b)

Figure 4.1 Serial port results for Arduino IDE (a) QRS- detection (b) Classification

The patient report that contains some of these outputs is uploaded to the mobile application through IoT for real-time monitoring. So, the mobile is displayed the vital patient condition as a report. This report is updated every 10 sec (the update time can be changed according to the doctor's decision and the internet speed). Moreover, this application controls the system by the ON/OFF button. The patient report in the mobile application is shown in Figure 4.2.

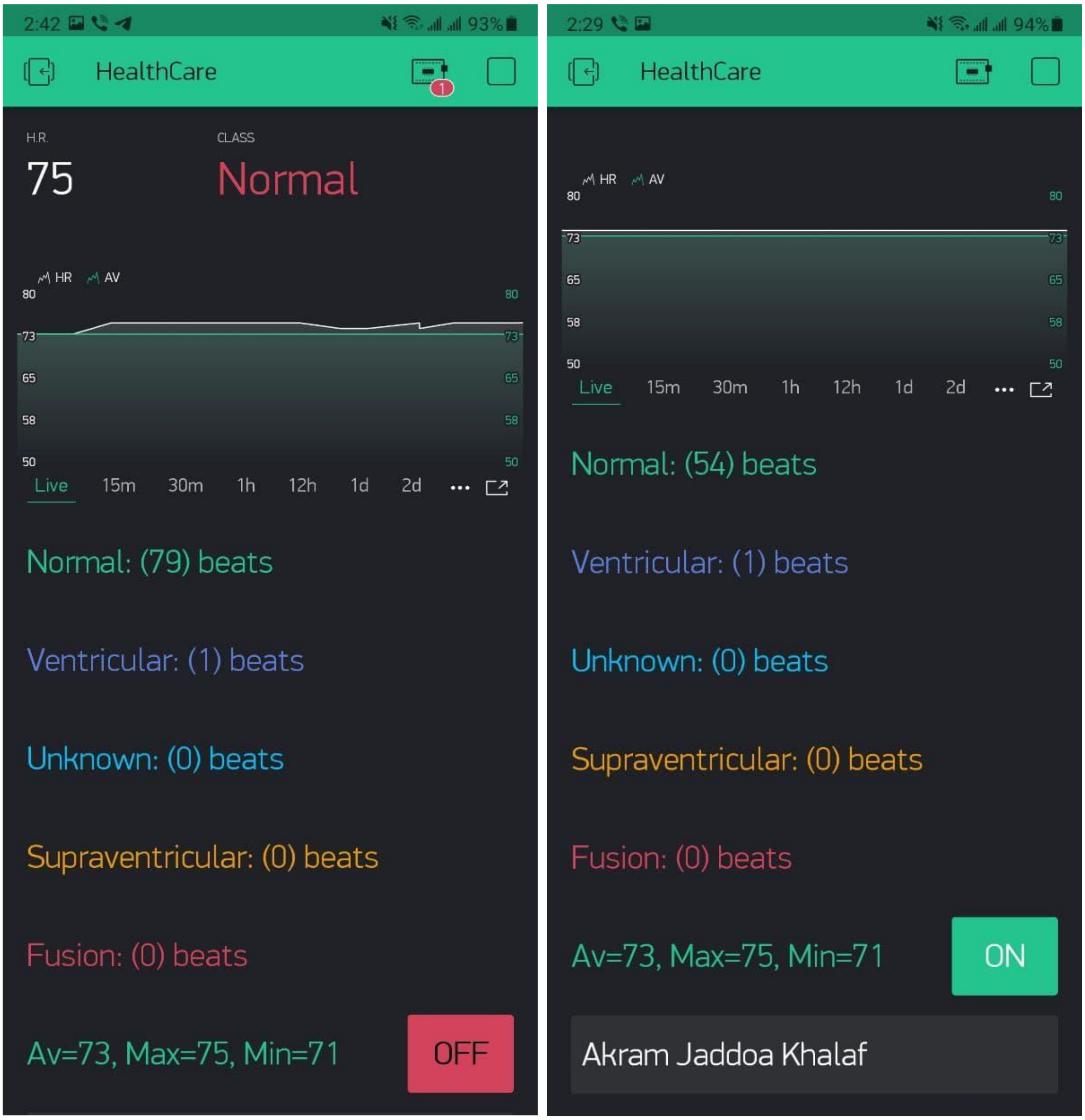

Figure 4.2 The mobile patient reports

The system stores the ECG samples and the patient report in the microSD-Card for offline analysis and data logger. The mobile application uploads the patient name that was entered using the application to store the name in the microSD-Card file, as shown in Figure 4.3.

Thus, for comparing the system results with the software evaluation, the results for hardware implementation are equivalent to the MATLAB results as summarized in Table 4.9, except for some missing results due to the program's initialization at starting. The running times were calculated, and the delay times:

- The average time for the first QRS-detection is 664 samples (1.84 s).
- The average time for the first classification is 2404 samples (6.678 s).
- The average QRS-detection and classification delay are calculated with an average of 237 samples (0.658 s).

Second:

Finally, the system was tested actual ECG signal reads from a human body. The card reads the ECG signal from the body at the same sampling frequency (360). After that, the node-MCU analyzed the ECG samples by executing the heartbeat detection and classification programming algorithm. The system results are promising for low computation wearable CDS devices based on IoT for long-time monitoring.

The device power consumption is calculated for the typical and the measured values of the hardware device parts. The Node-MCU, ECG card, and microSD-card are the device parts. The electrical energy Equation (4.1) is shown below to estimate the device battery life. The estimation is based on two different capacity batteries. The first is a serial two battery with 3.85*v* and 1850*mAh*; the second is a power bank with 5*v* and 3800*mAh*.

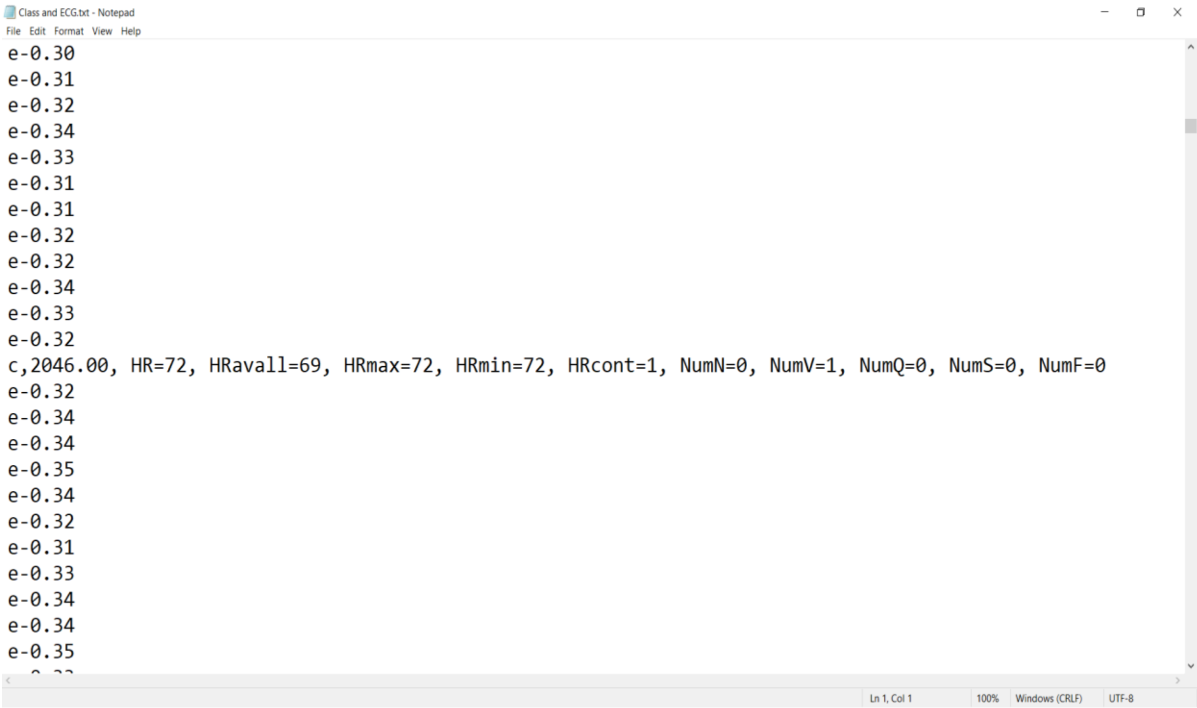

Class and ECG.txt - Notepad

File Edit Format View Help

```
e-0.30
e-0.31
e-0.32
e-0.34
e-0.33
e-0.31
e-0.31
e-0.32
e-0.32
e-0.34
e-0.33
e-0.32
c,2046.00, HR=72, HRavall=69, HRmax=72, HRmin=72, HRcont=1, NumN=0, NumV=1, NumQ=0, NumS=0, NumF=0
e-0.32
e-0.34
e-0.34
e-0.35
e-0.34
e-0.32
e-0.31
e-0.33
e-0.34
e-0.34
e-0.35
```

Ln 1, Col 1 100% Windows (CRLF) UTF-8

(a)

Class and ECG.txt - Notepad

File Edit Format View Help

```
e-0.38
e-0.38
e-0.38
e-0.39
e-0.40
e-0.39
e-0.38
e-0.38
e-0.38
e-0.38
e-0.40
e-0.38
c,25199.00, HR=75, HRavall=73, HRmax=75, HRmin=71, HRcont=80, NumN=79, NumV=1, NumQ=0, NumS=0, NumF=0
e-0.38
e-0.37
e-0.38
e-0.38
e-0.40
e-0.38
e-0.38
e-0.38
e-0.38
e-0.38
e-0.40
```

Ln 1, Col 1 100% Windows (CRLF) UTF-8

(b)

Figure 4.3 Micro-SD card file (a) at starting (b) at running

$$Energy(WattHour) = Power(Wat) \times Time(hour) \qquad (4.1)$$

$$E(Wh) = P(W) \times T(h)$$

The energy for the battery can be calculated from the following equations:

$$E_{battery}(Wh) = \left(2 \times 3.85(v)\right) \times 1850(mAh) \qquad (4.2)$$

$$E_{battery} = 14.245\ Wh$$

$$E_{powerbank}(Wh) = 5(v) \times 3800(mAh) \qquad (4.3)$$

$$E_{powerbank} = 19\ Wh$$

The Components typical power per each device part is determined from the following equations:

$$P_{nodeMCU}(W) = 3.3(v) \times 140(mA) \qquad (4.4)$$

$$P_{nodeMCU} = 462\ mW$$

$$P_{ECG}(W) = 3.3(v) \times 4.5(mA) \qquad (4.5)$$

$$P_{ECG} = 14.85\ mW$$

$$P_{microSD}(W) = 3.3(v) \times 30(mA) \tag{4.6}$$

$$P_{icoSD} = 99\ mW$$

The device battery life for typical power are:

$$T(h) = \frac{E_{battery}(Wh)}{P_{total}(W)} = \frac{E_{battery}(Wh)}{(P_{nodeMCU} + P_{ECG} + P_{microSD})(W)} \tag{4.7}$$

$$T_{battery} = \frac{14.245\ Wh}{(462 + 14.85 + 99)(mW)} = 24.74\ h \tag{4.8}$$

$$T_{powerbank} = \frac{19\ Wh}{(462 + 14.85 + 99)(mW)} = 32.99\ h \tag{4.9}$$

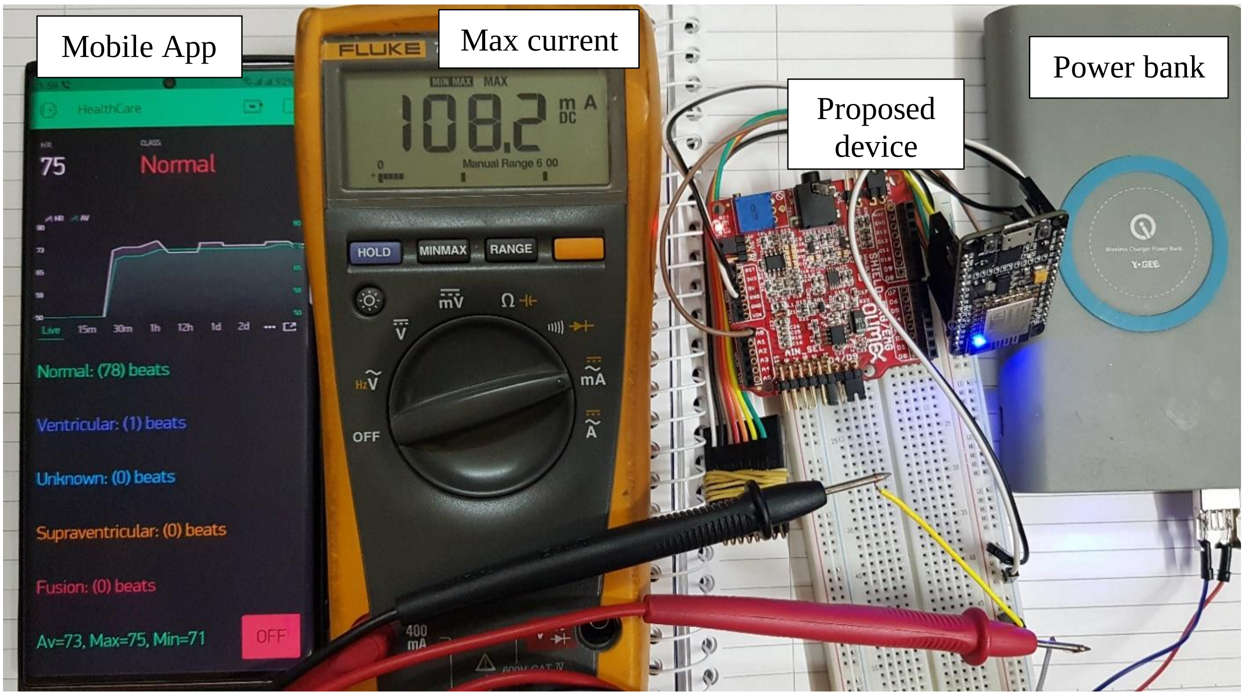

Figure 4.4 Measuring the maximum device power

The device measured power was calculated using an accurate multimeter, as shown in Figure 4.4. The device battery life for measured power are:

$$T(h) = \frac{E_{battery}(Wh)}{P_{\text{measured}}\,(W)} \tag{4.10}$$

$$T_{battery} = \frac{14.245\ Wh}{5v \times 108.2\ mA} = 26.33\ h \tag{4.11}$$

$$T_{powerbank} = \frac{19\ Wh}{5v \times 108.2\ mA} = 35.12\ h \tag{4.12}$$

Where: *E*: energy (Wh).

P: power (W).

T: time (h)

h: hour.

W: watt.

The battery life for the system based on the previous calculation is more than 24 hours (one day as shown in Equation (4.8)). The battery life can be reached 35 hours (Equation (4.12)) using the power bank. Therefore, the wearable system can be used for long-time patient monitoring.

The system cost is about (52$) according to the following parts prices:

No	Item	Price $
1	Node-MCU	7
2	ECG-card	24
3	SD	3
4	Cable	8
5	Battery	10
Total		52 $

4.3 QRS-Detection Proposed Algorithm Evaluation

The algorithm performance was evaluated using the MBADB with variable ECG signals used for testing and evaluating because it contains a variable ECG signal and variable noise. Furthermore, it is widely used from many other approaches for comparison purposes. This database contains 48 records with 30 minutes, two channels, 360 samples per second, and 11-bit resolution. In addition, the database contains positive and negative QRS, high and low QRS, baseline wander, power line interference, muscle noise, regular and irregular heartbeats, and normal and unnormal wave. All mentioned previously makes this database is suitable for evaluation reasons. Therefore, the first ECG channel is used from the database.

The proposed QRS-detection algorithm was implemented using the MATLAB program for software evaluation. The results are to evaluate the True Positive (TP), False Negative (FN), and False Positive (FP) values.

Sensitivity (Se), Positive_Predicitvity (PP), and Detection_Error_Rate (DER) illustrated in Equations (2.22),(2.23), and (2.24) are calculated for entirely database records only excepted the ventricular flutter beats in record 207 that are not included to evaluate the algorithm performance and compare the results with the other methods. Table 4.1 demonstrates the detection algorithm results for the MBADB. For example, record 105 and the overall record are determined as shown in the following calculations:

$$Se_{105}\% = \frac{TP}{TP + FN} \times 100 = \frac{2572}{2572 + 5} \times 100 = 99.81$$

$$PP_{105}\% = \frac{TP}{TP + FP} \times 100 = \frac{2572}{2572 + 15} \times 100 = 99.42$$

$$DER_{105}\% = \frac{FP + FN}{TP} \times 100 = \frac{15 + 5}{2572} \times 100 = 0.778$$

$$Se_{overall}\% = \frac{TP}{TP + FN} \times 100 = \frac{109494}{109494 + 130} \times 100 = 99.881$$

$$PP_{overall}\% = \frac{TP}{TP + FP} \times 100 = \frac{109494}{109494 + 115} \times 100 = 99.895$$

$$DER_{overall}\% = \frac{FP + FN}{TP} \times 100 = \frac{115 + 130}{109494} \times 100 = 0.224$$

The results show a promising QRS detection with high overall sensitivity and predictivity of 99.86% and 99.89%, respectively, and a low detection error rate of 0.224%. Moreover, it achieved a 99.75% average detection accuracy. A MATLAB 2020b 64-bit in 2.6 GHz Intel Ci7 computer is used for performance evaluation. The average computation time for the database of 30-minutes records is (1.196sec.), which is a low computation algorithm.

The database has difficult records for existing QRS-detection methods because it suffers from different types of noise, artifacts, irregular beats, and unnormal waves. Therefore, most detection errors occur from these records. Table 4.2 demonstrates the proposed algorithm, and some other algorithms are compared to the detection results errors (FP, FN) for specific records.

These results are based on the technique of searching all potential QRS points (QRS*) and separate these points depending on the QRS polarity. The algorithm improves the performance for negative QRS as in records (108,114)

Table 4.1 The QRS-detection results for MIT-BIH database records

Records No.	TP (Beats)	FP (Beats)	FN (Beats)	FP+FN=FT (Beats)	Se (%)	PP (%)	DER (%)
100	2273	0	0	0	100	100	0
101	1865	2	0	2	100	99.89	0.107
102	2187	0	0	0	100	100	0
103	2084	0	0	0	100	100	0
104	2229	1	0	1	100	99.96	0.045
105	2572	15	5	20	99.81	99.42	0.778
106	2027	0	0	0	100	100	0
107	2137	0	1	1	99.95	100	0.047
108	1763	2	5	7	99.72	99.89	0.397
109	2532	0	0	0	100	100	0
111	2124	0	1	1	99.95	100	0.047
112	2539	0	0	0	100	100	0
113	1795	0	0	0	100	100	0
114	1879	1	3	4	99.84	99.95	0.213
115	1953	0	0	0	100	100	0
116	2412	0	18	18	99.26	100	0.746
117	1535	0	0	0	100	100	0
118	2278	1	0	1	100	99.96	0.044
119	1987	0	0	0	100	100	0
121	1863	0	1	1	99.95	100	0.054
122	2476	0	0	0	100	100	0
123	1518	0	0	0	100	100	0
124	1619	1	0	1	100	99.94	0.062
200	2601	1	1	2	99.96	99.96	0.077
201	1963	0	8	8	99.59	100	0.408
202	2136	1	3	4	99.86	99.95	0.187
203	2980	25	23	48	99.23	99.17	1.611
205	2656	0	2	2	99.92	100	0.075
207	1860	30	11	41	99.41	98.41	2.204
208	2955	7	19	26	99.36	99.76	0.880
209	3005	2	0	2	100	99.93	0.067
210	2650	1	9	10	99.66	99.96	0.377
212	2748	1	0	1	100	99.96	0.036
213	3251	0	2	2	99.94	100	0.062
214	2262	2	3	5	99.87	99.91	0.221
215	3363	0	0	0	100	100	0
217	2208	1	2	3	99.91	99.95	0.136
219	2154	0	0	0	100	100	0
220	2048	0	0	0	100	100	0
221	2427	1	1	2	99.96	99.96	0.082
222	2483	1	2	3	99.92	99.96	0.121
223	2605	0	1	1	99.96	100	0.038
228	2053	12	6	18	99.71	99.42	0.877
230	2256	0	0	0	100	100	0
231	1571	0	0	0	100	100	0
232	1780	7	0	7	100	99.61	0.393
233	3079	0	0	0	100	100	0
234	2753	0	3	3	99.89	100	0.109
overall	109494	**115**	**130**	**245**	**99.881**	**99.895**	**0.224**

comparing with other methods. Detect the true QRS using two simple decisions based on the selected features. In addition to the slope, the level and the remaining features significantly reduce error detection. Some of these features are shown in Equation (3.15) and Equation (3.16) are reduced FN for high-frequency and noisy records (105, 200, 203, 222). The premature ventricular contraction these features are detected with low errors like records (116, 200, 203, 208, and 228).

Table 4.2 QRS detection methods comparison for specific records.

Rec. No.	***TP (B)***	**The proposed Method**			**[28]**			**[6]**			**[7]**			**[32]**			**[27]**			**[29]**		
		FP (B)	***FN (B)***	***FT (B)***	***FP (B)***	***FN (B)***	***FT (B)***	***FP (B)***	***FN (B)***	***FT (B)***	***FP (B)***	***FN (B)***	***FT (B)***	***FP (B)***	***FN (B)***	***FT (B)***	***FP (B)***	***FN (B)***	***FT (B)***	***FP (B)***	***FN (B)***	***FT (B)***
104	2229	1	0	**1**	12	12	**24**	6	6	**12**	1	0	**1**	113	2	**115**	12	18	**30**	9	4	**13**
105	2572	15	5	**20**	35	12	**47**	40	34	**74**	67	22	**89**	45	5	**50**	15	44	**59**	12	16	**28**
108	1763	2	5	**7**	21	8	**29**	34	52	**86**	199	22	**221**	79	115	**194**	25	35	**60**	34	15	**49**
114	1879	1	3	**4**	42	71	**113**	5	14	**19**	3	17	**20**	3	2	**5**	1	4	**5**	3	5	**8**
116	2412	0	18	**18**	2	23	**25**	1	30	**3**	3	22	**25**	3	22	**25**	4	15	**19**	11	8	**19**
200	2601	1	1	**2**	6	3	**9**	12	12	**24**	6	3	**9**	44	2	**46**	11	15	**26**	2	4	**6**
203	2980	25	23	**48**	17	74	**91**	19	182	**201**	53	30	**83**	80	27	**107**	25	36	**61**	22	25	**47**
208	2955	7	19	**26**	1	66	**67**	4	26	**30**	4	14	**18**	4	21	**25**	5	25	**30**	9	14	**23**
222	2483	1	2	**3**	5	7	**12**	0	1	**1**	101	81	**182**	4	9	**13**	2	2	**4**	3	1	**4**
228	2053	12	6	**18**	19	3	**22**	7	12	**19**	25	5	**30**	184	4	**188**	27	57	**84**	30	15	**45**

This algorithm presents a hybrid technique based on a decision tree and artificial neural networks for QRS detection. It consists of a particular five stages compared to the included three stages of the other methods. The most stages of other methods are included because it consists of more than one operation in each stage. On the other hand, our algorithm stage consists of one operation. Thus, there are several distinct features for the proposed algorithm:

- The algorithm is based on searching all possible QRS points (QRS^*) using the max or min moving window and remove the other point to reduce the computation. So, the ECG samples are reduced by the QRS* points only to increase the speed.

- The QRS*s are positive and negative depending on the peak polarity to improve the accuracy. Furthermore, there are no squaring samples to reduce the multiplication.
- The features extracted from QRS* are not depending on slope only. Moreover, depending on the level between these points and time to improve the detection.
- Two simple ANN's are used for QRS* positive and QRS* negative with high classification accuracy because it depends on the polarity.
- The low computation is from less data, no squaring all samples, and no back search for missing peaks based on RR interval calculation used for the conventional methods.

Finally, the overall evaluation performance comparison of the proposed algorithm with some other algorithm using the same MBADB are summarized in Table 4.3. These results describe that the performance of the proposed algorithm is achieved better than the other methods.

Table 4.3 Comparison of QRS-detection methods performance

Ref. No.	Year	Se (%)	PP (%)	DER (%)
The proposed method	**2020**	**99.881**	**99.895**	**0.224**
[30]	2019	99.833	99.881	0.287
[11]	2019	99.858	99.850	0.293
[29]	2018	99.832	99.834	0.334
[27]	2012	99.642	99.824	0.535
[26]	2009	99.769	99.642	0.590
[7]	1985	99.762	99.565	0.675
[6]	2015	99.442	99.679	0.883
[28]	2015	99.559	99.516	0.929
[32]	2020	99.240	99.383	1.387

The results for QRS detection algorithm of samples database records and of samples real case human body are showing in Figure 4.5 and Figure 4.6:

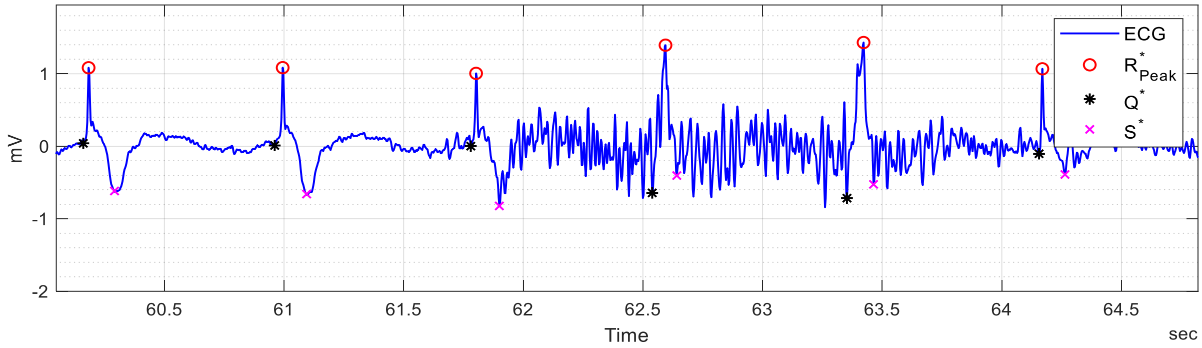

(a)

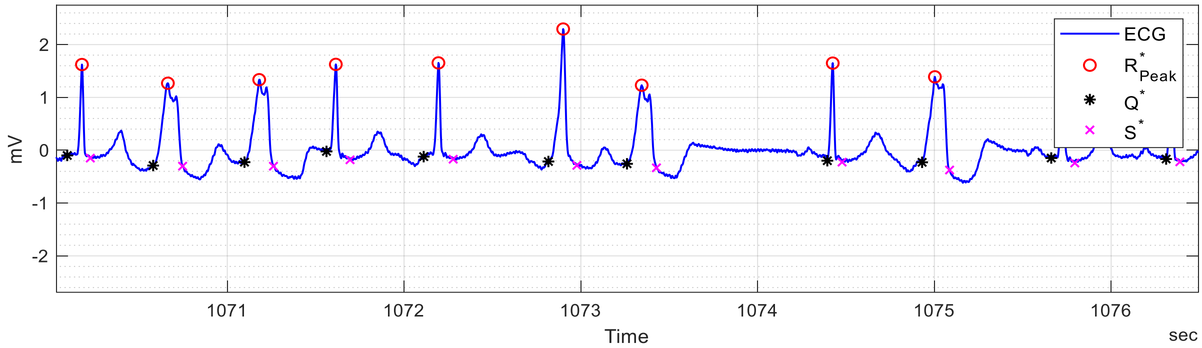

(b)

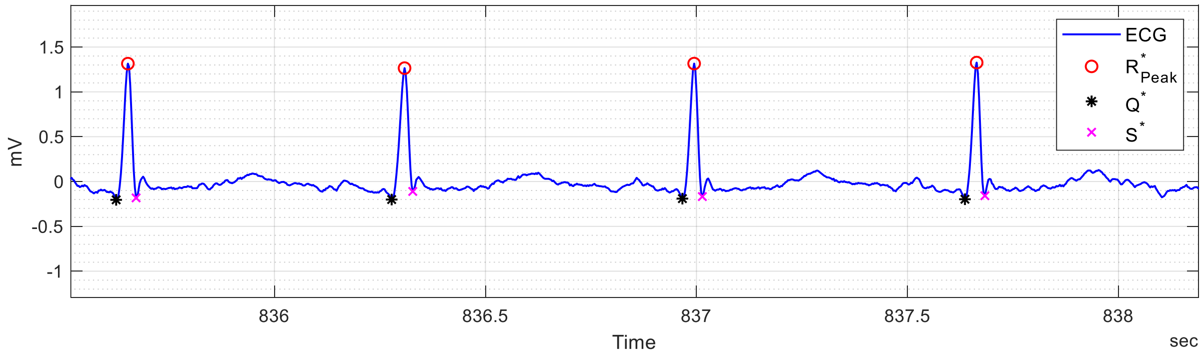

(c)

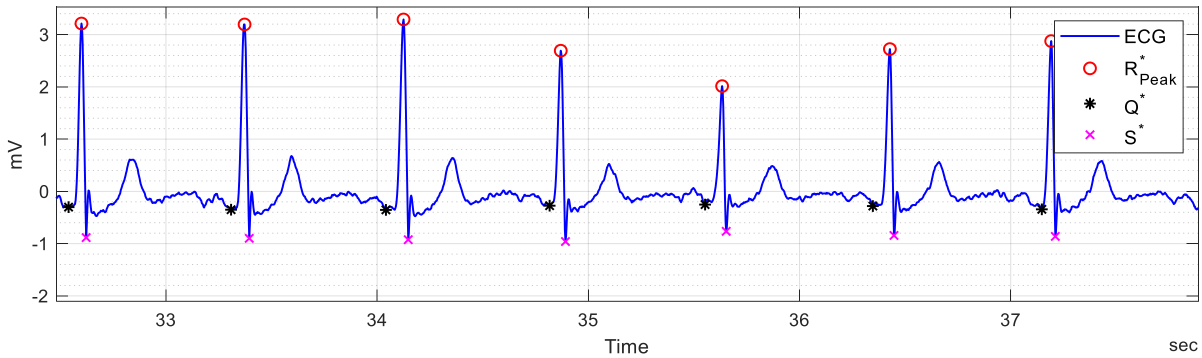

(d)

Figure 4.5 The results for records (a) 104 (b) 208 (c) 205 (d) 116

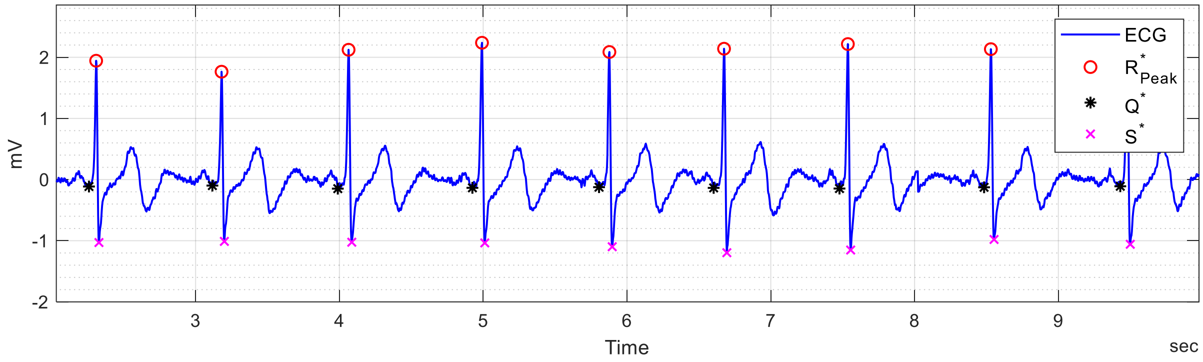

(a)

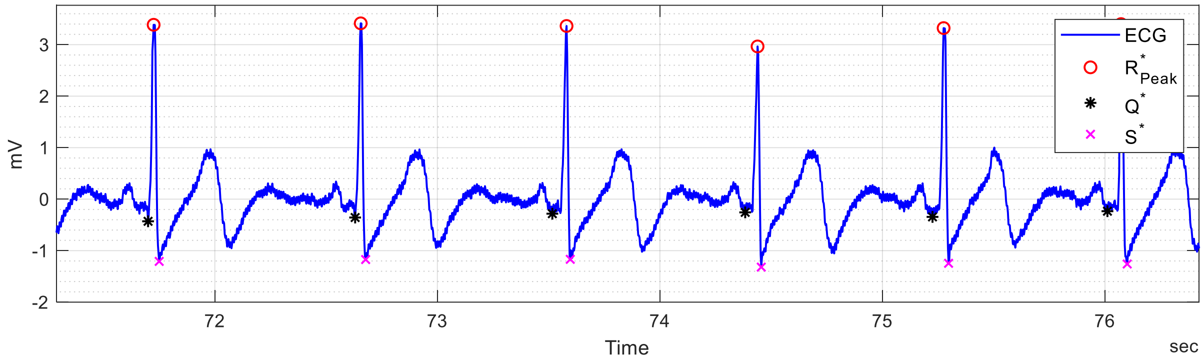

(b)

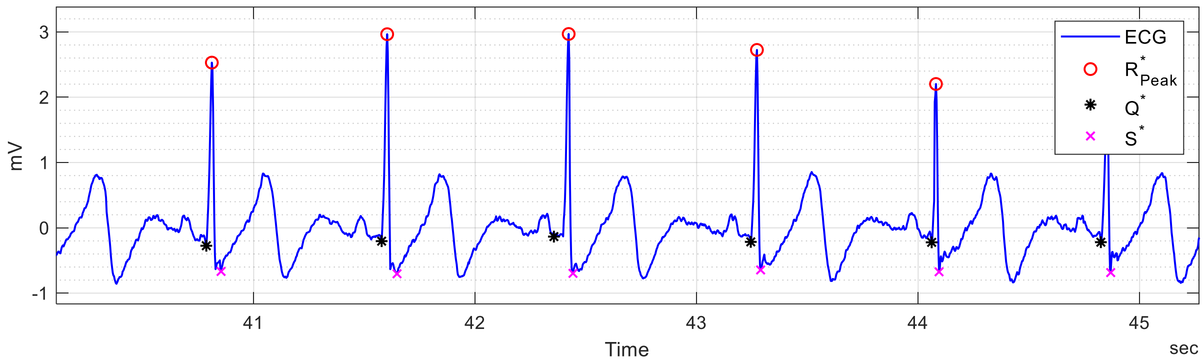

(c)

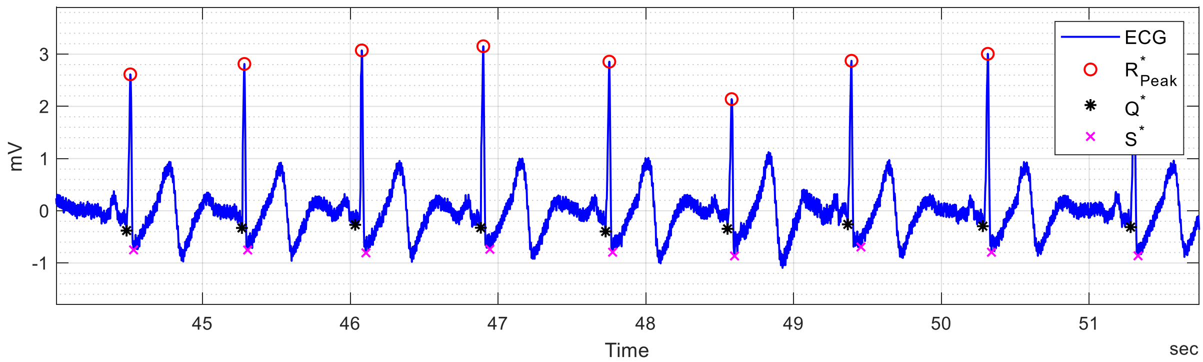

(d)

Figure 4.6 The results for (a) patient1 (b) patient2 (c) patient3 (d) patient4

In addition, the algorithm performance was evaluated based on the QT database. This database consists of 105 records with 50 minutes and a two-lead ECG. Also, many of these records are extracted from other ECG databases. The P, QRS, and T waves are annotated for these records. Table 4.4 shows promising results for QRS detection with high overall sensitivity and predictivity of 99.89% and 99.94%, respectively, and a low detection error rate of 0.167%.

Table 4.4 The QRS-detection results for QT database records

Records No.	TP (Beats)	FP (Beats)	FN (Beats)	FP+FN=FT (Beats)	Se (%)	PP (%)	DER (%)
Sel-100	1134	0	0	0	100.00	100.00	0
Sel-102	1088	0	0	0	100.00	100.00	0
Sel-103	1048	0	0	0	100.00	100.00	0
Sel-104	1109	0	1	1	99.91	100.00	0.090
Sel-114	862	1	1	2	99.88	99.88	0.232
Sel-116	1185	0	0	0	100.00	100.00	0
Sel-117	766	0	0	0	100.00	100.00	0
Sel-123	756	0	0	0	100.00	100.00	0
Sel-14046	1260	0	4	4	99.68	100.00	0.317
Sel-14157	1081	0	0	0	100.00	100.00	0
Sel-14172	663	0	0	0	100.00	100.00	0
Sel-15814	1036	0	0	0	100.00	100.00	0
Sel-16265	1031	0	0	0	100.00	100.00	0
Sel-16272	851	0	0	0	100.00	100.00	0
Sel-16273	1112	0	0	0	100.00	100.00	0
Sel-16420	1063	0	0	0	100.00	100.00	0
Sel-16483	1087	0	1	1	99.91	100.00	0.092
Sel-16539	922	0	0	0	100.00	100.00	0
Sel-16773	1008	0	0	0	100.00	100.00	0
Sel-16786	925	0	1	1	99.89	100.00	0.108
Sel-16795	761	0	0	0	100.00	100.00	0
Sel-17152	1628	0	0	0	100.00	100.00	0
Sel-17453	1047	0	0	0	100.00	100.00	0
Sel-213	1642	0	1	1	99.94	100.00	0.061
Sel-221	1247	0	2	2	99.84	100.00	0.160
Sel-223	1309	0	2	2	99.85	100.00	0.153
Sel-230	1077	0	0	0	100.00	100.00	0
Sel-231	732	0	0	0	100.00	100.00	0
Sel-232	865	0	0	0	100.00	100.00	0
Sel-233	1533	1	1	2	99.93	99.93	0.130
sel-30	1015	1	0	1	100.00	99.90	0.099
Sel-301	1351	0	2	2	99.85	100.00	0.148
Sel-302	1500	0	1	1	99.93	100.00	0.067
Sel-306	1040	0	1	1	99.90	100.00	0.096
Sel-307	853	0	0	0	100.00	100.00	0
Sel-308	1294	6	3	9	99.77	99.54	0.696
Sel-31	1087	0	0	0	100.00	100.00	0
Sel-310	2012	0	1	1	99.95	100.00	0.050
Sel-32	1193	7	7	14	99.42	99.42	1.174
Sel-33	523	3	0	3	100.00	99.43	0.574
Sel-34	896	1	0	1	100.00	99.89	0.112
Sel-35	881	2	19	21	97.89	99.77	2.384
Sel-36	947	2	1	3	99.89	99.79	0.317
Sel-37	668	2	0	2	100.00	99.70	0.299

Sel-38	1563	0	1	1	99.94	100.00	0.064
Sel-39	1170	1	0	1	100.00	99.91	0.085
Sel-40	1068	1	0	1	100.00	99.91	0.094
Sel-41	1363	5	3	8	99.78	99.63	0.587
Sel-42	1246	2	5	7	99.60	99.84	0.562
Sel-43	1428	2	0	2	100.00	99.86	0.140
Sel-44	1336	4	1	5	99.93	99.70	0.374
Sel-45	971	1	1	2	99.90	99.90	0.206
Sel-46	854	3	1	4	99.88	99.65	0.468
Sel-47	883	3	0	3	100.00	99.66	0.340
sel-48	1398	0	1	1	99.93	100.00	0.072
Sel-49	833	3	3	6	99.64	99.64	0.720
Sel-50	656	5	0	5	100.00	99.24	0.762
Sel-51	748	1	0	1	100.00	99.87	0.134
Sel-52	1416	2	7	9	99.51	99.86	0.636
Sel-803	1026	0	0	0	100.00	100.00	0
Sel-808	903	0	0	0	100.00	100.00	0
Sel-811	704	0	0	0	100.00	100.00	0
Sel-820	1159	0	0	0	100.00	100.00	0
Sel-821	1557	0	1	1	99.94	100.00	0.064
Sel-840	1180	0	1	1	99.92	100.00	0.085
Sel-847	801	0	0	0	100.00	100.00	0
Sel-853	1113	0	1	1	99.91	100.00	0.090
Sel-871	917	0	1	1	99.89	100.00	0.109
Sel-872	990	0	1	1	99.90	100.00	0.101
Sel-873	859	0	0	0	100.00	100.00	0
Sel-883	892	0	0	0	100.00	100.00	0
Sel-891	1267	1	0	1	100.00	99.92	0.079
Sele-0104	804	0	0	0	100.00	100.00	0
Sele-0106	896	0	0	0	100.00	100.00	0
Sele-0107	812	0	0	0	100.00	100.00	0
Sele-0110	872	0	0	0	100.00	100.00	0
Sele-0111	907	0	0	0	100.00	100.00	0
Sele-0112	684	1	0	1	100.00	99.85	0.146
Sele-0114	699	0	1	1	99.86	100.00	0.143
Sele-0116	558	1	0	1	100.00	99.82	0.179
Sele-0121	1436	0	3	3	99.79	100.00	0.209
Sele-0122	1415	0	1	1	99.93	100.00	0.071
Sele-0124	1121	0	0	0	100.00	100.00	0
Sele-0126	945	0	0	0	100.00	100.00	0
Sele-0129	671	1	31	32	95.58	99.85	4.769
Sele-0133	840	0	1	1	99.88	100.00	0.119
Sele-0136	809	0	0	0	100.00	100.00	0
Sele-0166	813	0	1	1	99.88	100.00	0.123
Sele-0170	897	0	0	0	100.00	100.00	0
Sele-0203	1246	0	0	0	100.00	100.00	0
Sele-0210	1063	0	0	0	100.00	100.00	0
Sele-0211	1575	0	0	0	100.00	100.00	0
Sele-0303	1045	0	0	0	100.00	100.00	0
Sele-0405	1216	0	1	1	99.92	100.00	0.082
Sele-0406	959	0	0	0	100.00	100.00	0
Sele-0409	1737	0	0	0	100.00	100.00	0
Sele-0411	1202	0	0	0	100.00	100.00	0
Sele-0509	1028	0	0	0	100.00	100.00	0
Sele-0603	870	0	1	1	99.89	100.00	0.115
Sele-0604	1031	0	0	0	100.00	100.00	0
Sele-0606	1442	0	4	4	99.72	100.00	0.277
Sele-0607	1184	0	2	2	99.83	100.00	0.169
Sele-0609	1127	0	0	0	100.00	100.00	0
Sele-0612	751	0	0	0	100.00	100.00	0
Sele-0704	1094	0	0	0	100.00	100.00	0
overall	**111,138**	**63**	**123**	**186**	**99.89**	**99.94**	**0.167**

4.4 Verification and Comparison of MIT-BIH Arrhythmia Database

This work focuses on the verification and comparison of the MBADB used for the QRS-detection algorithm. The proposed heartbeats filter function can apply to all MIT-BIH databases from the PhysioNet site. The reviewed QRS- detection methods are not using the same number of heartbeats for the MBADB. This number should be standard for this database because it depends on the original database's beats number. Simultaneously, not all the QRS-detection methods consider the same number of beats for the same database records. The revision for the existing QRS-detection methods using the MBADB has summarized the errors for these methods based on the beats for records shown in Table 4.5. The incorrect records are indicated by grey colour, the Total (T), and Errors (E) in this table. The methods should use the same number of beats without any difference, but the errors are occurring by researchers. All the reviewed methods are revised, compared, and verified based on beats number for each database record. The total beats number summarizes in Table 4.6, total error per record, and total error per database for different methods to evaluate these methods' incorrectness.

The total number of beats for the MBADB used from the reviewed methods is calculated; this number should be 109,494 heartbeats for all database records, as shown in section 3.4. The beat errors for these methods compared to the correct number of beats for this database are determined to find the number of methods that used the correct beat's value. Also, the other methods contained errors start from 1 beat to 1400 beats for the overall database. The percentage of references numbers for each error per the total references that were reviewed is shown in Table 4.6. Moreover, it shows the total number of errors for each reference per each record (sum of the absolute values of errors) and the total number of errors for each reference per overall database, which takes a positive or negative value.

Table 4.5 The beat annotation for the reviewed methods

Rec	[69] [70] [30] [71] [72] [73] [29] [74] [75] [76] [77] [78] [6] [79] [80] [81] [27] [26] [82] [83]	[12]	[84] [85] [86] [87] [88]	[89]	[90]	[91]	[92]	[93]	[94]	[95] [96] [97]	[98] [99] [100]	[101]	[102]	[103]	[104]	[105]	[106]
100	2273	2273	2273	2273	2273	2273	2272	2272	2272	2273	2273	2273	2273	2273	2271	2273	2272
101	1865	1865	1865	1865	1865	1865	1865	1865	1865	1865	1865	1865	1865	1865	1864	1865	1864
102	2187	2187	2187	2187	2187	2187	2187	2187	2187	2187	2187	2187	2187	2187	2186	2187	2187
103	2084	2084	2084	2084	2084	2084	2084	2084	2084	2084	2084	2084	2084	2084	2083	2084	2084
104	2229	2229	2229	2229	2229	2229	2228	2228	2228	2229	2229	2229	2229	2230	2228	2229	2227
105	2572	2572	2572	2572	2572	2572	2572	2572	2572	2572	2572	2572	2572	2572	2571	2572	2555
106	2027	2027	2027	2027	2027	2027	2027	2027	2027	2027	2027	2027	2027	2027	2026	2027	2027
107	2137	2136	2137	2137	2137	2137	2136	2137	2137	2137	2137	2137	2137	2137	2136	2137	2135
108	1763	1763	1763	1763	1763	1763	1763	1763	1763	1774	1774	1760	1774	1763	1762	1763	1761
109	2532	2532	2532	2532	2532	2532	2532	2532	2532	2532	2532	2532	2532	2532	2531	2532	2532
111	2124	2124	2124	2124	2124	2124	2124	2124	2124	2124	2124	2124	2124	2124	2123	2124	2124
112	2539	2539	2539	2539	2539	2539	2539	2539	2539	2539	2539	2539	2539	2539	2538	2539	2539
113	1795	1795	1795	1795	1795	1795	1794	1794	1794	1795	1795	1795	1795	1795	1793	1795	1794
114	1879	1879	1879	1879	1879	1879	1879	1878	1879	1879	1879	1872	1879	1879	1878	1879	1879
115	1953	1953	1953	1953	1953	1953	1953	1953	1953	1953	1953	1952	1953	1953	1952	1953	1952
116	2412	2412	2412	2412	2412	2412	2412	2412	2412	2412	2412	2412	2412	2412	2411	2412	2410
117	1535	1535	1535	1535	1535	1535	1535	1535	1535	1535	1535	1535	1535	1535	1534	1535	1535
118	2278	2278	2278	2278	2278	2278	2278	2278	2277	2278	2278	2278	2278	2288	2277	2278	2278
119	1987	1987	1987	1987	1987	1987	1987	1987	1987	1987	1987	1987	1987	1987	1986	1987	1987
121	1863	1863	1863	1863	1863	1863	1863	1862	1862	1863	1863	1863	1863	1863	1862	1863	1863
122	2476	2476	2476	2476	2476	2476	2476	2476	2476	2476	2476	2476	2476	2476	2475	2476	2476
123	1518	1518	1518	1518	1518	1518	1518	1518	1518	1518	1518	1518	1518	1518	1517	1518	1518
124	1619	1619	1619	1619	1619	1619	1619	1619	1619	1619	1619	1619	1619	1619	1618	1619	1619
200	2601	2601	2601	2601	2601	2601	2601	2601	2601	2601	2601	2601	2601	2601	2600	2601	2581
201	1963	1963	1963	1963	1963	1963	1963	1963	1962	1963	1963	1963	1963	1963	1962	1963	1950
202	2136	2136	2136	2136	2136	2135	2136	2136	2136	2136	2136	2136	2136	2136	2135	2136	2133
203	2980	2980	2980	2980	2980	2980	2980	2980	2980	2980	2980	2980	2980	2980	2979	2980	2949
205	2656	2656	2656	2656	2656	2656	2656	2656	2655	2656	2656	2656	2656	2656	2655	2656	2647
207	1860	1860	1862	1860	1862	1860	1860	1860	1860	1860	1862	1862	1860	1862	1859	1794	1859
208	2955	2955	2955	2955	2955	2955	2955	2955	2955	2955	2955	2955	2955	2946	2954	2955	2921
209	3005	3005	3005	3004	3005	3004	3005	3004	3004	3004	3004	3004	3004	3005	3004	3005	3002
210	2650	2650	2650	2650	2650	2650	2650	2650	2650	2650	2650	2650	2650	2647	2649	2650	2644
212	2748	2748	2748	2748	2748	2748	2748	2748	2748	2748	2748	2748	2748	2748	2747	2748	2747
213	3251	3251	3251	3251	3251	3251	3250	3250	3250	3251	3251	3251	3251	3251	3249	3251	3249
214	2262	2262	2262	2261	2261	2261	2262	2261	2261	2265	2265	2265	2265	2254	2261	2262	2261
215	3363	3363	3363	3363	3363	3361	3363	3363	3363	3363	3363	3363	3363	3353	3362	3363	3362
217	2208	2208	2208	2208	2208	2208	2208	2208	2208	2209	2209	2209	2209	2208	2207	2208	2208
219	2154	2154	2154	2154	2154	2154	2154	2154	2154	2154	2154	2154	2154	2154	2153	2154	2154
220	2048	2048	2048	2048	2048	2048	2047	2048	2047	2048	2048	2048	2048	2048	2047	2048	2047
221	2427	2427	2427	2427	2427	2427	2427	2427	2426	2427	2427	2427	2407	2427	2426	2427	2427
222	2483	2483	2483	2483	2483	2483	2483	2483	2483	2483	2483	2483	2483	2484	2482	2483	2482
223	2605	2605	2605	2605	2605	2605	2605	2605	2605	2605	2605	2605	2605	2605	2604	2605	2603
228	2053	2053	2053	2053	2053	2053	2053	2053	2053	2053	2053	2048	2053	2053	2052	2053	2053
230	2256	2256	2256	2256	2256	2256	2256	2256	2256	2256	2256	2256	2256	2256	2255	2256	2256
231	1571	1571	1571	1571	1571	1571	1571	1571	1571	1571	1571	1571	1571	1571	1570	1571	1571
232	1780	1780	1780	1780	1780	1779	1780	1780	1780	1780	1780	1780	1780	1780	1779	1780	1780
233	3079	3079	3079	3079	3079	3079	3079	3079	3078	3079	3079	3079	3079	3079	3078	3079	3071
234	2753	2753	2753	2753	2753	2753	2753	2753	2753	2753	2753	2753	2753	2753	2752	2753	2753
T	109494	109493	109496	109492	109495	109488	109488	109486	109481	109508	109510	109483	109488	109478	109443	109428	109328
E	0	1	2	2	3	6	6	8	13	16	18	23	36	44	51	66	166

Table 4.5 The beat annotation for the reviewed methods (continue)

Rec	[11]	[107]	[108] [109] [110] [111] [112] [7]	[113]	[114]	[115]	[116]	[32] [117] [118]	[119]	[120]	[121]	[122]	[123]	[124]	[125]	[126]	[127]
100	2269	2273	2273	2273	2267	2265	2273	2273	2273	2273	2273	2273	2274	2270	2273	2273	2272
101	1862	1864	1865	1865	1859	1860	1865	1865	1865	1865	1865	1865	1866	1862	1865	1873	1864
102	2183	2187	2187	2187	2181	2180	2187	2187	2187	2187	2187	2187	2187	2186	2187	2186	2186
103	2081	2084	2084	2084	2081	2078	2084	2084	2084	2084	2084	2084	2084	2083	2084	2084	2083
104	2225	2226	2230	2230	2224	2222	2230	2229	2229	2230	2229	2229	2229	2219	2229	2235	2228
105	2582	2566	2572	2572	2564	2565	2572	2572	2572	2572	2572	2572	2602	2559	2572	2578	2571
106	2024	2023	2027	2027	2024	2021	2027	2027	2027	2027	2027	2027	2026	2025	2027	2096	2026
107	2133	2135	2137	2137	2131	2131	2137	2137	2137	2137	2137	2137	2136	2135	2137	2138	2136
108	1761	1759	1763	1763	1757	1757	1763	1763	1763	1763	1763	1763	1763	1747	1774	1763	1762
109	2528	2527	2532	2532	2526	2524	2532	2532	2532	2532	2532	2532	2533	2531	2532	2519	1649
111	2121	2123	2124	2124	2120	2118	2124	2124	2124	2124	2124	2124	2123	2120	2124	2124	2123
112	2535	2539	2539	2539	2536	2531	2539	2539	2539	2539	2539	2539	2539	2537	2539	2549	2538
113	1791	1795	1795	1797	1791	1789	1795	1795	1795	1795	1795	1795	1794	1792	1795	1795	1794
114	1875	1832	1879	1879	1872	1872	1879	1879	1879	1879	1879	1879	1890	1878	1879	1885	1878
115	1949	1953	1953	1953	1945	1946	1953	1953	1953	1953	1953	1953	1953	1950	1953	1960	1952
116	2408	2392	2412	2412	2409	2404	2412	2412	2412	2412	2412	2412	2395	2407	2412	2401	2411
117	1532	1535	1535	1535	1532	1530	1535	1535	1535	1535	1535	1535	1535	1534	1535	1538	1534
118	2275	2278	2275	2275	2273	2271	2275	2278	2278	2278	2278	2278	2278	2275	2288	2298	2277
119	1984	1987	1987	1987	1985	1981	1987	1987	1987	1987	1987	1987	1988	1985	1987	2010	1986
121	1859	1863	1863	1863	1858	1856	1863	1863	1863	1863	1863	1863	1863	1860	1863	1871	1862
122	2472	2476	2476	2476	2471	2468	2476	2476	2476	2476	2476	2476	2476	2475	2476	2477	2475
123	1515	1518	1518	1518	1514	1513	1518	1518	1518	1518	1518	1518	1519	1517	1518	1518	1517
124	1616	1619	1619	1619	1613	1613	1619	1619	1619	1618	1619	1619	1619	1618	1619	1602	1618
200	2597	2600	2601	2601	2595	2593	2607	2601	2601	2601	2601	2601	2601	2560	2601	2599	2600
201	1961	1934	1963	1963	1946	1959	1963	1963	1963	1963	1963	1963	1949	1954	2000	1963	1962
202	2132	2132	2136	2136	2134	2128	2136	2136	2136	2136	2136	2136	2138	2134	2136	2135	2135
203	3003	2926	2982	2978	2976	2973	2982	2980	2980	2980	2980	2980	2988	2962	2980	2982	2979
205	2652	2653	2656	2656	2650	2648	2656	2656	2656	2656	2656	2656	2656	2654	2656	2657	2655
207	1855	1857	1862	1862	1856	1850	1862	2332	2332	2332	2332	1543	2324	2246	2332	1862	2331
208	2951	2940	2956	2954	2953	2946	2956	2955	2955	2955	2955	2955	2953	2937	2955	2952	2954
209	3001	3005	3004	3004	2999	2997	3004	3005	3004	3005	3005	3006	3006	3002	3005	3051	3004
210	2646	2628	2647	2647	2645	2642	2647	2650	2650	2650	2650	2640	2652	2640	2650	2645	2649
212	2744	2748	2748	2748	2746	2740	2748	2748	2748	2748	2748	2748	2748	2746	2748	2761	2747
213	3246	3250	3251	3251	3245	3241	3251	3251	3251	3251	3251	3471	3250	3247	3251	3245	3250
214	2258	2258	2262	2262	2255	2254	2262	2262	2262	2262	2262	2259	2262	2259	2262	2273	2261
215	3358	3363	3363	3362	3357	3353	3363	3363	3363	3363	3363	3363	3362	3360	3363	3398	3362
217	2205	2207	2208	2208	2202	2202	2208	2208	2208	2208	2208	2208	2208	2207	2208	2270	2207
219	2151	2154	2154	2154	2150	2147	2154	2154	2154	2154	2154	2154	2154	2152	2287	2154	2153
220	2044	2047	2048	2048	2041	2041	2048	2048	2048	2048	2048	2048	2048	2047	2048	2068	2047
221	2423	2426	2427	2427	2422	2420	2427	2427	2427	2427	2457	2427	2427	2426	2427	2447	2426
222	2478	2481	2484	2484	2492	2474	2484	2483	2483	2483	2483	2483	2485	2481	2483	2624	2482
223	2601	2604	2605	2605	2603	2581	2605	2605	2605	2605	2605	2589	2604	2604	2605	2636	2604
228	2050	2050	2053	2053	2048	2047	2053	2053	2053	2053	2053	2053	2060	2051	2053	2116	2052
230	2252	2256	2256	2256	2252	2248	2256	2256	2256	2256	2256	2256	2256	2253	2256	2257	2255
231	1568	1571	1886	1886	1566	1565	1186	1571	1571	1571	1571	1571	1571	1570	1573	1569	1570
232	1778	1780	1780	1767	1719	1776	1780	1780	1780	1780	1780	1780	1783	1779	1780	1734	1779
233	3074	3078	3079	3076	3135	3069	3079	3079	3079	3079	3079	3079	3077	3076	3079	3074	3078
234	2749	2753	2753	2753	2747	2745	2735	2753	2753	2753	2753	2753	2751	2751	2753	2763	2752
T	109357	109255	109809	109788	109267	109134	109097	109966	109965	109966	109996	109369	109985	109663	110159	110008	109036
E	203	239	329	348	357	360	423	472	473	474	502	567	579	603	665	738	1400

The beats errors per all data record up to 1400 beats and 29% of the total reviewed methods use the correct beats number. On the other hand, 71% are using incorrect beats numbers. Also, the number of incorrect methods is higher than the number of correct methods based on the comparison. So, this work is proposed. Each record in the database for the reviewed methods has been studied for beats errors calculation. The number of references that contain errors for each record is described in Figure 4.7. For each record, the percentage of the reference number that occurs error per all references is calculated to evaluate the record error reasons. The records error percentage is started from 53% for record no. 207 to 9% for records (102, 103, 112, 117, 119, 122, 123, and 230).

The difference between these methods for the same records used from the same database is shown in Table 4.6 and Figure 4.7. After the results are studied, the following obvious points are established:

- The correct number of beats is 109,494 beats without adding or removing any data.
- The designed function extracts the correct heartbeats number of all records for the MIT-BIH arrhythmia database.
- If the beats number exceed the correct number:
  - Some non-beat annotations have been added and should be mentioned in the methods.
  - The data has been repeated for record and should be mentioned in the methods.
- If the beats number less than the correct number:
  - Some beat annotations have been removed and should be mentioned in the methods.
- This database contains some errors before digitalization and verification.

Table 4.6 Total beat annotations and errors for the reviewed methods

References	Count of Ref	Percentage Ref	Total beats	Total errors per record	Total Errors per database
[69] [70] [30] [71] [72] [73] [29] [74] [75] [76] [77] [78] [6] [79] [80] [81] [27] [26] [82] [83]	20	29%	109494	0	0
[12]	1	1%	109493	1	-1
[84] [85] [86] [87] [88] [89]	6	9%	109496	2	2
[90]	1	1%	109495	3	1
[91]	1	1%	109488	6	-6
[92]	1	1%	109488	6	-6
[93]	1	1%	109486	8	-8
[94]	1	1%	109481	13	-13
[95] [96] [97]	3	4%	109508	16	14
[98] [99] [100]	3	4%	109510	18	16
[101]	1	1%	109483	23	-11
[102]	1	1%	109488	36	-6
[103]	1	1%	109478	44	-16
[104]	1	1%	109443	51	-51
[105]	1	1%	109428	66	-66
[106]	1	1%	109328	166	-166
[11]	1	1%	109357	203	-137
[107]	1	1%	109255	239	-239
[108] [109] [110] [111] [112] [7]	6	9%	109809	329	315
[113]	1	1%	109788	348	294
[114]	1	1%	109267	357	-227
[115]	1	1%	109134	360	-360
[116]	1	1%	109097	423	-397
[32] [117] [118]	3	4%	109966	472	472
[119]	1	1%	109965	473	471
[120]	1	1%	109966	474	472
[121]	1	1%	109996	502	502
[122]	1	1%	109369	567	-125
[123]	1	1%	109985	579	491
[124]	1	1%	109663	603	169
[125]	1	1%	110159	665	665
[126]	1	1%	110008	738	514
[127]	1	1%	109036	1400	-458
Total	68	100%			

- The WFDB toolbox does not include the beats or non-beats filter for the (rdann) function that reads the annotations files.
- The copy and paste records beat numbers between the researcher without verification.
- A high number of annotation types (39 annotations) confuse the researchers.
- According to Figure 4.7:
  - The most errors occur in the record no. 207 because many researchers are counting the 472 ventricular flutter waves, but these waves are considered as non-beat annotations based on the annotation's description of PhysioNet.
  - Records no. 209 is the second and records no. 214 is the third most error beats for the reviewed methods, but the number of errors is low and not exceeds eight beats and nine beats, respectively.
  - The lowest error records (102, 103, 112, 117, 119, 122, 123, and 230) because these records contain the lowest non-beat annotations.

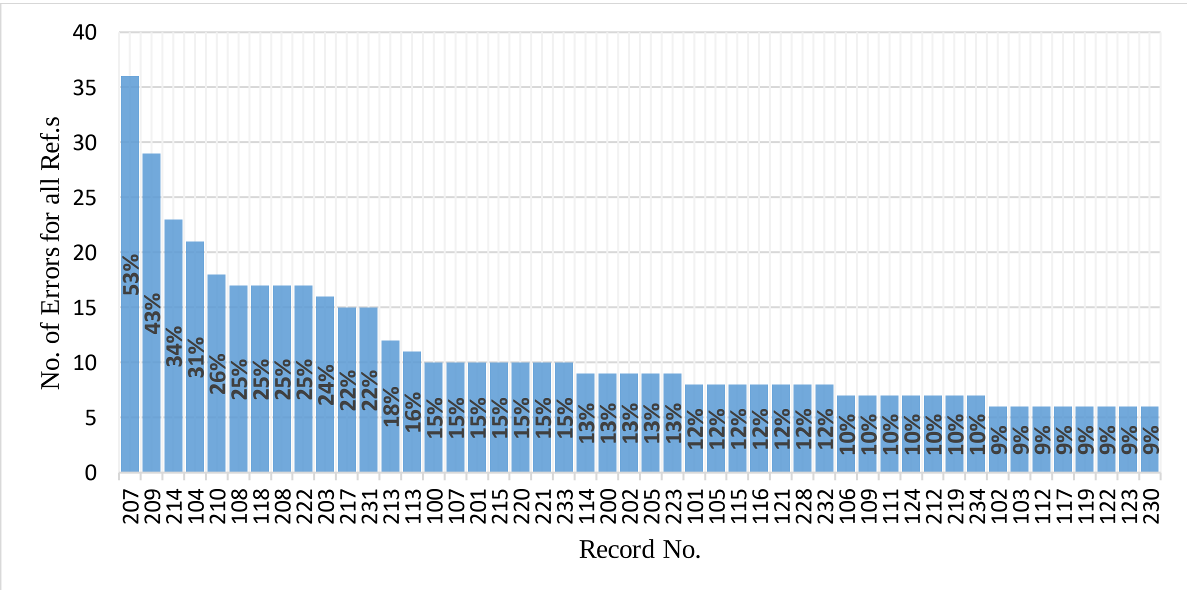

Figure 4.7 Records errors per overall references

4.5 Normality Heartbeat Classification Proposed Method Evaluation

The MIT-BIH arrhythmia is the database for method evaluation performance. Its widely used, and it consists of a variable ECG signal that is suffered from different types of noise. The 103,192 heartbeats from 45 records are used excepted the records 102, 104, and 114 that are not included. These heartbeats are divided into 73,028 normal and 30,164 abnormal heartbeats. These beats are trained, tested, and evaluated in a 2.6 GHz Intel Ci7 computer using 64-bit MATLAB 2020b. The average classification time for each record of the evaluation database is (1.67 Sec). From this time, the method is low computational based on the algorithm simplicity. The proposed algorithm's promising results show an accuracy of 98.97%, Sensitivity of 99.42%, and a high Positive_Predicitvit of 99.13%.

The parameters: true positive (TP), true negative (TN), false negative (FN), and false positive (FP), false total (FT) are calculated from the confusion matrix, as shown in Figure 4.8. The performance is evaluated based on Accuracy (Acc), Sensitivity (Se), and Positive_Predicitvity (PP) that illustrated in Equations (2.21), (2.22), and (2.23).

The Equations (2.21), (2.22), and (2.23) are calculated for the 103,192 beats to evaluate the algorithm performance and compare the results with the other methods. The evaluation performance comparison of the proposed algorithm with other not the high computational algorithms using the same MBADB is summarized in Table 4.7. The proposed algorithm performance is better than the other methods, as the results described. These results are promising from the accuracy and low computational. The following points can describe the reason for low computation:

- It is a simple ANN with a single hidden layer.
- Most features that are extracted for QRS-detection are used for heartbeats classification.

- The rest of the features are simply extracted.
- It processes the input obtained by features instead of raw ECG signals.

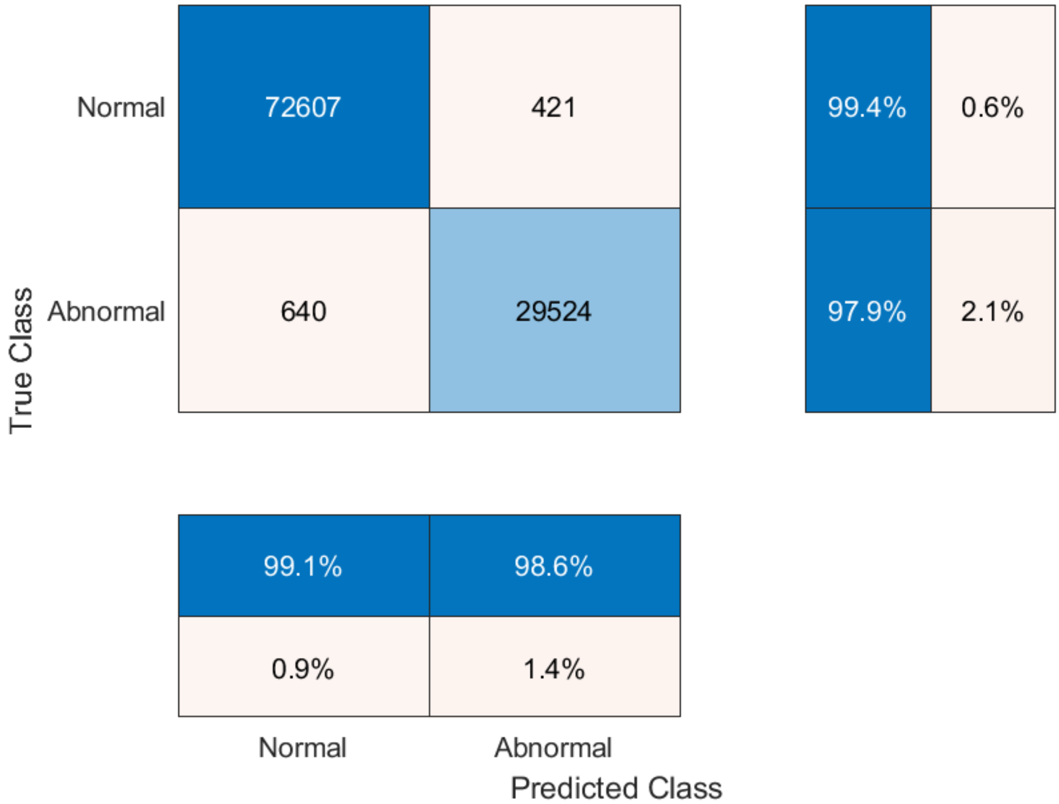

Figure 4.8 The result confusion matrix

The performance measures (Acc, Se, and PP) showed in Equations (2.21), (2.22), and (2.23) are calculated for the overall record as shown below:

$$Se_{overall}\% = \frac{TP}{TP + FN} \times 100 = \frac{72607}{72607 + 421} \times 100 = 99.42$$

$$PP_{overall}\% = \frac{TP}{TP + FP} \times 100 = \frac{72607}{72607 + 640} \times 100 = 99.13$$

$$Acc_{\ overall}\% = \frac{TP + TN}{TP + TN + FP + FN} \times 100$$

$$= \frac{72607 + 29524}{103192} \times 100 = 98.97$$

Table 4.7 The method's performance comparison

Method	Classes	Data size	Acc%	Se%	PP%
The proposed method	2	103,192	**98.97**	**99.42**	**99.13**
[44]	15	104,986	97.70	-	-
[22]	13	blocks	95.00	-	-
[39]	5	100,688	94.30	-	-
[43]	5	100,647	93.40	-	-
[41]	2	-	93.19	95.00	-
[128]	5	98,794	92.40	-	-
[38]	2	blocks	88.10	92.40	-
[37]	6	blocks	87.00	-	-
[129]	5	100,731	83.00	-	-

The accuracy of 98.97%, sensitivity of 99.42%, and positive predictivity of 99.13% are promising results for a low computation algorithm. It is a new approach for real-time applications with low resources and high efficiency compared to other classifier approaches.

4.6 Five Classes Heartbeat Classification Proposed Method Evaluation

The method was evaluated based on the MIT-BIH arrhythmia database. Because it consists of a variable ECG signal that is suffered from different types of noise and variable heartbeats types (15-classes), this database is suitable for evaluation. The database consists of two channels, 48 records with 11-bit resolution at 360 sampling rates.

In this work, the number of heartbeats is 103,192 from 45 records excepted the records 102, 104, and 114 that are not included. The 45 records are lead-II ECG-signal. According to the knowledge base, these heartbeats are divided, as shown in Figure 3.21. According to the AAMI, five classes are 88,490 (N), 7,143 (V), 3,888 (Q), 2,876 (S), and 795 (F). The regularity property is extracted from the R and R time of the four RR-before beats and one RR-after beat. So, this property is extracted from the RR-interval features. The heart rate is extracted directly from the average heart rate features (F_{24}), as shown in Equation (3.35).

The new method (SMANN) is evaluated and compared with the traditional ANN performance evaluation. First, the traditional ANN method with all input features without any selection is evaluated using the 103,192 heartbeats from 45 records. Second, the SMANN with selective input features is evaluated using the same heartbeats from the same records. These heartbeats are divided into six selective properties to train the SMANN and produce six masks for each selective property.

The performance measures Accuracy (Acc), Sensitivity (Se), and Positive_Predicitvity (PP) illustrated in Equations (2.21), (2.22), and (2.23) are calculated for all classes. For example, the normal class and the overall classes are calculated of SMANN as follows:

$$TP_N = 88474$$

$$TN_N = 2861 + 8 + 0 + 0 + 13 + 7134 + 0 + 0 + 0 + 0 + 764 + 1 + 0 + 0 + 1 + 3879 = 14661$$

$$FP_N = 2 + 1 + 30 + 8 = 41$$

$$FN_N = 3 + 1 + 9 + 3 = 16$$

$$Se_N\% = \frac{TP_N}{TP_N + FN_N} \times 100 = \frac{88474}{88474 + 16} \times 100 = 99.982$$

$$PP_N\% = \frac{TP_N}{TP_N + FP_N} \times 100 = \frac{88474}{88474 + 41} \times 100 = 99.954$$

$$Se_{overall}\% = \Big((Se_N \times No_N) + (Se_S \times No_S) + (Se_V \times No_V) + (Se_F \times No_F) + \big(Se_Q \times No_Q\big)\Big)/total$$

$$Se_{overall}\% = \big((99.98 \times 88490) + (99.48 \times 2876) + (99.87 \times 7143) + (96.1 \times 795) + (99.77 \times 3888)\big)/103192 = 99.922$$

$$PP_{overall}\% = \Big((PP_N \times No_N) + (PP_S \times No_S) + (PP_V \times No_V) + (PP_F \times No_F) + \big(PP_Q \times No_Q\big)\Big)/total$$

$$PP_{overall}\% = \big((99.95 \times 88490) + (99.62 \times 2876) + (99.8 \times 7143) + (98.7 \times 795) + (99.9 \times 3888)\big) / 103192 = 99.922$$

$$Acc_{\ overall}\% = \frac{Correct}{Total} \times 100 = \frac{88474 + 2861 + 7134 + 764 + 3879}{103192} \times 100 = 99.9224$$

Where: TP_N, TN_N, FP_N, and FN_N are the normal class parameters

The parameters as shown in Figure 4.9: TP, TN, FT, FN, and FP were calculated to evaluate the performance for both ANN and SMANN. The FT is the most important parameter because a patient is diagnosed with the wrong heartbeat class. The performance is evaluated based on the overall Accuracy (Acc), Sensitivity (Se), and Positive_Predicitvity (PP). The Equations (2.21), (2.22), and (2.23)were calculated for both ANN and SMANN based on each class. The equation results are presented in Table 4.8 and Table 4.9.

The Equations (2.21), (2.22), and (2.23) were calculated for the 103,192 beats to evaluate the algorithm performance and compare the results with the other methods. The method was trained, tested, and evaluated in a 2.6 GHz Intel Ci7 computer using 64-bit MATLAB 2020b. The proposed method's promising results show an Acc of 99.9224%, overall Se of 99.9224%, and overall high PP of 99.9222% (The overall Se and PP are the average weighted values). The total errors (FT) for the proposed method based on SMANN is 80 comparing with the 583 errors for the same method with traditional ANN. This low error leads to durability for diagnosing the patient's heartbeats and assists the clinical decision-

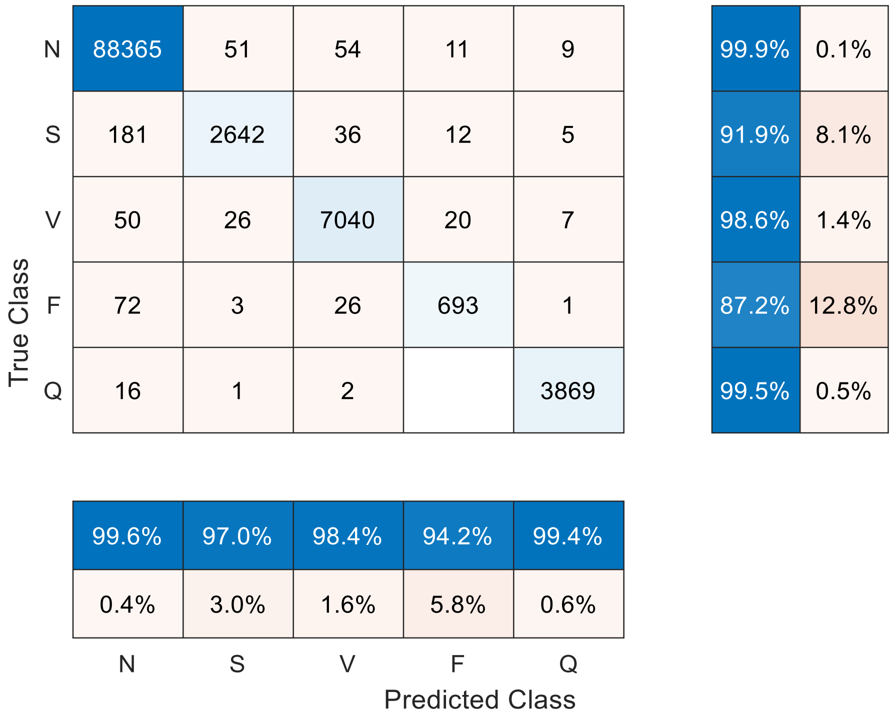

(a)

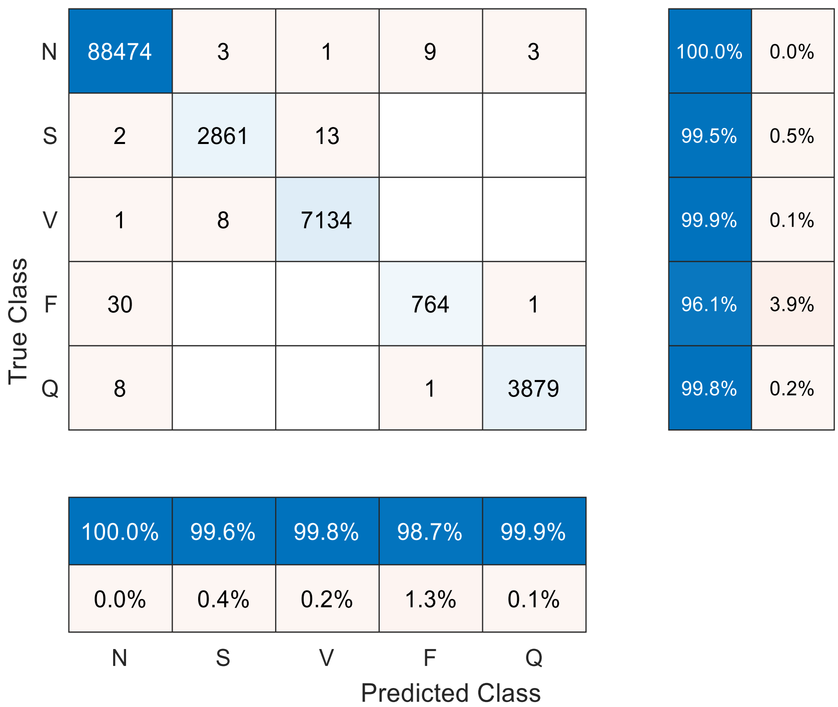

(b)

Figure 4.9 The confusion matrix for (a) ANN and (b) SMANN

Table 4.8 The performance for the ANN

		True					
	Class	**N**	**S**	**V**	**F**	**Q**	**Pre. sum**
Predicted	**N**	88365	181	50	72	16	88684
	S	51	2642	26	3	1	2723
	V	54	36	7040	26	2	7158
	F	11	12	20	693	0	736
	Q	9	5	7	1	3869	3891
	true sum	88490	2876	7143	795	3888	103,192
							Total
Parameters	**TP**	88365	2642	7040	693	3869	102,609
	TN	14383	100235	95931	102354	99282	
	FP	319	81	118	43	22	583
	FN	125	234	103	102	19	583
	Total	103,192	103,192	103,192	103,192	103,192	
Performance		**Per Class**					**Overall**
	Se %	99.8587	91.8637	98.5580	87.1698	99.5113	99.4350
	PP %	99.6403	97.0253	98.3514	94.1576	99.4345	99.4282
	Acc %						99.4350

Table 4.9 The performance for the SMANN

		True					
	Class	**N**	**S**	**V**	**F**	**Q**	**Pre. sum**
Predicted	**N**	88474	2	1	30	8	88515
	S	3	2861	8	0	0	2872
	V	1	13	7134	0	0	7148
	F	9	0	0	764	1	774
	Q	3	0	0	1	3879	3883
	true sum	88490	2876	7143	795	3888	103,192
							Total
Parameters	**TP**	88474	2861	7134	764	3879	103112
	TN	14661	100305	96035	102387	99300	
	FP	41	11	14	10	4	80
	FN	16	15	9	31	9	80
	Total	103192	103192	103192	103192	103192	
Performance		**Per Class**					**Overall**
	Se %	99.9819	99.4784	99.874	96.1006	99.7685	99.9224
	PP %	99.9536	99.6169	99.8041	98.7080	99.8969	99.9222
	Acc %						99.9224

maker for long-time or real-time ECG signals. The improvements for SMANN over the ANN are:

- The sensitivity of the fusion class is improved to be 96.1 % for the SMANN instead of the ANN 87.17 %.
- The positive_predicitvity of the fusion class is improved to be 98.7 % for the SMANN instead of the ANN 94.16 %.
- The sensitivity of the supraventricular ectopic class is improved to be 99.47 % for the SMANN instead of the ANN 91.86 %.
- The positive_predicitvity of the supraventricular ectopic class is improved to be 99.62 % for the SMANN instead of the ANN 97.03 %.
- All classes for SMANN have high sensitivity and high positive_predicitvity.
- The ANN classification sensitivity and positive_predicitvity are variable from high for some classes and moderate for the other classes.

The evaluation performance comparison of the proposed method with other not high computational algorithms using the same MBADB is summarized in Table 4.10. The proposed method performance is better than the other methods, as the results described. These results are promising according to the accuracy and low computational.

Table 4.10 The methods performance comparison

Method	Types	Data size	Acc%	Se%	PP%
The proposed SMANN	5	103,192	**99.922**	**99.922**	**99.922**
The proposed-ANN			**99.435**	**99.435**	**99.428**
[44]	15	104,986	97.70	-	-
[22]	13	blocks	95.00	-	-
[39]	5	100,688	94.30	-	-
[43]	5	100,647	93.40	-	-
[41]	2	-	93.19	95.00	-
[128]	5	98,794	92.40	-	-
[38]	2	blocks	88.10	92.40	-
[37]	6	blocks	87.00	-	-
[129]	5	100,731	83.00	-	-

Chapter 5: Conclusions and Future Works

Contents

Chapter Five:
Conclusions and Future Works

5.1 Conclusions

The conclusions are summarized into the following aspects for each objective:

- The QRS detection algorithm is based on novel techniques:
  - The features are extracted with simple calculation from some ECG signal points (predicted-QRS) and eliminate the most unexpected QRS samples to simplify the processes.
  - The QRS level values with the slope are used to improve the accuracy.
  - Separating the QRS classifier (ANN) by polarity improves the accuracy. Therefore, each ANN can classify the data more accurately and less complicated to achieve better performance.
- The proposed BF function should be added to the MATLAB-WFDB Toolbox in order to filter the annotations files to remove the non-beat annotations correctly and extract the standard beat values. Because the non-beat annotations for the MBADB database affected the results of the QRS-detection methods in two ways:
  - First, the proposed methods' evaluation accuracy is not calculated correctly because the number of database beats is incorrect.
  - Second, the methods based on machine learning are trained depending on incorrect information. So, the learning operation was not proper, and results of the methods are not correct.

- For the proposed heartbeat normality classification method:
  - A new features extraction method reused the QRS detection features and mixed them with the RR interval to achieve better performance based on low computation.
  - It focuses on the normal and abnormal to diagnose any abnormal in the general case and exclude the normal beats for the normal patient’s data that no need for any more analysis.
- The five classes proposed classification is based on the low computational novel SMANN method to improve the performance without adding complexity. Also:
  - The QRS-shape, RR-interval, and between-RR new mixed features are the most relevant for the heartbeat classification.
- Designing a low computational heartbeat detection and classification algorithm is implemented in low resource wearable devices. Also:
  - The proposed CDS wearable system purpose is to improve the quality of life and to save more lives.
  - The accomplished system is low cost according to the total cost of 52$.

5.2 Future Works

The wearable system can be developed by applying some of the following suggestions:

- Adding temperature, accelerometer, and SpO2 sensors for the wearable system. Improving the diagnostic by including the new sensors reading for the data analysis.
- Extend the heartbeat classification method based on the SMANN from five to fifteen classes of the heartbeat within the MBADB.
- Implement a wearable system for the fifteen classes heartbeat classification method.

- Evaluate and test the SMANN method by adding more selectivity of new properties from the same ECG database.
- Evaluate and test the SMANN method for different applications based on various databases.

References

[1] O. World Health, "Global health estimates 2016: estimated deaths by age, sex, and cause," ed, 2016.

[2] S. K. Berkaya, A. K. Uysal, E. S. Gunal, S. Ergin, S. Gunal, and M. B. Gulmezoglu, "A survey on ECG analysis," *Biomedical Signal Processing and Control*, vol. 43, pp. 216-235, 2018.

[3] R. Ghorbani Afkhami, G. Azarnia, and M. A. Tinati, "Cardiac arrhythmia classification using statistical and mixture modeling features of ECG signals," *Pattern Recognition Letters*, vol. 70, pp. 45-51, 2016.

[4] T. F. Romdhane, H. Alhichri, R. Ouni, and M. Atri, "Electrocardiogram heartbeat classification based on a deep convolutional neural network and focal loss," *Computers in Biology and Medicine*, vol. 123, p. 103866, 2020.

[5] J. Hampton and J. Hampton, *The ECG Made Easy*. Elsevier Health Sciences, 2019.

[6] D. Castells-Rufas and J. Carrabina, "Simple real-time QRS detector with the MaMeMi filter," *Biomedical Signal Processing and Control*, vol. 21, pp. 137-145, 2015.

[7] J. Pan and W. J. Tompkins, "A Real-Time QRS Detection Algorithm," *IEEE Transactions on Biomedical Engineering*, vol. BME-32, no. 3, pp. 230-236, 1985.

[8] F. Murat, O. Yildirim, M. Talo, U. B. Baloglu, Y. Demir, and U. R. Acharya, "Application of deep learning techniques for heartbeats detection using ECG signals-analysis and review," *Computers in Biology and Medicine*, vol. 120, p. 103726, 2020.

[9] Z. Ebrahimi, M. Loni, M. Daneshtalab, and A. Gharehbaghi, "A review on deep learning methods for ECG arrhythmia classification," *Expert Systems with Applications: X*, vol. 7, p. 100033, 2020.

[10] M. Alfaras, M. C. Soriano, and S. Ortín, "A Fast Machine Learning Model for ECG-Based Heartbeat Classification and Arrhythmia Detection," (in English), *Frontiers in Physics,* Original Research vol. 7, no. 103, 2019.

[11] W. Chin, C. Chang, C. Tseng, Y. Huang, and T. Jiang, "Bayesian Real-Time QRS Complex Detector for Healthcare System," *IEEE Internet of Things Journal*, vol. 6, no. 3, pp. 5540-5549, 2019.

[12] M. Elgendi, M. Jonkman, and F. De Boer, "Frequency Bands Effects on QRS Detection," presented at the Proceedings of the Third International Conference on Bio-inspired Systems and Signal Processing, 2010.

[13] B. Kohler, C. Hennig, and R. Orglmeister, "The principles of software QRS detection," *IEEE Engineering in Medicine and Biology Magazine,* vol. 21, no. 1, pp. 42-57, 2002.

[14] P. Pławiak and U. R. Acharya, "Novel deep genetic ensemble of classifiers for arrhythmia detection using ECG signals," *Neural Computing and Applications*, vol. 32, no. 15, pp. 11137-11161, 2020.

[15] N. N. Anuar *et al.*, "Cardiovascular Disease Prediction from Electrocardiogram by Using Machine Learning," *International Journal of Online and Biomedical Engineering,* 2020.

[16] G. Ciaburro and B. Venkateswaran, *Neural Networks with R: Smart models using CNN, RNN, deep learning, and artificial intelligence principles*. Packt Publishing Ltd, 2017.

[17] S. Seneviratne *et al.*, "A Survey of Wearable Devices and Challenges," *IEEE Communications Surveys & Tutorials*, vol. 19, no. 4, pp. 2573-2620, 2017.

[18] P. Bonato, "Wearable Sensors and Systems," *IEEE Engineering in Medicine and Biology Magazine*, vol. 29, no. 3, pp. 25-36, 2010.

[19] L. Atzori, A. Iera, and G. Morabito, "The Internet of Things: A survey," *Computer Networks*, vol. 54, no. 15, pp. 2787-2805, 2010.

[20] G. B. Moody and R. G. Mark, "The impact of the MIT-BIH Arrhythmia Database," *IEEE Engineering in Medicine and Biology Magazine,* vol. 20, no. 3, pp. 45-50, 2001.

[21] ANSI/AAMI, "Testing and reporting performance results of cardiac rhythm and ST segment measurement algorithms," *American National Standards Institute, Inc. (ANSI), Association for the Advancement of Medical Instrumentation (AAMI), ANSI/AAMI/ISO EC57, 1998-(R),* 2008.

[22] P. Pławiak, "Novel methodology of cardiac health recognition based on ECG signals and evolutionary-neural system," *Expert Systems with Applications,* vol. 92, pp. 334-349, 2018.

[23] O. Pahlm and L. Sörnmo, "Software QRS detection in ambulatory monitoring — a review," *Medical and Biological Engineering and Computing,* vol. 22, no. 4, pp. 289-297, 1984.

[24] Q. Xue, Y. H. Hu, and W. J. Tompkins, "Neural-network-based adaptive matched filtering for QRS detection," *IEEE Transactions on Biomedical Engineering,* vol. 39, no. 4, pp. 317-329, 1992.

[25] J. C. T. B. Moraes, M. M. Freitas, F. N. Vilani, and E. V. Costa, "A QRS complex detection algorithm using electrocardiogram leads," in *Computers in Cardiology*, 2002, pp. 205-208.

[26] M. Adnane, Z. Jiang, and S. Choi, "Development of QRS detection algorithm designed for wearable cardiorespiratory system," *Computer Methods and Programs in Biomedicine,* vol. 93, no. 1, pp. 20-31, 2009.

[27] Z. Zidelmal, A. Amirou, M. Adnane, and A. Belouchrani, "QRS detection based on wavelet coefficients," *Computer Methods and Programs in Biomedicine,* vol. 107, no. 3, pp. 490-496, 2012.

[28] B. S. Shaik, G. V. S. S. K. R. Naganjaneyulu, T. Chandrasheker, and A. V. Narasimhadhan, "A Method for QRS Delineation Based on STFT Using Adaptive Threshold," *Procedia Computer Science,* vol. 54, pp. 646-653, 2015.

[29] Ö. Yakut and E. D. Bolat, "An improved QRS complex detection method having low computational load," *Biomedical Signal Processing and Control,* vol. 42, pp. 230-241, 2018.

[30] A. Sharma, S. Patidar, A. Upadhyay, and U. Rajendra Acharya, "Accurate tunable-Q wavelet transform based method for QRS complex detection," *Computers & Electrical Engineering,* vol. 75, pp. 101-111, 2019.

[31] W. Cai and D. Hu, "QRS Complex Detection Using Novel Deep Learning Neural Networks," *IEEE Access,* vol. 8, pp. 97082-97089, 2020.

[32] Z. Zhang, Q. Yu, Q. Zhang, N. Ning, and J. Li, "A Kalman filtering based adaptive threshold algorithm for QRS complex detection," *Biomedical Signal Processing and Control,* vol. 58, p. 101827, 2020.

[33] M. K. Das and S. Ari, "ECG Beats Classification Using Mixture of Features," *International Scholarly Research Notices,* vol. 2014, p. 178436, 2014.

[34] M. Sadrawi *et al.*, "Arrhythmia Evaluation in Wearable ECG Devices," *Sensors,* vol. 17, no. 11, p. 2445, 2017.

[35] G. Sannino and G. De Pietro, "A deep learning approach for ECG-based heartbeat classification for arrhythmia detection," *Future Generation Computer Systems,* vol. 86, pp. 446-455, 2018.

[36] O. Faust, A. Shenfield, M. Kareem, T. R. San, H. Fujita, and U. R. Acharya, "Automated detection of atrial fibrillation using long short-term memory network with RR interval signals," *Computers in Biology and Medicine,* vol. 102, pp. 327-335, 2018.

[37] E. Izci, M. A. Ozdemir, R. Sadighzadeh, and A. Akan, "Arrhythmia Detection on ECG Signals by Using Empirical Mode Decomposition," in *2018 Medical Technologies National Congress (TIPTEKNO)*, 2018, pp. 1-4.

[38] S. Singh, S. K. Pandey, U. Pawar, and R. R. Janghel, "Classification of ECG Arrhythmia using Recurrent Neural Networks," *Procedia Computer Science*, vol. 132, pp. 1290-1297, 2018.

[39] L. B. Marinho, N. d. M. M. Nascimento, J. W. M. Souza, M. V. Gurgel, P. P. Rebouças Filho, and V. H. C. de Albuquerque, "A novel electrocardiogram feature extraction approach for cardiac arrhythmia classification," *Future Generation Computer Systems,* vol. 97, pp. 564-577, 2019.

[40] X. Hua *et al.*, "A novel method for ECG signal classification via one-dimensional convolutional neural network," *Multimedia Systems,* 2020.

[41] D. K. Atal and M. Singh, "Arrhythmia Classification with ECG signals based on the Optimization-Enabled Deep Convolutional Neural Network," *Computer Methods and Programs in Biomedicine,* vol. 196, p. 105607, 2020.

[42] A. Ullah, S. M. Anwar, M. Bilal, and R. M. Mehmood, "Classification of Arrhythmia by Using Deep Learning with 2-D ECG Spectral Image Representation," *Remote Sensing,* vol. 12, no. 10, p. 1685, 2020.

[43] H. Wang *et al.*, "A high-precision arrhythmia classification method based on dual fully connected neural network," *Biomedical Signal Processing and Control,* vol. 58, p. 101874, 2020.

[44] H. Yang and Z. Wei, "Arrhythmia Recognition and Classification Using Combined Parametric and Visual Pattern Features of ECG Morphology," *IEEE Access,* vol. 8, pp. 47103-47117, 2020.

[45] J. W. Zheng, Z. B. Zhang, T. H. Wu, and Y. Zhang, "A wearable mobihealth care system supporting real-time diagnosis and alarm," *Medical & Biological Engineering & Computing,* vol. 45, no. 9, pp. 877-885, 2007.

[46] J. J. Oresko *et al.*, "A Wearable Smartphone-Based Platform for Real-Time Cardiovascular Disease Detection Via Electrocardiogram

Processing," *IEEE Transactions on Information Technology in Biomedicine,* vol. 14, no. 3, pp. 734-740, 2010.

[47] J. Liu, F. Xie, Y. Zhou, Q. Zou, and J. Wu, "A wearable health monitoring system with multi-parameters," in *2013 6th International Conference on Biomedical Engineering and Informatics*, 2013, pp. 332-336.

[48] D. Sopic, A. Aminifar, A. Aminifar, and D. Atienza, "Real-Time Event-Driven Classification Technique for Early Detection and Prevention of Myocardial Infarction on Wearable Systems," *IEEE Transactions on Biomedical Circuits and Systems,* vol. 12, no. 5, pp. 982-992, 2018.

[49] Y. Xia *et al.*, "An Automatic Cardiac Arrhythmia Classification System With Wearable Electrocardiogram," *IEEE Access,* vol. 6, pp. 16529-16538, 2018.

[50] A. Amirshahi and M. Hashemi, "ECG Classification Algorithm Based on STDP and R-STDP Neural Networks for Real-Time Monitoring on Ultra Low-Power Personal Wearable Devices," *IEEE Transactions on Biomedical Circuits and Systems,* vol. 13, no. 6, pp. 1483-1493, 2019.

[51] A. Bonfiglio and D. De Rossi, *Wearable monitoring systems*. Springer Science & Business Media, 2010.

[52] S. Patel, H. Park, P. Bonato, L. Chan, and M. Rodgers, "A review of wearable sensors and systems with application in rehabilitation," *Journal of NeuroEngineering and Rehabilitation,* vol. 9, no. 1, p. 21, 2012.

[53] P. Wang and Q. Liu, *Biomedical sensors and measurement*. Springer Science & Business Media, 2011.

[54] G. Zhou, Y. Wang, and L. J. A. i. B. Cui, "Biomedical sensor, device and measurement systems," vol. 177, 2015.

[55] S. Chaudhuri, T. D. Pawar, and S. Duttagupta, *Ambulation analysis in wearable ECG*. Springer, 2009.

[56] T. Tagawa, T. Tamura, and P. A. Oberg, *Biomedical sensors and instruments*. CRC press, 2019.

[57] S. Smith, *Digital signal processing: a practical guide for engineers and scientists*. Elsevier, 2013.

[58] W. Dargie and C. Poellabauer, *Fundamentals of wireless sensor networks: theory and practice*. John Wiley & Sons, 2010.

[59] L. K. Hansen and P. Salamon, "Neural network ensembles," *IEEE Transactions on Pattern Analysis and Machine Intelligence,* vol. 12, no. 10, pp. 993-1001, 1990.

[60] S. Kiranyaz, T. Ince, and M. Gabbouj, "Real-Time Patient-Specific ECG Classification by 1-D Convolutional Neural Networks," *IEEE Transactions on Biomedical Engineering,* vol. 63, no. 3, pp. 664-675, 2016.

[61] L. V. Fausett, *Fundamentals of neural networks: architectures, algorithms and applications*. Pearson Education India, 2006.

[62] J. M. Zurada, *Introduction to artificial neural systems*. West St. Paul, 1992.

[63] S. Xu and L. Chen, "A novel approach for determining the optimal number of hidden layer neurons for FNN’s and its application in data mining," presented at the 5th International Conference on Information Technology and Applications (ICITA 2008), 2008.

[64] K. G. Sheela and S. N. Deepa, "Review on Methods to Fix Number of Hidden Neurons in Neural Networks," *Mathematical Problems in Engineering,* vol. 2013, p. 425740, 2013.

[65] F. Provost and R. Kohavi, "Glossary of terms," *Journal of Machine Learning,* vol. 30, no. 2-3, pp. 271-274, 1998.

[66] T. Fawcett, "An introduction to ROC analysis," *Pattern Recognition Letters,* vol. 27, no. 8, pp. 861-874, 2006.

[67] R. A. Rayan, C. Tsagkaris, and R. B. Iryna, "The Internet of Things for Healthcare: Applications, Selected Cases and Challenges," in *IoT in Healthcare and Ambient Assisted Living*: Springer, 2021, pp. 1-15.

[68] F. Al-Turjman and I. Baali, "Machine learning for wearable IoT-based applications: A survey," *Trans Emerging Tel Tech,* vol. n/a, no. n/a, p. e3635, 2019.

[69] A. J. Khalaf and S. J. Mohammed, "A QRS-Detection Algorithm for Real-Time Applications," *International Journal of Intelligent Engineering and Systems,* vol. 14, no. 1, pp. 356-367, 2021.

[70] C. Nayak, S. K. Saha, R. Kar, and D. Mandal, "An Efficient and Robust Digital Fractional Order Differentiator Based ECG Pre-Processor Design for QRS Detection," *IEEE Transactions on Biomedical Circuits and Systems,* vol. 13, no. 4, pp. 682-696, 2019.

[71] A. Bajaj and S. Kumar, "QRS complex detection using fractional Stockwell transform and fractional Stockwell Shannon energy," *Biomedical Signal Processing and Control,* vol. 54, p. 101628, 2019.

[72] T. Nguyen, X. Qin, A. Dinh, and F. Bui, "Low Resource Complexity R-peak Detection Based on Triangle Template Matching and Moving Average Filter," *sensors,* vol. 19, no. 18, p. 3997, 2019.

[73] C. Nayak, S. K. Saha, R. Kar, and D. Mandal, "Optimal SSA-based wideband digital differentiator design for cardiac QRS complex detection application," *Int J Numer Model,* vol. 32, no. 2, p. e2524, 2019.

[74] D. Yang and Y. Zhang, "A real-time QRS detector based on low-pass differentiator and hilbert transform," in *MATEC Web of Conferences*, 2018, vol. 175, p. 02008: EDP Sciences.

[75] T. Sharma and K. K. Sharma, "QRS complex detection in ECG signals using locally adaptive weighted total variation denoising," *Computers in Biology and Medicine,* vol. 87, pp. 187-199, 2017.

[76] S. Jain, A. Kumar, V. J. I. S. Bajaj, Measurement, and Technology, "Technique for QRS complex detection using particle swarm optimisation," *IET Science, Measurement & Technology,* vol. 10, no. 6, pp. 626-636, 2016.

[77] T. Sharma and K. K. Sharma, "QRS Complex Detection in ECG Signals Using the Synchrosqueezed Wavelet Transform," *IETE Journal of Research*, vol. 62, no. 6, pp. 885-892, 2016.

[78] S. Yazdani and J.-M. Vesin, "Extraction of QRS fiducial points from the ECG using adaptive mathematical morphology," *Digital Signal Processing*, vol. 56, pp. 100-109, 2016.

[79] F. Bouaziz, D. Boutana, and M. J. I. S. P. Benidir, "Multiresolution wavelet-based QRS complex detection algorithm suited to several abnormal morphologies," *IET Signal Process*, vol. 8, no. 7, pp. 774-782, 2014.

[80] G. Nallathambi and J. C. Príncipe, "Integrate and fire pulse train automaton for QRS detection," (in eng), *IEEE Trans Biomed Eng*, vol. 61, no. 2, pp. 317-26, 2014.

[81] Y. Li, H. Yan, F. Hong, and J. Song, "A new approach of QRS complex detection based on matched filtering and triangle character analysis," (in eng), *Australas Phys Eng Sci Med*, vol. 35, no. 3, pp. 341-56, 2012.

[82] F. Chiarugi, V. Sakkalis, D. Emmanouilidou, T. Krontiris, M. Varanini, and I. Tollis, "Adaptive threshold QRS detector with best channel selection based on a noise rating system," in *2007 Computers in Cardiology*, 2007, pp. 157-160.

[83] M. Cvikl, F. Jager, and A. Zemva, "Hardware Implementation of a Modified Delay-Coordinate Mapping-Based QRS Complex Detection Algorithm," *EURASIP Journal on Advances in Signal Processing*, vol. 2007, no. 1, p. 057286, 2007.

[84] M. S. Manikandan and B. Ramkumar, "Straightforward and robust QRS detection algorithm for wearable cardiac monitor," *Healthcare Technology Letters*, vol. 1, no. 1, pp. 40-44, 2014.

[85] M. S. Manikandan and K. P. Soman, "A novel method for detecting R-peaks in electrocardiogram (ECG) signal," *Biomedical Signal Processing and Control,* vol. 7, no. 2, pp. 118-128, 2012.

[86] J. Lewandowski, H. E. Arochena, R. N. G. Naguib, and K. Chao, "A simple real-time QRS detection algorithm utilizing curve-length concept with combined adaptive threshold for electrocardiogram signal classification," in *TENCON 2012 IEEE Region 10 Conference*, 2012, pp. 1-6.

[87] N. S. V. K. Chaitanya, A. Radhakrishnan, G. R. Reddy, and M. S. Manikandan, "A simple and robust QRS detection algorithm for wireless medical body area network," in *2011 International Conference on Emerging Trends in Networks and Computer Communications (ETNCC)*, 2011, pp. 153-158.

[88] B. Huang and Y. Wang, "Detecting QRS Complexes of Two-Channel ECG Signals by Using Combined Wavelet Entropy," in *2009 3rd International Conference on Bioinformatics and Biomedical Engineering*, 2009, pp. 1-4.

[89] F. Abdelliche, A. Charef, and S. Ladaci, "Complex fractional and complex Morlet wavelets for QRS complex detection," in *ICFDA'14 International Conference on Fractional Differentiation and Its Applications 2014*, 2014, pp. 1-5.

[90] W. Zhu, H. Zhao, and X. Chen, "A new QRS detector based on empirical mode decomposition," in *IEEE 10th INTERNATIONAL CONFERENCE ON SIGNAL PROCESSING PROCEEDINGS*, 2010, pp. 1-4.

[91] S. A. Chouakri, F. Bereksi-Reguig, and A. Taleb-Ahmed, "QRS complex detection based on multi wavelet packet decomposition," *Applied Mathematics and Computation,* vol. 217, no. 23, pp. 9508-9525, 2011.

[92] P. Phukpattaranont, "QRS detection algorithm based on the quadratic filter," *Expert Systems with Applications,* vol. 42, no. 11, pp. 4867-4877, 2015.

[93] J.-W. Lee, K.-S. Kim, B. Lee, B. Lee, and M.-H. Lee, "A Real Time QRS Detection Using Delay-Coordinate Mapping for the Microcontroller Implementation," *Annals of Biomedical Engineering,* vol. 30, no. 9, pp. 1140-1151, 2002.

[94] L. Jeongwhan, J. Keesam, Y. Jiyoung, and L. Myoungho, "A simple real-time QRS detection algorithm," in *Proceedings of 18th Annual International Conference of the IEEE Engineering in Medicine and Biology Society*, 1996, vol. 4, pp. 1396-1398 vol.4.

[95] C. J. Deepu and Y. Lian, "A Joint QRS Detection and Data Compression Scheme for Wearable Sensors," *IEEE Transactions on Biomedical Engineering,* vol. 62, no. 1, pp. 165-175, 2015.

[96] M. R. Arefin and R. Fazel-Rezai, "Computationally efficient QRS detection analysis based on dual-slope method," (in eng), *Annu Int Conf IEEE Eng Med Biol Soc,* vol. 2014, pp. 2274-7, 2014.

[97] Y. Wang, C. J. Deepu, and Y. Lian, "A computationally efficient QRS detection algorithm for wearable ECG sensors," in *2011 Annual International Conference of the IEEE Engineering in Medicine and Biology Society*, 2011, pp. 5641-5644.

[98] C. F. Zhang and T. Bae, "VLSI Friendly ECG QRS Complex Detector for Body Sensor Networks," *IEEE Journal on Emerging and Selected Topics in Circuits and Systems,* vol. 2, no. 1, pp. 52-59, 2012.

[99] F. Zhang and Y. Lian, "QRS Detection Based on Morphological Filter and Energy Envelope for Applications in Body Sensor Networks," *Journal of Signal Processing Systems,* vol. 64, no. 2, pp. 187-194, 2011.

[100] F. Zhang and Y. Lian, "QRS Detection Based on Multiscale Mathematical Morphology for Wearable ECG Devices in Body Area Networks," *IEEE*

Transactions on Biomedical Circuits and Systems, vol. 3, no. 4, pp. 220-228, 2009.

[101] K. Arbateni and A. Bennia, "Sigmoidal radial basis function ANN for QRS complex detection," *Neurocomputing,* vol. 145, pp. 438-450, 2014/12/05/ 2014.

[102] L. D. Sharma and R. K. Sunkaria, "A robust QRS detection using novel pre-processing techniques and kurtosis based enhanced efficiency," *Measurement*, vol. 87, pp. 194-204, 2016.

[103] P. Li *et al.*, "A 410-nW Efficient QRS Processor for Mobile ECG Monitoring in 0.18-μm CMOS," *IEEE Transactions on Biomedical Circuits and Systems,* vol. 11, no. 6, pp. 1356-1365, 2017.

[104] C.-L. Chen and C.-T. Chuang, "A QRS Detection and R Point Recognition Method for Wearable Single-Lead ECG Devices," *Sensors* vol. 17, no. 9, p. 1969, 2017.

[105] N. Ravanshad, H. Rezaee-Dehsorkh, R. Lotfi, and Y. Lian, "A Level-Crossing Based QRS-Detection Algorithm for Wearable ECG Sensors," *IEEE Journal of Biomedical and Health Informatics,* vol. 18, no. 1, pp. 183-192, 2014.

[106] S. Torbey, S. G. Akl, and D. P. Redfearn, "Multi-lead QRS detection using window pairs," in *2012 Annual International Conference of the IEEE Engineering in Medicine and Biology Society*, 2012, pp. 3143-3146.

[107] B. S. Shaik, G. V. S. S. K. R. Naganjaneyulu, and A. V. Narasimhadhan, "A novel approach for QRS delineation in ECG signal based on chirplet transform," in *2015 IEEE International Conference on Electronics, Computing and Communication Technologies (CONECCT)*, 2015, pp. 1-5.

[108] A. Karimipour and M. R. Homaeinezhad, "Real-time electrocardiogram P-QRS-T detection–delineation algorithm based on quality-supported

analysis of characteristic templates," *Computers in Biology and Medicine,* vol. 52, pp. 153-165, 2014.

[109] S. K. Salih, S. Aljunid, A. Yahya, and K. J. I. J. o. C. S. I. Ghailan, "A novel approach for detecting QRS complex of ECG signal," *International Journal of Computer Science Issues,* vol. 9, no. 6, pp. 205-215, 2012.

[110] S. Taouli, F. J. G. J. o. C. S. Bereksi-Reguig, and Technology, "Detection of QRS complexes in ECG signals based on empirical mode decomposition," *Global Journal of Computer Science and Technology* vol. 11, no. 20, 2011.

[111] Y.-C. Yeh and W.-J. Wang, "QRS complexes detection for ECG signal: The Difference Operation Method," *Computer Methods and Programs in Biomedicine,* vol. 91, no. 3, pp. 245-254, 2008.

[112] M. Paoletti and C. Marchesi, "Discovering dangerous patterns in long-term ambulatory ECG recordings using a fast QRS detection algorithm and explorative data analysis," *Computer Methods and Programs in Biomedicine,* vol. 82, no. 1, pp. 20-30, 2006.

[113] Z.-E. Hadj Slimane and A. Naït-Ali, "QRS complex detection using Empirical Mode Decomposition," *Digital Signal Processing,* vol. 20, no. 4, pp. 1221-1228, 2010.

[114] P. S. Hamilton and W. J. Tompkins, "Quantitative Investigation of QRS Detection Rules Using the MIT/BIH Arrhythmia Database," *IEEE Transactions on Biomedical Engineering,* vol. BME-33, no. 12, pp. 1157-1165, 1986.

[115] C. Ieong *et al.*, "A 0.83-$\mu {\rm W}$ QRS Detection Processor Using Quadratic Spline Wavelet Transform for Wireless ECG Acquisition in 0.35- $\mu{\rm m}$ CMOS," *IEEE Transactions on Biomedical Circuits and Systems,* vol. 6, no. 6, pp. 586-595, 2012.

[116] J. P. Sahoo, M. K. Das, S. Ari, S. J. I. J. o. S. Behera, and I. S. Engineering, "Autocorrelation and Hilbert transform-based QRS complex detection in

ECG signal," *International Journal of Signal and Imaging Systems Engineering,* vol. 7, no. 1, pp. 52-58, 2014.

[117] X. Lu, M. Pan, and Y. Yu, "QRS Detection Based on Improved Adaptive Threshold," *Journal of Healthcare Engineering,* vol. 2018, p. 5694595, 2018.

[118] X. Zhang and Y. Lian, "A 300-mV 220-nW Event-Driven ADC With Real-Time QRS Detection for Wearable ECG Sensors," *IEEE Transactions on Biomedical Circuits and Systems,* vol. 8, no. 6, pp. 834-843, 2014.

[119] S. Farashi, "A multiresolution time-dependent entropy method for QRS complex detection," *Biomedical Signal Processing and Control,* vol. 24, pp. 63-71, 2016.

[120] A. Chen *et al.*, "A Real Time QRS Detection Algorithm Based on ET and PD Controlled Threshold Strategy," *Sensors,* vol. 20, no. 14, p. 4003, 2020.

[121] X. Tang, Q. Hu, and W. Tang, "A Real-Time QRS Detection System With PR/RT Interval and ST Segment Measurements for Wearable ECG Sensors Using Parallel Delta Modulators," *IEEE Transactions on Biomedical Circuits and Systems,* vol. 12, no. 4, pp. 751-761, 2018.

[122] Y. Zhao, Z. Shang, and Y. Lian, "User Adaptive QRS Detection Based on One Target Clustering and Correlation Coefficient," in *2018 IEEE Biomedical Circuits and Systems Conference (BioCAS)*, 2018, pp. 1-4.

[123] M. Elgendi, A. Mohamed, and R. Ward, "Efficient ECG Compression and QRS Detection for E-Health Applications," *Scientific Reports,* vol. 7, no. 1, p. 459, 2017.

[124] J. Darrington, "Towards real time QRS detection: A fast method using minimal pre-processing," *Biomedical Signal Processing and Control,* vol. 1, no. 2, pp. 169-176, 2006.

[125] A. Ghaffari, H. Golbayani, and M. Ghasemi, "A new mathematical based QRS detector using continuous wavelet transform," *Computers & Electrical Engineering,* vol. 34, no. 2, pp. 81-91, 2008.

[126] Z. Hou, Y. Dong, J. Xiang, X. Li, and B. Yang, "A Real-Time QRS Detection Method Based on Phase Portraits and Box-Scoring Calculation," *IEEE Sensors Journal,* vol. 18, no. 9, pp. 3694-3702, 2018.

[127] J. Rahul, M. Sora, and L. D. Sharma, "Exploratory data analysis based efficient QRS-complex detection technique with minimal computational load," *Physical and Engineering Sciences in Medicine,* vol. 43, no. 3, pp. 1049-1067, 2018.

[128] G. Garcia, G. Moreira, D. Menotti, and E. Luz, "Inter-Patient ECG Heartbeat Classification with Temporal VCG Optimized by PSO," *Scientific Reports,* vol. 7, no. 1, p. 10543, 2017.

[129] C. Philip de, M. O. Dwyer, and R. B. Reilly, "Automatic classification of heartbeats using ECG morphology and heartbeat interval features," *IEEE Transactions on Biomedical Engineering,* vol. 51, no. 7, pp. 1196-1206, 2004.

Appendix A. ESP8266 Specifications

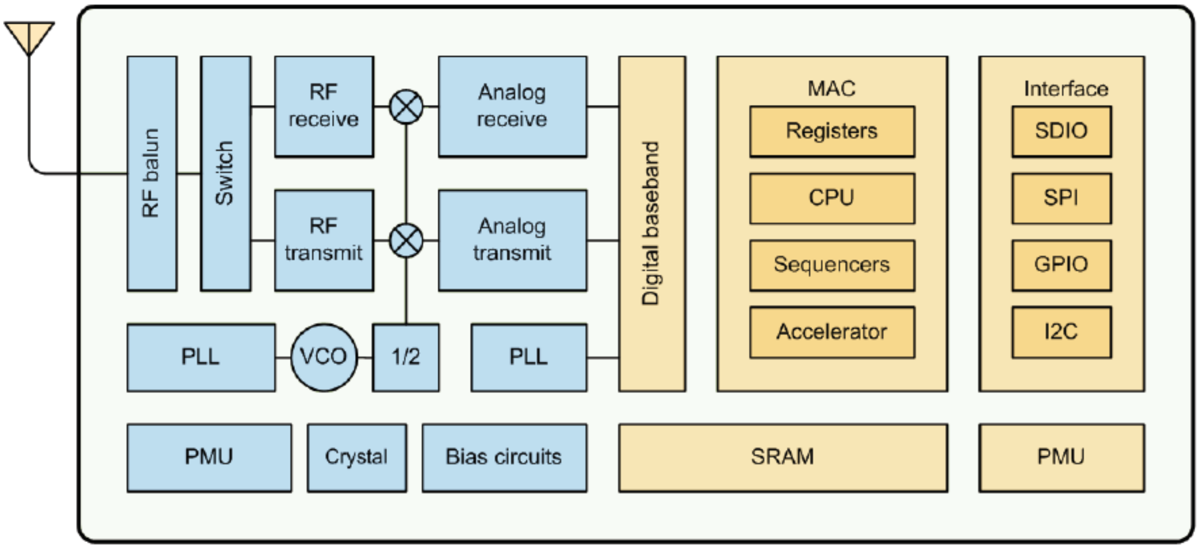

ESP8266EX Block Diagram

Features

- 802.11 b/g/n
- Integrated low power 32-bit MCU
- Integrated 10-bit ADC
- Integrated TCP/IP protocol stack
- Integrated TR switch, balun, LNA, power amplifier and matching network
- Integrated PLL, regulators, and power management units
- Supports antenna diversity
- WiFi 2.4 GHz, support WPA/WPA2
- Support STA/AP/STA+AP operation modes
- Support Smart Link Function for both Android and iOS devices
- SDIO 2.0, (H) SPI, UART, I2C, I2S, IR Remote Control, PWM, GPIO
- STBC, 1x1 MIMO, 2x1 MIMO
- A-MPDU & A-MSDU aggregation & 0.4s guard interval
- Deep sleep power <10uA, Power down leakage current < 5uA
- Wake up and transmit packets in < 2ms
- Standby power consumption of < 1.0mW (DTIM3)

- +20 dBm output power in 802.11b mode
- Operating temperature range -40C ~ 125C
- FCC, CE, TELEC, WiFi Alliance, and SRRC certified

ESP8266EX Electrical Characteristics

Parameters		Conditions	Min	Typical	Max	Unit
Storage Temperature Range			-40	Normal	125	°C
Maximum Soldering Temperature		IPC/JEDEC J-STD-020			260	°C
Working Voltage Value			3.0	3.3	3.6	V
I/O	V_{IL}/V_{IH}		$-0.3/0.75V_{IO}$		$0.25V_{IO}/3.6$	V
	V_{OL}/V_{OH}		$N/0.8V_{IO}$		$0.1V_{IO}/N$	
	I_{MAX}				12	mA
Electrostatic Discharge (HBM)		TAMB=25°C			2	KV
Electrostatic Discharge (CDM)		TAMB=25°C			0.5	KV

Pin Definitions of GPIOs

Variables	Symbol	Min	Max	Unit
Input Low Voltage	V_{IL}	-0.3	$0.25 \times V_{IO}$	V
Input High Voltage	V_{IH}	$0.75 \times V_{IO}$	3.3	V
Input Leakage Current	I_{IL}		50	nA
Output Low Voltage	V_{OL}		$0.1 \times V_{IO}$	V
Output High Voltage	V_{OH}	$0.8 \times V_{IO}$		V
Input Pin Resistance Value	C_{pad}		2	pF
VDDIO	V_{IO}	1.8	3.3	V
Maximum Driving Power	I_{MAX}		12	mA
Temerpature	T_{amb}	-40	125	°C

Appendix B. OLIMEX ECG Specifications

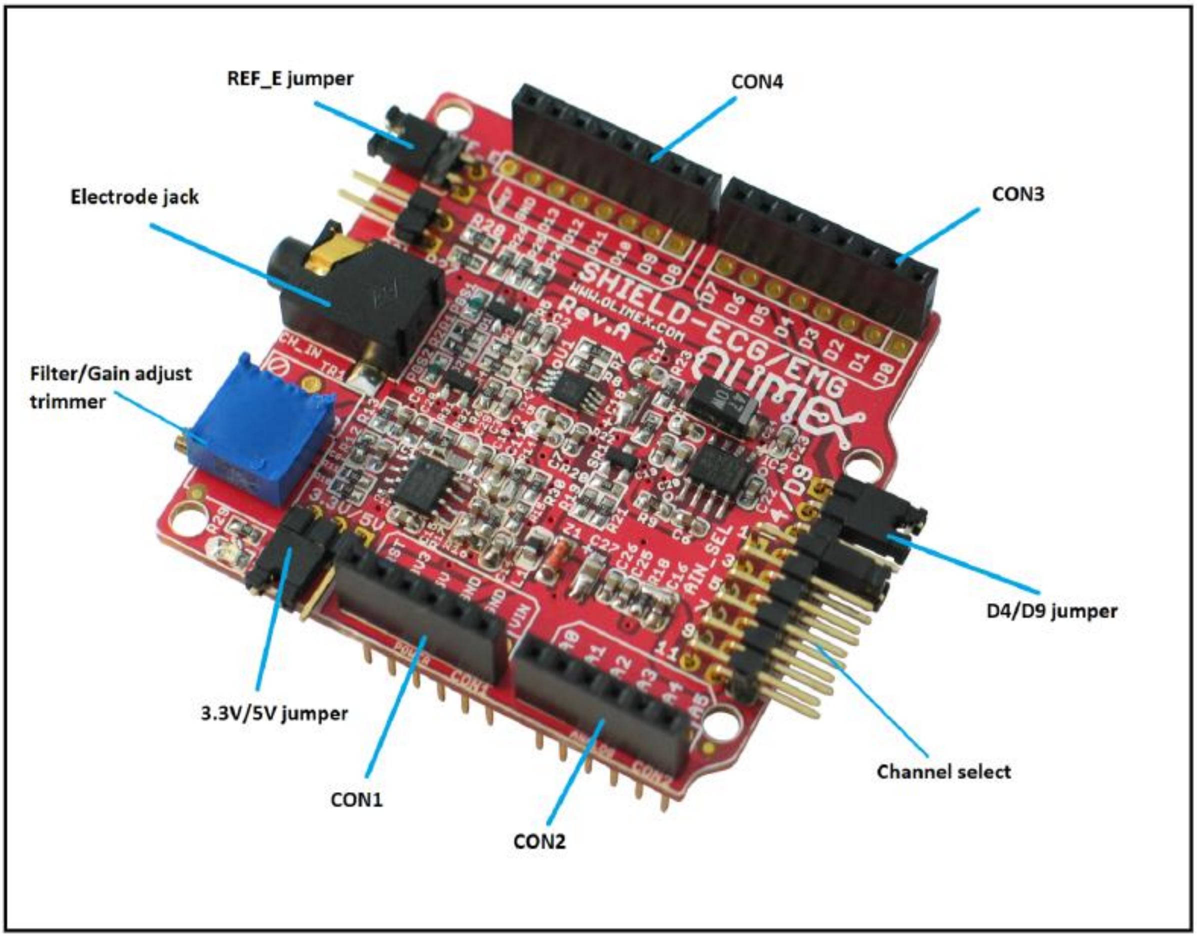

ECG BOARD DESCRIPTION

ECG card pins

Pin #	POWER CON1	ANALOG CON2	DIGITAL CON3	DIGITAL CON4
1	RST	A0	D0	D8
2	3.3V	A1	D1	D9
3	5V	A2	D2	D10
4	GND	A3	D3	D11
5	GND	A4	D4	D12
6	Vin	A5	D5	D13
7	-	-	D6	GND
8	-	-	D7	AREF

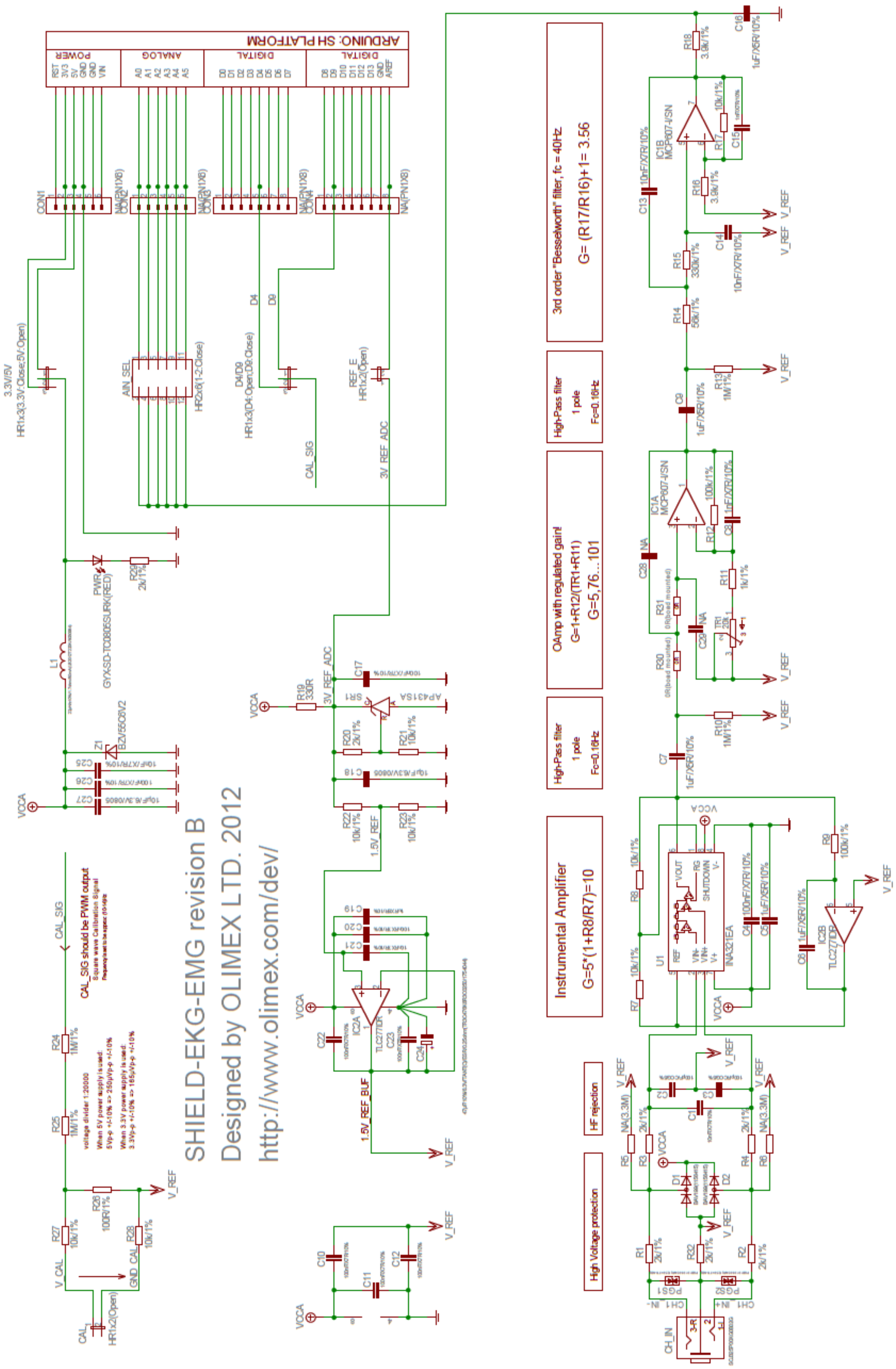

ECG card circuit

Appendix C. The QRS detection growing results for MBADB

The QRS-detection results for single hidden neuron

Records No.	TP (Beats)	FP (Beats)	FN (Beats)	FP+FN=FT (Beats)	Se (%)	PP (%)	DER (%)
100	2273	0	1	1	99.96	100.00	0.04
101	1865	3	0	3	100.00	99.84	0.16
102	2187	0	0	0	100.00	100.00	0.00
103	2084	0	0	0	100.00	100.00	0.00
104	2229	8	1	9	99.96	99.64	0.40
105	2572	52	7	59	99.73	98.02	2.29
106	2027	0	4	4	99.80	100.00	0.20
107	2137	0	2	2	99.91	100.00	0.09
108	1763	10	14	24	99.21	99.44	1.36
109	2532	0	3	3	99.88	100.00	0.12
111	2124	0	1	1	99.95	100.00	0.05
112	2539	2	0	2	100.00	99.92	0.08
113	1795	0	1	1	99.94	100.00	0.06
114	1879	2	7	9	99.63	99.89	0.48
115	1953	0	0	0	100.00	100.00	0.00
116	2412	2	18	20	99.26	99.92	0.83
117	1535	0	0	0	100.00	100.00	0.00
118	2278	2	0	2	100.00	99.91	0.09
119	1987	0	0	0	100.00	100.00	0.00
121	1863	0	2	2	99.89	100.00	0.11
122	2476	1	0	1	100.00	99.96	0.04
123	1518	0	0	0	100.00	100.00	0.00
124	1619	1	0	1	100.00	99.94	0.06
200	2601	7	4	11	99.85	99.73	0.42
201	1963	0	27	27	98.64	100.00	1.38
202	2136	0	4	4	99.81	100.00	0.19
203	2980	54	38	92	98.74	98.22	3.09
205	2656	0	5	5	99.81	100.00	0.19
207	1860	120	34	154	98.20	93.94	8.28
208	2955	9	41	50	98.63	99.70	1.69
209	3005	5	0	5	100.00	99.83	0.17
210	2650	7	30	37	98.88	99.74	1.40
212	2748	1	0	1	100.00	99.96	0.04
213	3251	0	3	3	99.91	100.00	0.09
214	2262	2	4	6	99.82	99.91	0.27
215	3363	1	0	1	100.00	99.97	0.03
217	2208	2	2	4	99.91	99.91	0.18
219	2154	0	0	0	100.00	100.00	0.00
220	2048	0	1	1	99.95	100.00	0.05
221	2427	1	3	4	99.88	99.96	0.16
222	2483	0	1	1	99.96	100.00	0.04
223	2605	0	1	1	99.96	100.00	0.04
228	2053	30	12	42	99.42	98.56	2.05
230	2256	0	0	0	100.00	100.00	0.00
231	1571	0	0	0	100.00	100.00	0.00
232	1780	3	0	3	100.00	99.83	0.17
233	3079	0	0	0	100.00	100.00	0.00
234	2753	0	4	4	99.85	100.00	0.15
overall	109494	325	275	600	99.75	99.70	0.55

The QRS-detection results for four hidden neurons

Records No.	TP (Beats)	FP (Beats)	FN (Beats)	FP+FN=FT (Beats)	Se (%)	PP (%)	DER (%)
100	2273	0	1	1	99.96	100.00	0.04
101	1865	3	1	4	99.95	99.84	0.21
102	2187	0	1	1	99.95	100.00	0.05
103	2084	0	0	0	100.00	100.00	0.00
104	2229	5	3	8	99.87	99.78	0.36
105	2572	37	14	51	99.46	98.58	1.98
106	2027	0	1	1	99.95	100.00	0.05
107	2137	0	2	2	99.91	100.00	0.09
108	1763	9	13	22	99.27	99.49	1.25
109	2532	1	3	4	99.88	99.96	0.16
111	2124	0	1	1	99.95	100.00	0.05
112	2539	0	0	0	100.00	100.00	0.00
113	1795	0	1	1	99.94	100.00	0.06
114	1879	2	6	8	99.68	99.89	0.43
115	1953	0	0	0	100.00	100.00	0.00
116	2412	0	18	18	99.26	100.00	0.75
117	1535	0	0	0	100.00	100.00	0.00
118	2278	1	0	1	100.00	99.96	0.04
119	1987	0	0	0	100.00	100.00	0.00
121	1863	0	2	2	99.89	100.00	0.11
122	2476	0	0	0	100.00	100.00	0.00
123	1518	0	0	0	100.00	100.00	0.00
124	1619	1	0	1	100.00	99.94	0.06
200	2601	5	1	6	99.96	99.81	0.23
201	1963	0	26	26	98.69	100.00	1.32
202	2136	0	4	4	99.81	100.00	0.19
203	2980	40	37	77	98.77	98.68	2.58
205	2656	0	4	4	99.85	100.00	0.15
207	1860	61	32	93	98.31	96.82	5.00
208	2955	8	29	37	99.03	99.73	1.25
209	3005	4	0	4	100.00	99.87	0.13
210	2650	3	24	27	99.10	99.89	1.02
212	2748	1	0	1	100.00	99.96	0.04
213	3251	0	4	4	99.88	100.00	0.12
214	2262	2	4	6	99.82	99.91	0.27
215	3363	0	0	0	100.00	100.00	0.00
217	2208	1	2	3	99.91	99.95	0.14
219	2154	0	0	0	100.00	100.00	0.00
220	2048	0	1	1	99.95	100.00	0.05
221	2427	1	2	3	99.92	99.96	0.12
222	2483	0	3	3	99.88	100.00	0.12
223	2605	0	1	1	99.96	100.00	0.04
228	2053	21	10	31	99.52	98.99	1.51
230	2256	0	0	0	100.00	100.00	0.00
231	1571	0	0	0	100.00	100.00	0.00
232	1780	2	0	2	100.00	99.89	0.11
233	3079	0	1	1	99.97	100.00	0.03
234	2753	0	4	4	99.85	100.00	0.15
overall	109494	208	256	464	99.77	99.81	0.42

The QRS-detection results for eight hidden neurons

Records No.	TP (Beats)	FP (Beats)	FN (Beats)	FP+FN=FT (Beats)	Se (%)	PP (%)	DER (%)
100	2273	0	1	1	99.96	100.00	0.04
101	1865	3	0	3	100.00	99.84	0.16
102	2187	0	0	0	100.00	100.00	0.00
103	2084	0	0	0	100.00	100.00	0.00
104	2229	3	1	4	99.96	99.87	0.18
105	2572	37	7	44	99.73	98.58	1.71
106	2027	0	2	2	99.90	100.00	0.10
107	2137	0	3	3	99.86	100.00	0.14
108	1763	10	9	19	99.49	99.44	1.08
109	2532	0	4	4	99.84	100.00	0.16
111	2124	0	1	1	99.95	100.00	0.05
112	2539	0	0	0	100.00	100.00	0.00
113	1795	0	1	1	99.94	100.00	0.06
114	1879	1	5	6	99.73	99.95	0.32
115	1953	0	0	0	100.00	100.00	0.00
116	2412	2	18	20	99.26	99.92	0.83
117	1535	0	0	0	100.00	100.00	0.00
118	2278	1	0	1	100.00	99.96	0.04
119	1987	0	0	0	100.00	100.00	0.00
121	1863	0	1	1	99.95	100.00	0.05
122	2476	0	0	0	100.00	100.00	0.00
123	1518	0	0	0	100.00	100.00	0.00
124	1619	1	0	1	100.00	99.94	0.06
200	2601	2	1	3	99.96	99.92	0.12
201	1963	0	17	17	99.14	100.00	0.87
202	2136	0	3	3	99.86	100.00	0.14
203	2980	33	34	67	98.87	98.90	2.25
205	2656	0	4	4	99.85	100.00	0.15
207	1860	67	12	79	99.36	96.52	4.25
208	2955	8	26	34	99.13	99.73	1.15
209	3005	3	0	3	100.00	99.90	0.10
210	2650	5	14	19	99.47	99.81	0.72
212	2748	2	0	2	100.00	99.93	0.07
213	3251	0	2	2	99.94	100.00	0.06
214	2262	2	3	5	99.87	99.91	0.22
215	3363	0	0	0	100.00	100.00	0.00
217	2208	1	2	3	99.91	99.95	0.14
219	2154	0	0	0	100.00	100.00	0.00
220	2048	0	1	1	99.95	100.00	0.05
221	2427	1	2	3	99.92	99.96	0.12
222	2483	1	1	2	99.96	99.96	0.08
223	2605	0	1	1	99.96	100.00	0.04
228	2053	17	7	24	99.66	99.18	1.17
230	2256	0	0	0	100.00	100.00	0.00
231	1571	0	0	0	100.00	100.00	0.00
232	1780	2	0	2	100.00	99.89	0.11
233	3079	0	0	0	100.00	100.00	0.00
234	2753	0	5	5	99.82	100.00	0.18
overall	109494	202	188	390	99.83	99.82	0.36

The QRS-detection results for fourteen hidden neurons

Records No.	TP (Beats)	FP (Beats)	FN (Beats)	FP+FN=FT (Beats)	Se (%)	PP (%)	DER (%)
100	2273	0	1	1	99.96	100.00	0.04
101	1865	2	0	2	100.00	99.89	0.11
102	2187	0	0	0	100.00	100.00	0.00
103	2084	0	0	0	100.00	100.00	0.00
104	2229	1	1	2	99.96	99.96	0.09
105	2572	18	6	24	99.77	99.31	0.93
106	2027	0	2	2	99.90	100.00	0.10
107	2137	0	2	2	99.91	100.00	0.09
108	1763	6	9	15	99.49	99.66	0.85
109	2532	0	3	3	99.88	100.00	0.12
111	2124	0	1	1	99.95	100.00	0.05
112	2539	0	0	0	100.00	100.00	0.00
113	1795	0	1	1	99.94	100.00	0.06
114	1879	2	2	4	99.89	99.89	0.21
115	1953	0	0	0	100.00	100.00	0.00
116	2412	0	18	18	99.26	100.00	0.75
117	1535	0	0	0	100.00	100.00	0.00
118	2278	0	0	0	100.00	100.00	0.00
119	1987	0	0	0	100.00	100.00	0.00
121	1863	0	1	1	99.95	100.00	0.05
122	2476	0	0	0	100.00	100.00	0.00
123	1518	0	0	0	100.00	100.00	0.00
124	1619	1	0	1	100.00	99.94	0.06
200	2601	2	2	4	99.92	99.92	0.15
201	1963	0	13	13	99.34	100.00	0.66
202	2136	1	3	4	99.86	99.95	0.19
203	2980	27	29	56	99.04	99.10	1.88
205	2656	0	4	4	99.85	100.00	0.15
207	1860	30	20	50	98.94	98.41	2.69
208	2955	7	18	25	99.39	99.76	0.85
209	3005	3	0	3	100.00	99.90	0.10
210	2650	3	9	12	99.66	99.89	0.45
212	2748	2	0	2	100.00	99.93	0.07
213	3251	0	2	2	99.94	100.00	0.06
214	2262	2	3	5	99.87	99.91	0.22
215	3363	0	0	0	100.00	100.00	0.00
217	2208	1	2	3	99.91	99.95	0.14
219	2154	0	0	0	100.00	100.00	0.00
220	2048	0	1	1	99.95	100.00	0.05
221	2427	0	1	1	99.96	100.00	0.04
222	2483	0	1	1	99.96	100.00	0.04
223	2605	0	1	1	99.96	100.00	0.04
228	2053	15	5	20	99.76	99.27	0.97
230	2256	0	0	0	100.00	100.00	0.00
231	1571	0	0	0	100.00	100.00	0.00
232	1780	2	0	2	100.00	99.89	0.11
233	3079	0	0	0	100.00	100.00	0.00
234	2753	0	4	4	99.85	100.00	0.15
overall	109494	125	165	290	99.85	99.89	0.26

الخلاصة

يعد مخطط كهربائية القلب (ECG) إشارة جسم طبية حيوية اساسية حيث تُظهر نشاط القلب وتشخص أمراض القلب والأوعية الدموية. قام العديد من الباحثين بالتحقيق في الكشف عن نبضات القلب وتصنيفها بناءً على تخطيط القلب ECG لتحقيق طريقة عالية الأداء ولأنها تتعلق بحياة الإنسان وكنتيجة للتقدم الحاصل في التكنولوجيا القابل للارتداء.

إن خوارزمية اكتشاف QRS (نبضات القلب) اساسي لمعالجة إشارة تخطيط القلب في تطبيقات الرعاية الصحية. في العديدة من الطرق، يتم تحليل إشارة مخطط كهربائية القلب لتصنيف أنواع أو فئات مختلفة من نبضات القلب. تبدأ هذه الفئات من الضربات العادية أو غير الطبيعية وتصل إلى أنواع عديدة بناءً على طرق التصنيف والتنوع في انواع الضربات المتوفرة في قاعدة البيانات.

تمثل خوارزمية اكتشاف وتصنيف نبضات القلب ذات الخطأ المنخفض مع الحسابات المنخفضة تحديًا كبيرًا للباحثين. المشكلة الرئيسية في تحسين الأداء تودي الى زيادة الحسابات، كما هو الحال في العديد من الطرق الحالية للكشف والتصنيف. علاوة على ذلك، فإن طرق الحساب العالية غير مناسبة للتنفيذ في الأجهزة القابلة للارتداء وتطبيقات الإنترنت ذات معدل البيانات المنخفض. من ناحية أخرى، بالنسبة لقاعدة بيانات عدم انتظام ضربات القلبMIT-BIH ، يتم حساب أرقام نبضات قلب مختلفة من الباحثين اعتمادًا على الاختلاف في فهم ملف التعليقات التوضيحية.

هذه الأطروحة طورت نظام رعاية صحية يمكن ارتداؤه عالي الدقة ومنخفض حسابيًا يعتمد على الذكاء الاصطناعي (AI) وإنترنت الأشياء (IoT) باستخدام طرق مقترحة للكشف عن دقات القلب وتصنيفها. ومن أجل تحقيق ذلك :أولاً، تم تصميم خوارزمية كشف QRS ذات اكتشاف أخطاء منخفضة. تتميز الخوارزمية المقترحة بحساب منخفض وأداء عالٍ تعتمد على تقنيات جديدة لاستخراج الميزات وتصنيف هجين بواسطة الشبكات العصبية الاصطناعية (ANN) وأشجار القرار. ثانيًا، تم توحيد رقم دقات القلب لقاعدة بيانات عدم انتظام ضربات القلب MIT-BIH بعد تطوير دالة جديدة لـ MATLAB Waveform Database Toolbox (WFDB). ثالثًا، تم تطوير طريقة تصنيف بحسابات منخفضة ودقة عالية لضربات القلب الطبيعية وغير الطبيعية بناءً على الميزات الجديدة المختلطة والمعاد استخدامها على اساس الشبكات العصبية الاصطناعية. رابعًا، تم تصميم طريقة تصنيف عالية الدقة لخمس فئات

من ضربات القلب وفقًا لطريقة جديدة تسمى الشبكة العصبية الاصطناعية ذات القناع الانتقائي (SMANN) مناسبة للتطبيقات الحسابية المنخفضة. يعطي SMANN بُعدًا جديدًا لـ ANN بدلاً من البعد التسلسلي لطرق التعلم العميق.SMANN عبارة عن شبكه عصبية اصطناعية ذات أقنعة متعددة ، يتم استخدام كل قناع للبيانات الانتقائية التي يتم فصلها حسب مميزاتها. علاوة على ذلك، يتم استخدام مزيج جديد من الميزات من ميزات مرحلة اكتشاف QRS المعاد استخدامها والميزات الأخرى من فترة RR وبين RR لتقليل حسابات استخراج الميزات. أخيرًا، تم تصميم وتنفيذ نظام ذكي يمكن ارتداؤه للكشف عن نبضات القلب وتصنيفها باستخدام Node-MCU مع إنترنت الأشياء بناءً على خوارزمية اكتشاف QRS المقترحة وطريقة تصنيف الفئات الخمس المقترحة.

تم تقييم خوارزمية الكشف المقترحة وأداء طرق التصنيف المقترحة باستخدام برنامج MATLAB على أساس قاعدة بيانات MIT-BIH لعدم انتظام ضربات القلب. نتائج أداء التقييم لخوارزمية اكتشاف QRS المقترحة ذات حساسية عالية (٩٩.٨٨٪)، واكتشاف معدل خطأ منخفض (٠.٢٢٤٪)، وتنبؤ عالي بنسبة ٩٩.٨٩٪. اما نتائج طريقة التصنيف للحالة الطبيعية لها دقة ٩٨.٩٧٪ وحساسية ٩٩.٤٢٪ وتوقع إيجابي ٩٩.١٣٪. بعد ذلك، كانت نتائج تصنيف الطريقة المقترحة للفئات الخمس ذات دقة عالية تصل إلى ٩٩.٩٢٢٤٪؛ إجمالي أخطاء التصنيف لـ SMANN هي ٨٠ من أصل ١٠٣١٩٢ ومقارنة بـ ٥٨٣ خطأ لشبكة ANN التقليدية. وبالتالي، يعد SMANN منهجًا جديدًا لتحسين الأداء بموارد منخفضة. اخيراً كانت نتائج النظام المنجز القابل للارتداء واعدة للكشف عن دقات القلب في الوقت الفعلي وتصنيفها كمراقبة للمرضى عبر الإنترنت وبدونه ذات تكلفة منخفضة تبلغ تقريباً ٥٢ دولارًا.

جمهورية العراق
وزارة التعليم العالي والبحث العلمي
جامعة بابل / كلية الهندسة
قسم الهندسة الكهربائية

تصميم وتنفيذ وتحليل الأداء لنظام تحليل نبضات القلب الذكي

اطروحة
مقدمة إلى كلية الهندسة في جامعة بابل
وهي جزء من متطلبات الحصول على درجة الدكتوراه
فلسفة في هندسة الالكترونيك والاتصالات

من قبل
أكرم جدوع خلف احمد

بأشراف
الأستاذ الدكتور
سمير جاسم محمد

تشرين الأول ٢٠٢١ | ربيع الثاني ١٤٤٣